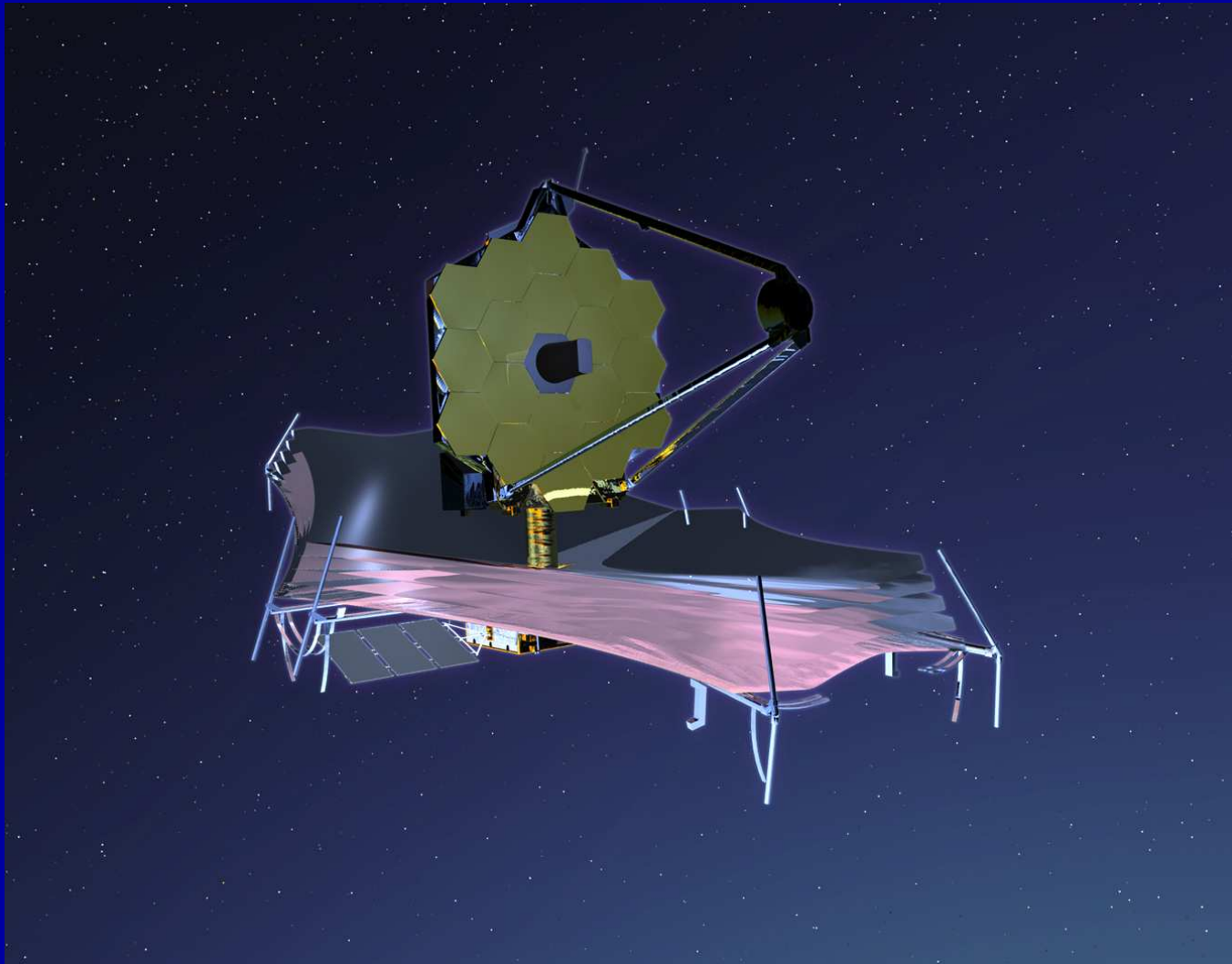


How can the James Webb Space Telescope Measure First Light, Reionization, & Galaxy Assembly?

Rogier Windhorst (Arizona State University)

Collaborators: S. Cohen, R. Jansen, N. Hathi (ASU), C. Conselice & H. Yan (Caltech)



Colloquium at CASA/ARL, University of Colorado, Feb, 5 2007

Outline

- (1) What is JWST and how will it be deployed?
- (2) What instruments and sensitivity will JWST have?
- (3) How JWST can measure First Light and Reionization
- (4) How JWST can measure Galaxy Assembly
- (5) Predicted Galaxy Appearance for JWST at $z \simeq 1-15$
- (6) What can WFC3 do, in particular in parallel to COS?
- (7) Summary and Conclusions

Sponsored by NASA/JWST

"Brilliantly done...breathtaking in its vision."
The New York Times

JAMES WEBB

Author of The Emperor's General



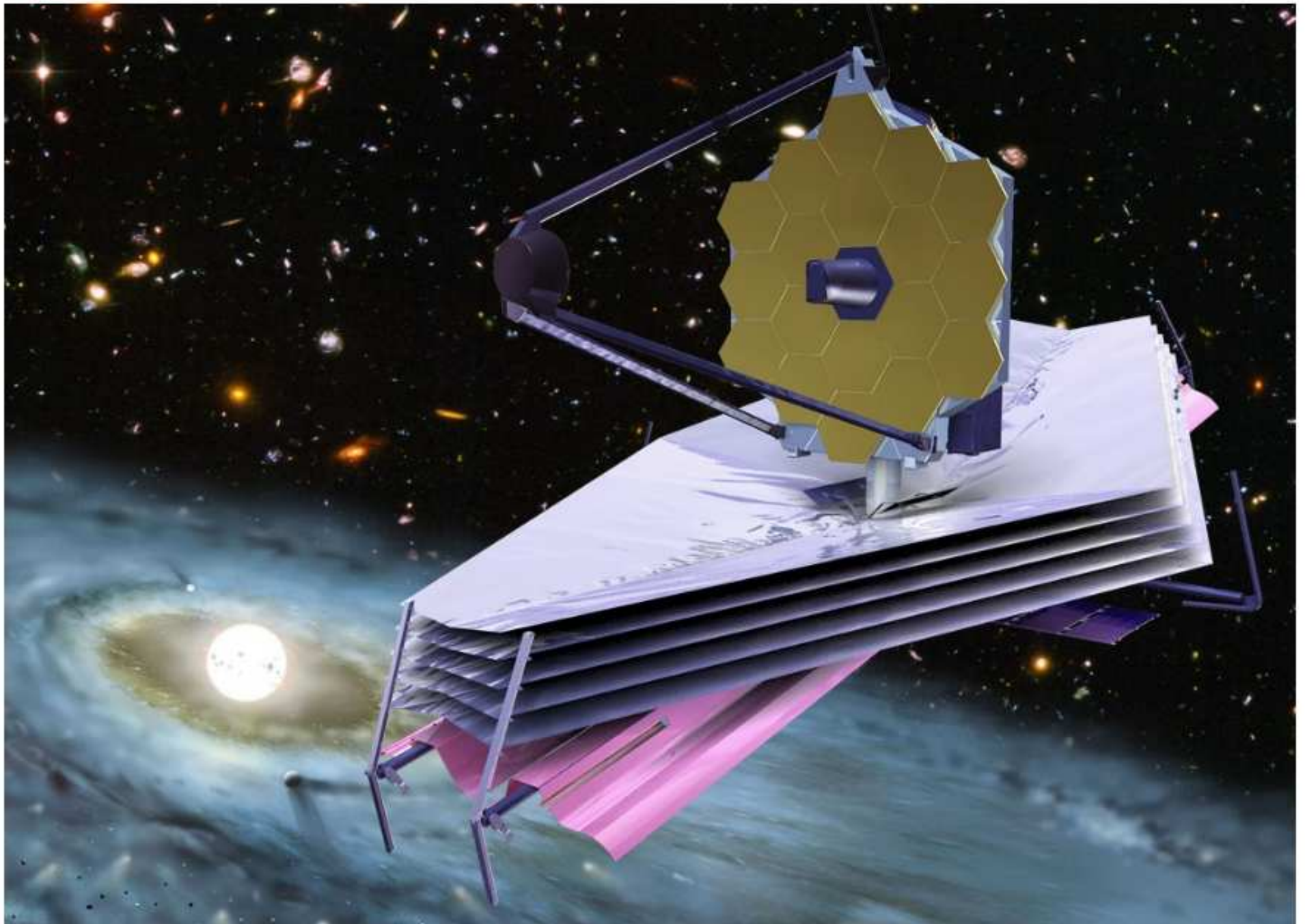
A NOVEL

**SOMETHING
TO DIE FOR**

Need hard-working grad students & postdocs in $\gtrsim 2013$... It'll be worth it!



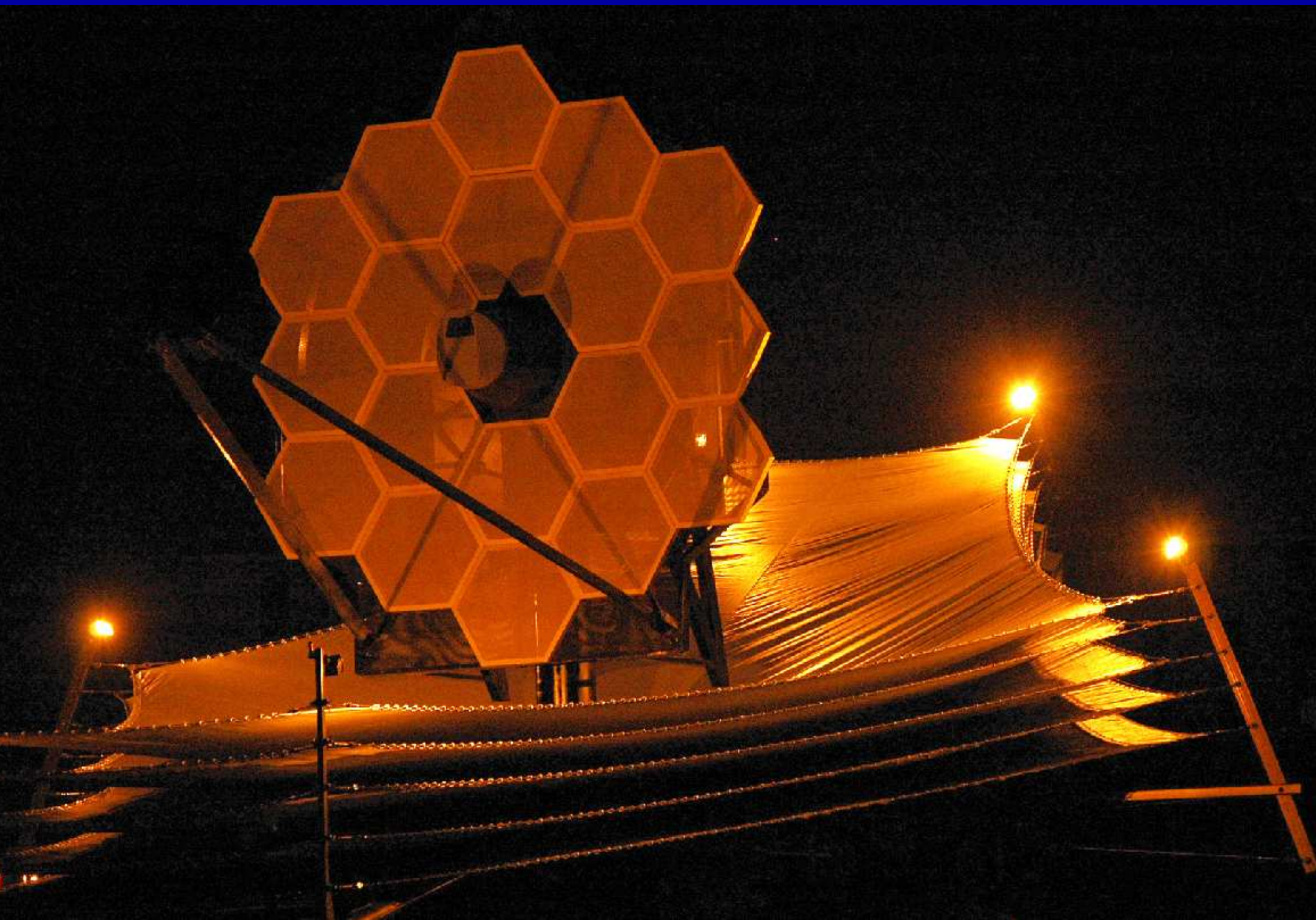
James Webb Space Telescope



- (1) What is the James Webb Space Telescope (JWST)?



- A fully deployable 6.5 meter (25 m^2) segmented IR telescope for imaging and spectroscopy from 0.6 to $28 \mu\text{m}$, to be launched by NASA $\gtrsim 2013$. It has a nested array of sun-shields to keep its ambient temperature at 35-45 K, allowing faint imaging ($AB \lesssim 31.5$) and spectroscopy ($AB \lesssim 29 \text{ mag}$).



Life size model of JWST: on display at the Jan. 2007 AAS mtg in Seattle.

- (1) How will JWST travel to its L2 orbit?

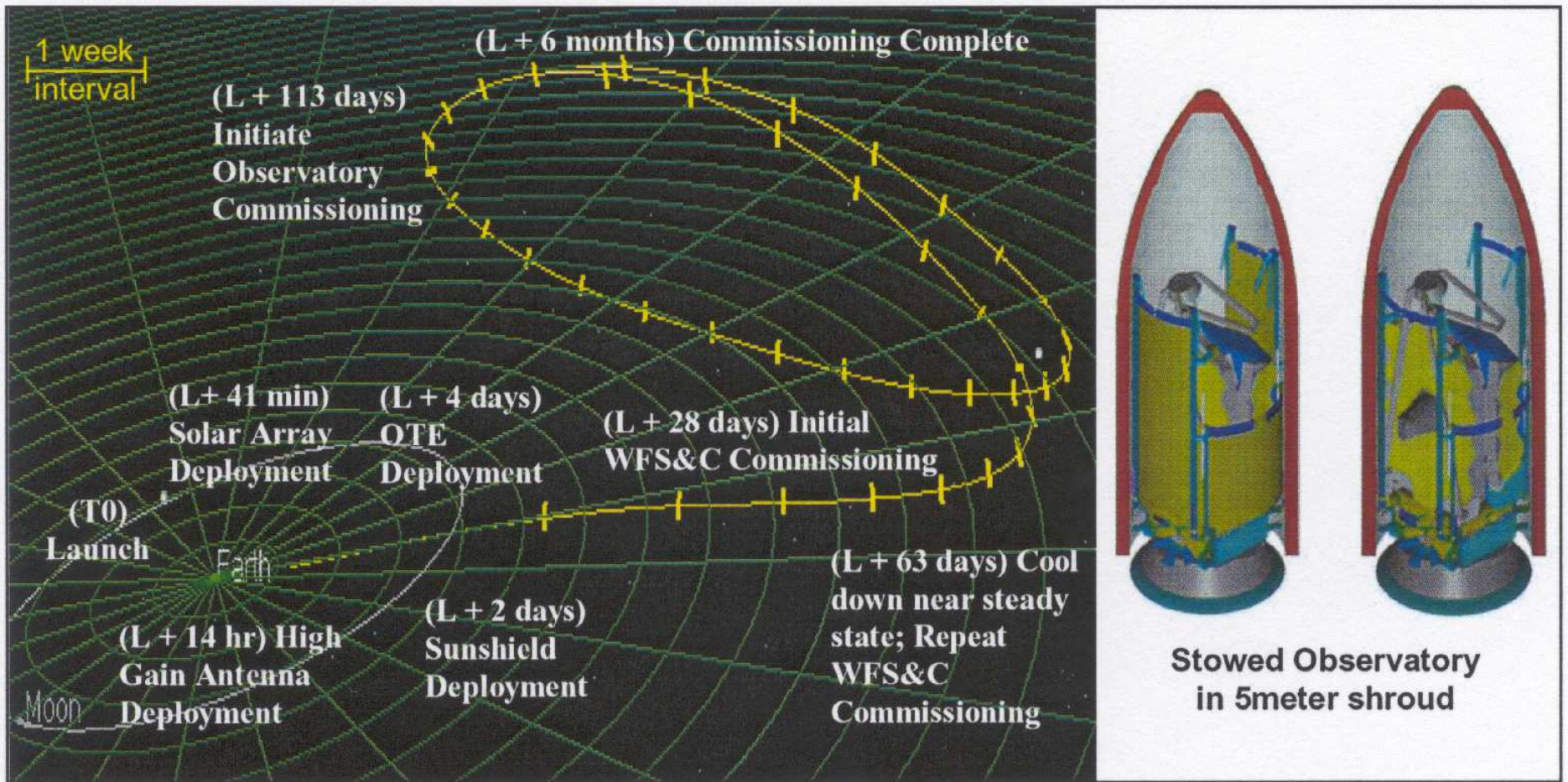


Figure 52. JWST orbit and trajectory to L2, and stowed view in 5 meter shroud.

After launch in ≈ 2013 with an Ariane V vehicle, JWST will orbit around the the Earth–Sun Lagrange point L2. From there, JWST can cover the whole sky in segments that move along in RA with the Earth, have an observing efficiency $\approx 70\%$, and send data back to Earth every day.

- (1) How will the JWST be automatically deployed?

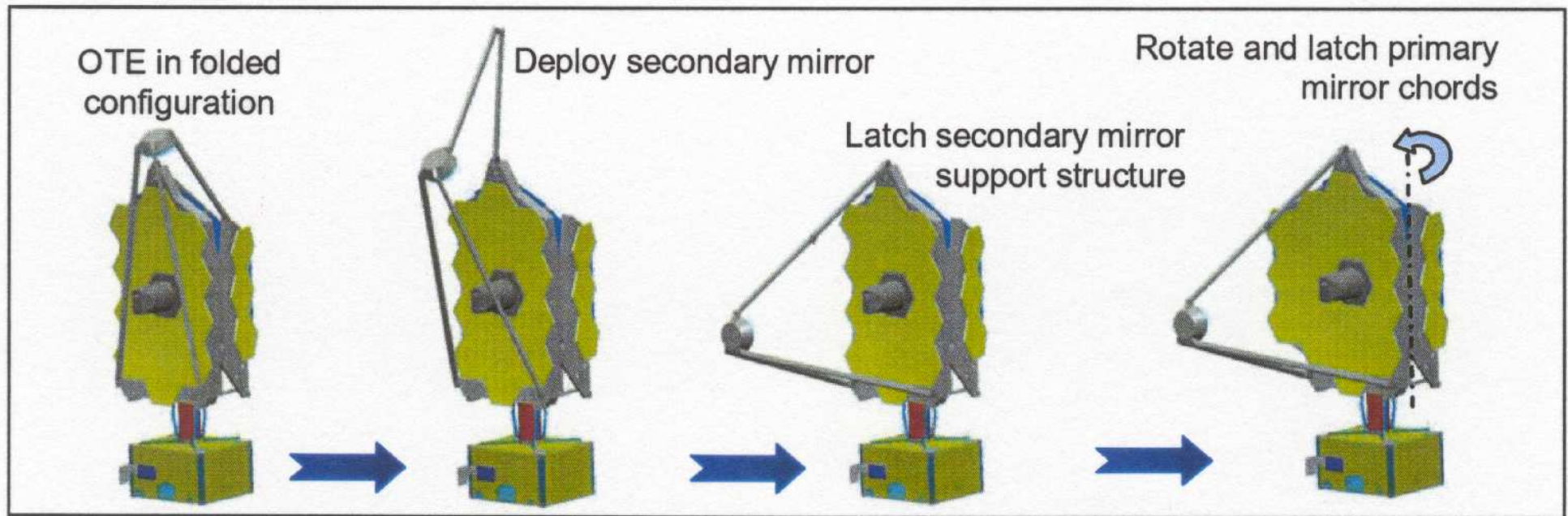
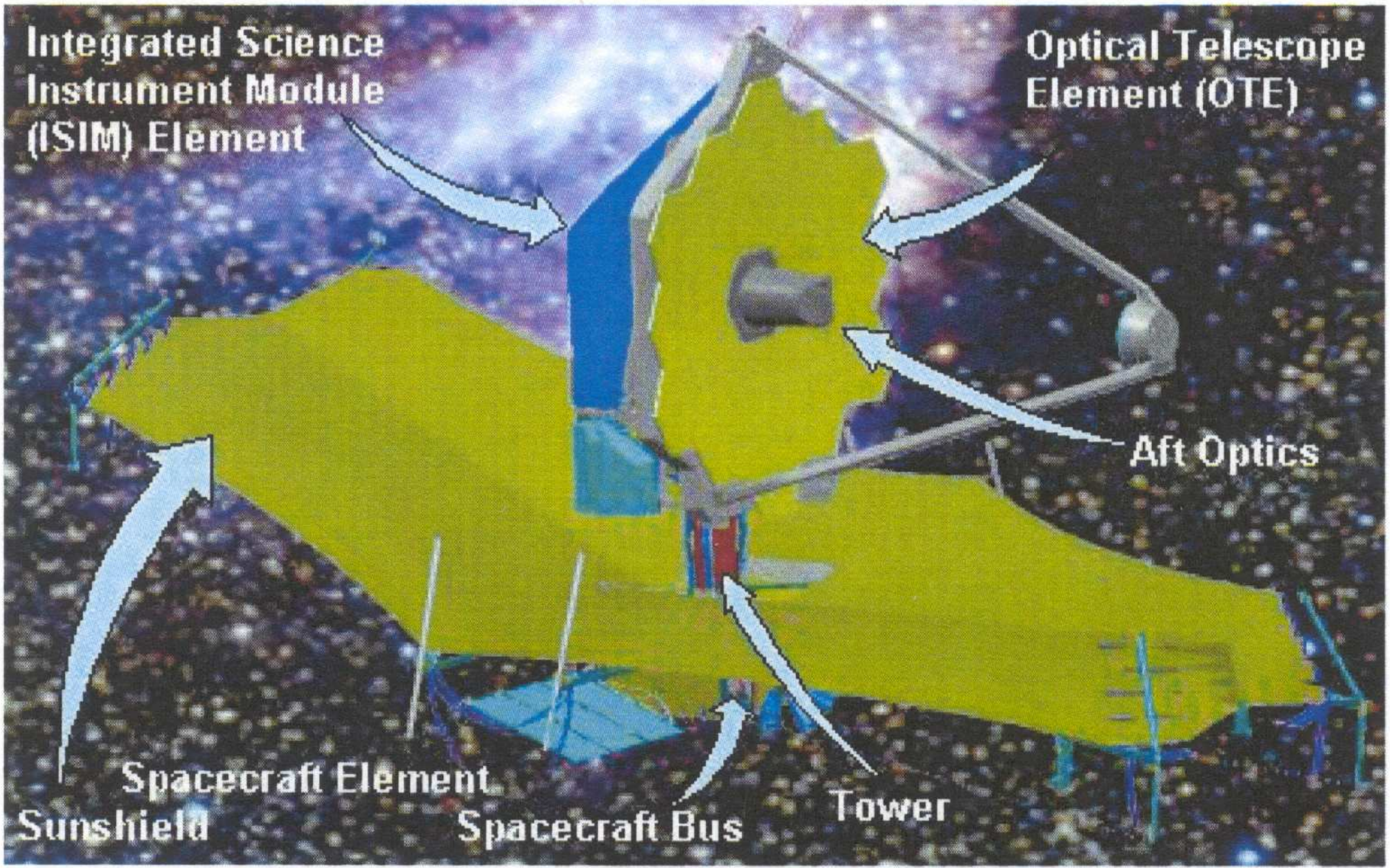


Figure 53. Telescope Deployment Sequence (Deployment steps 4 and 5)

During its several month journey to L2 (shown on a previous page), JWST will be automatically deployed in phases (as shown here), its instruments will be tested, and it will then be inserted into an L2 halo orbit.

From an orbit around the the Earth–Sun Lagrange point L2, JWST can cover the whole sky in segments, have an observing efficiency $\gtrsim 70\%$, and send data back to Earth every day.



JWST mission reviewed in Gardner, J. P., et al.2006, Space Science Reviews, 123, 485–606; astro-ph/0606175)

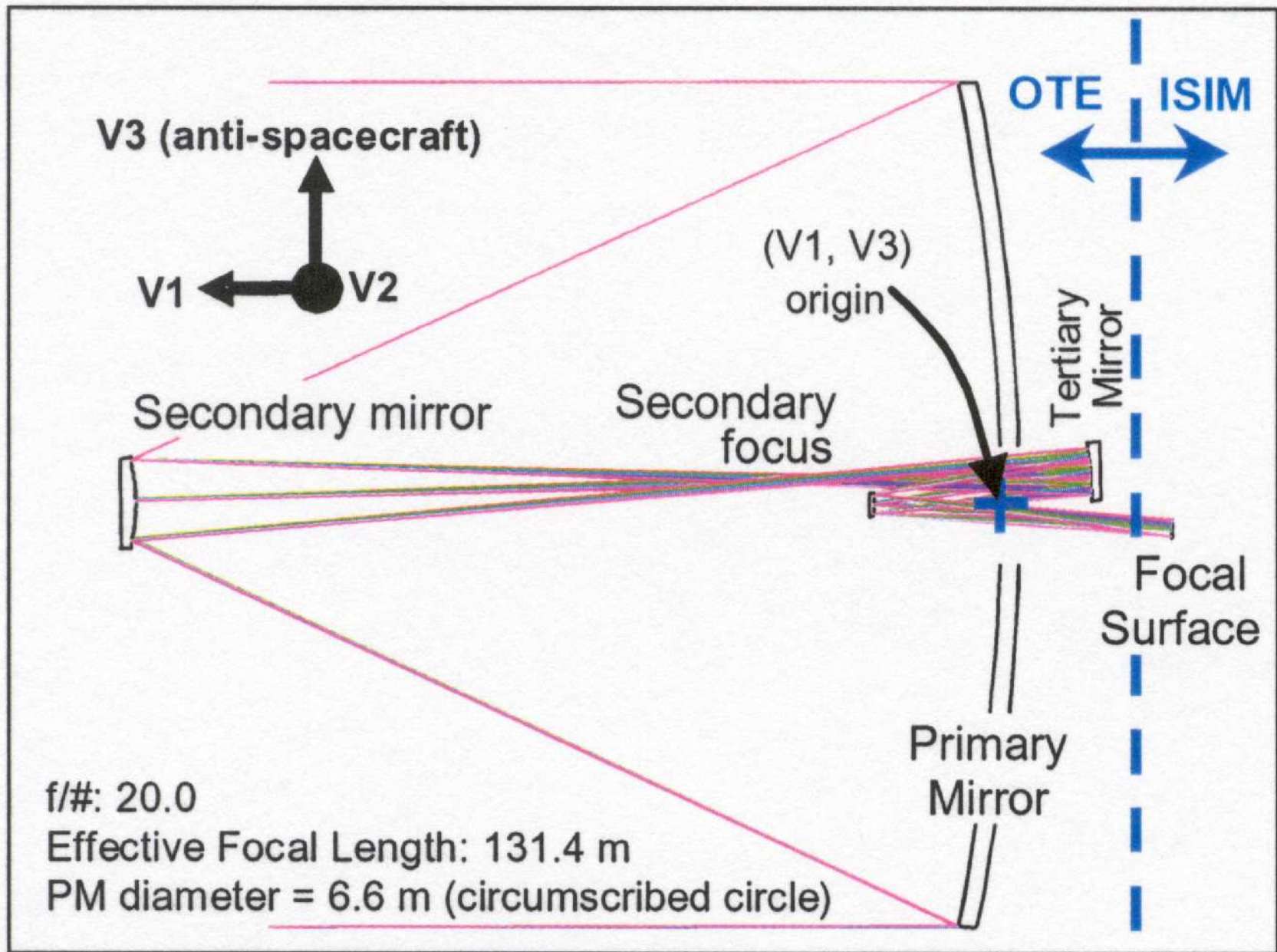
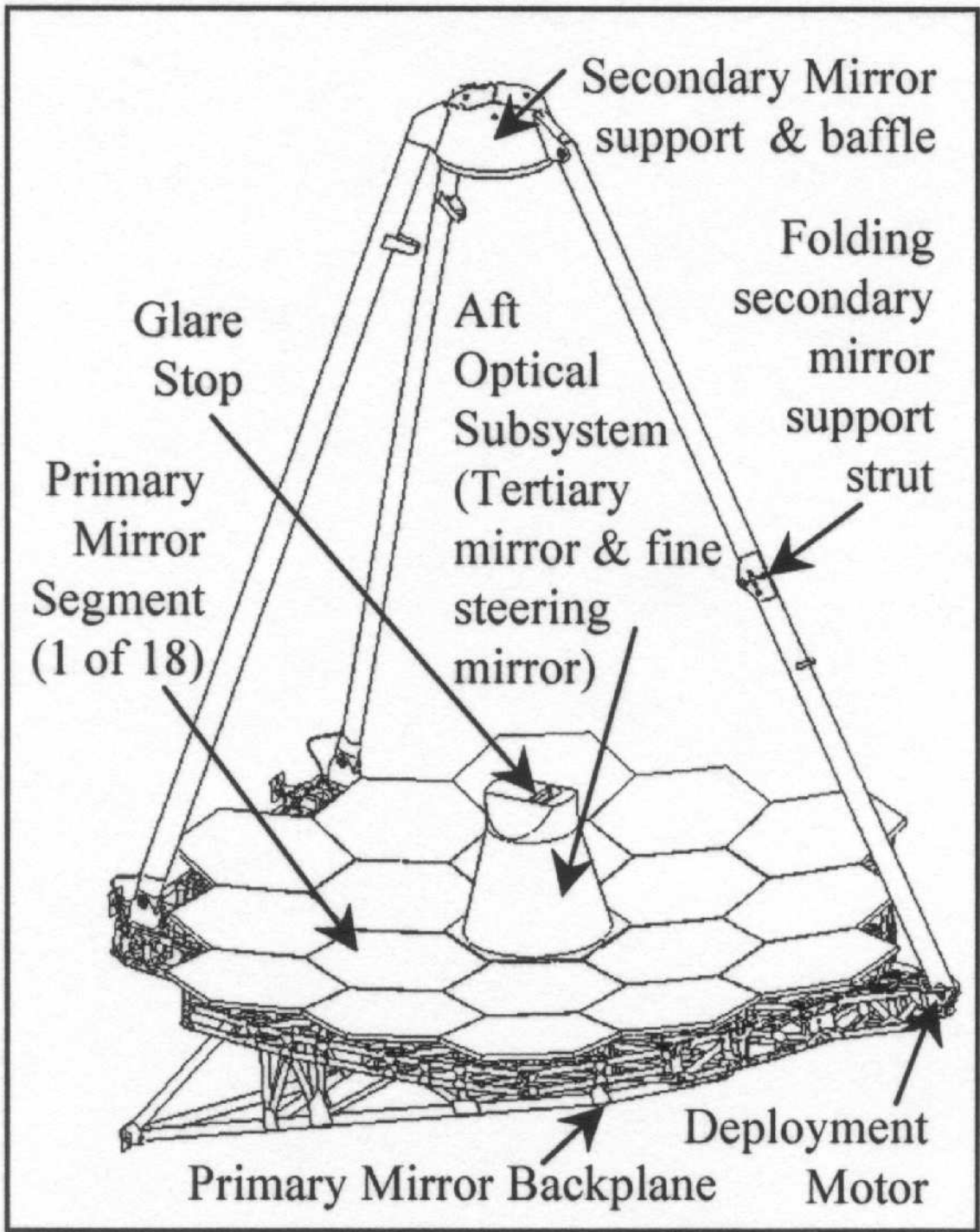


Figure 33. OTE optical layout



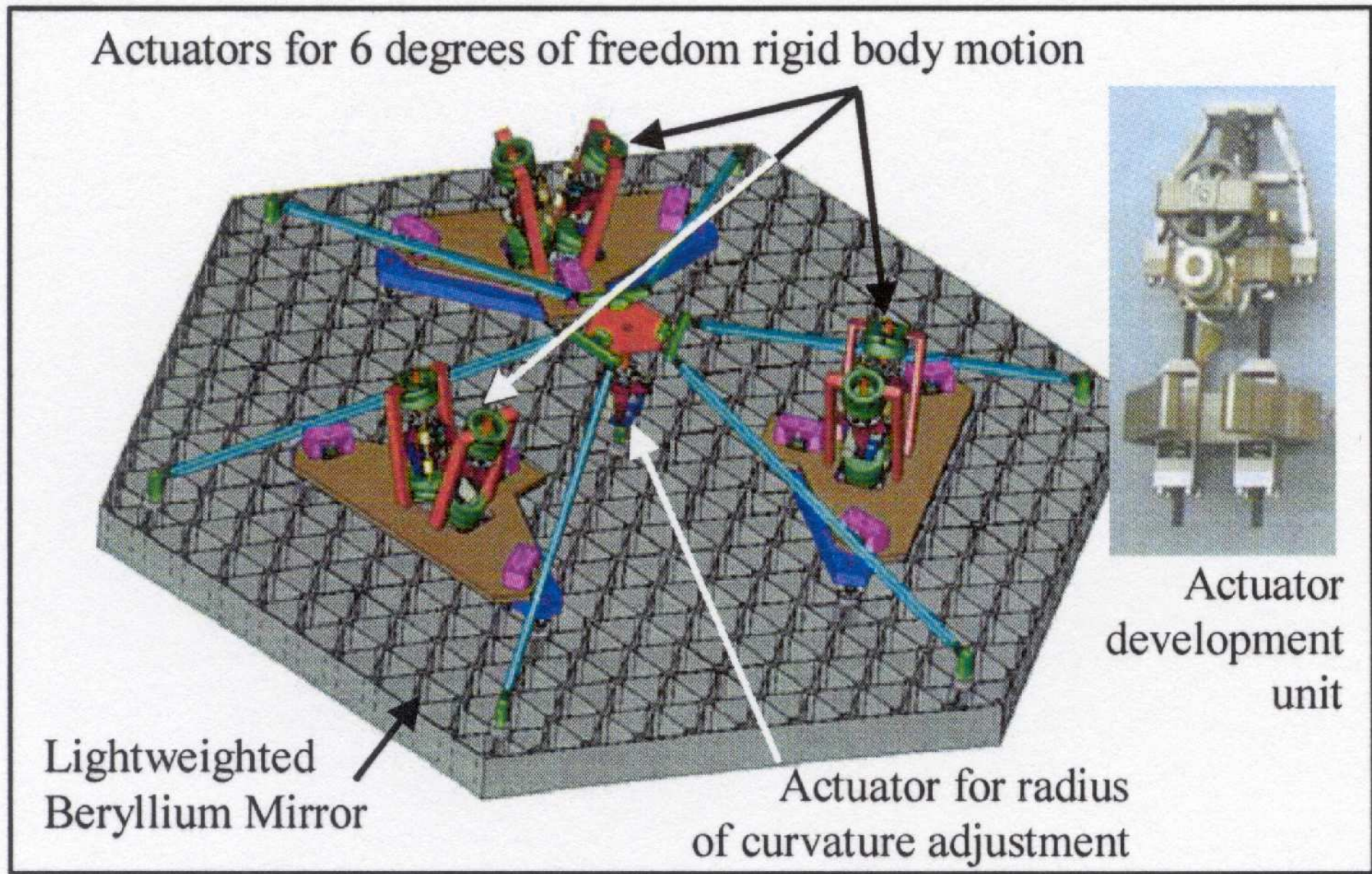
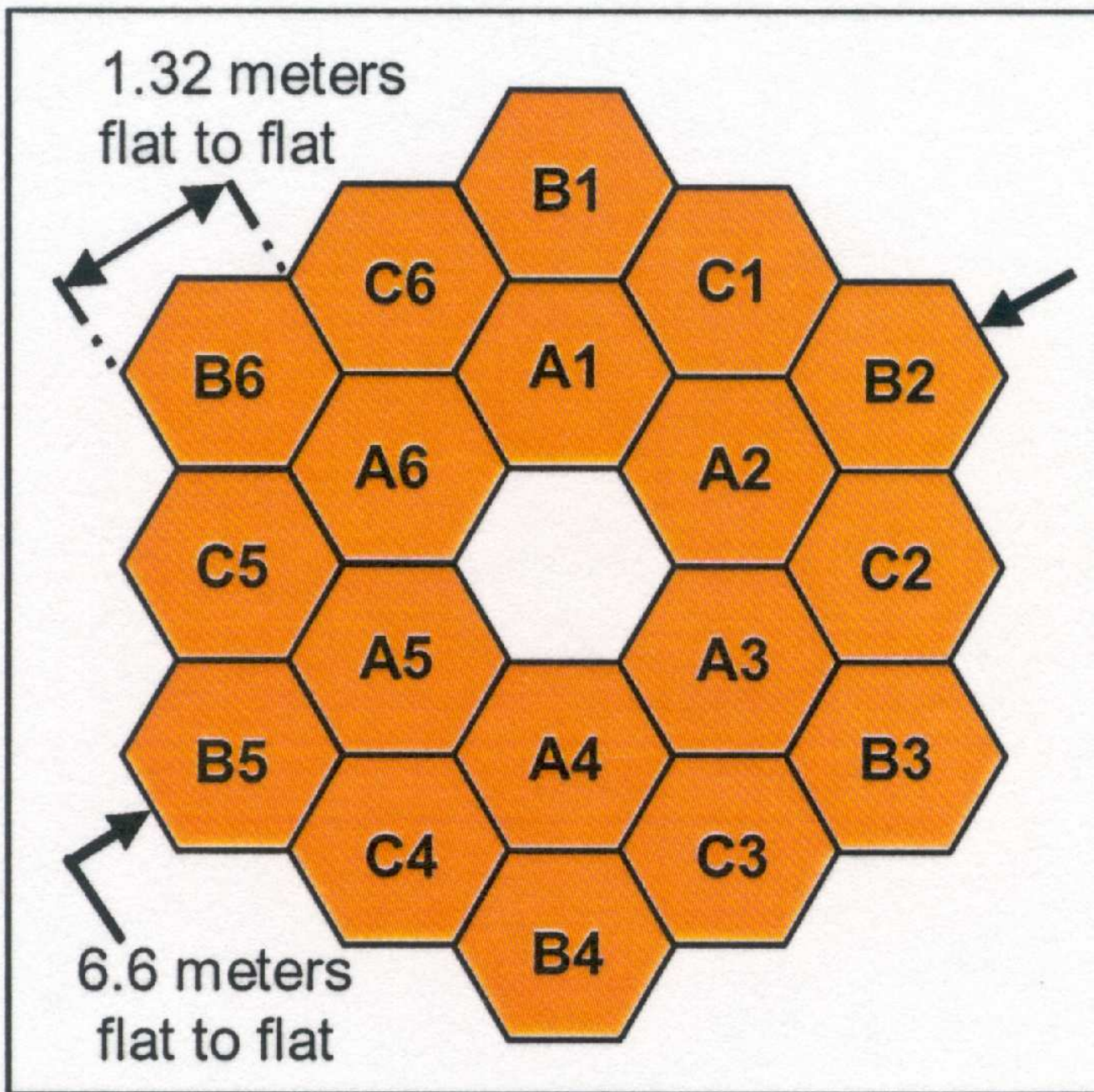


Figure 36. Rear view of a primary mirror segment.

Active mirror segment support through hexapods, like Keck whiffle-trees.

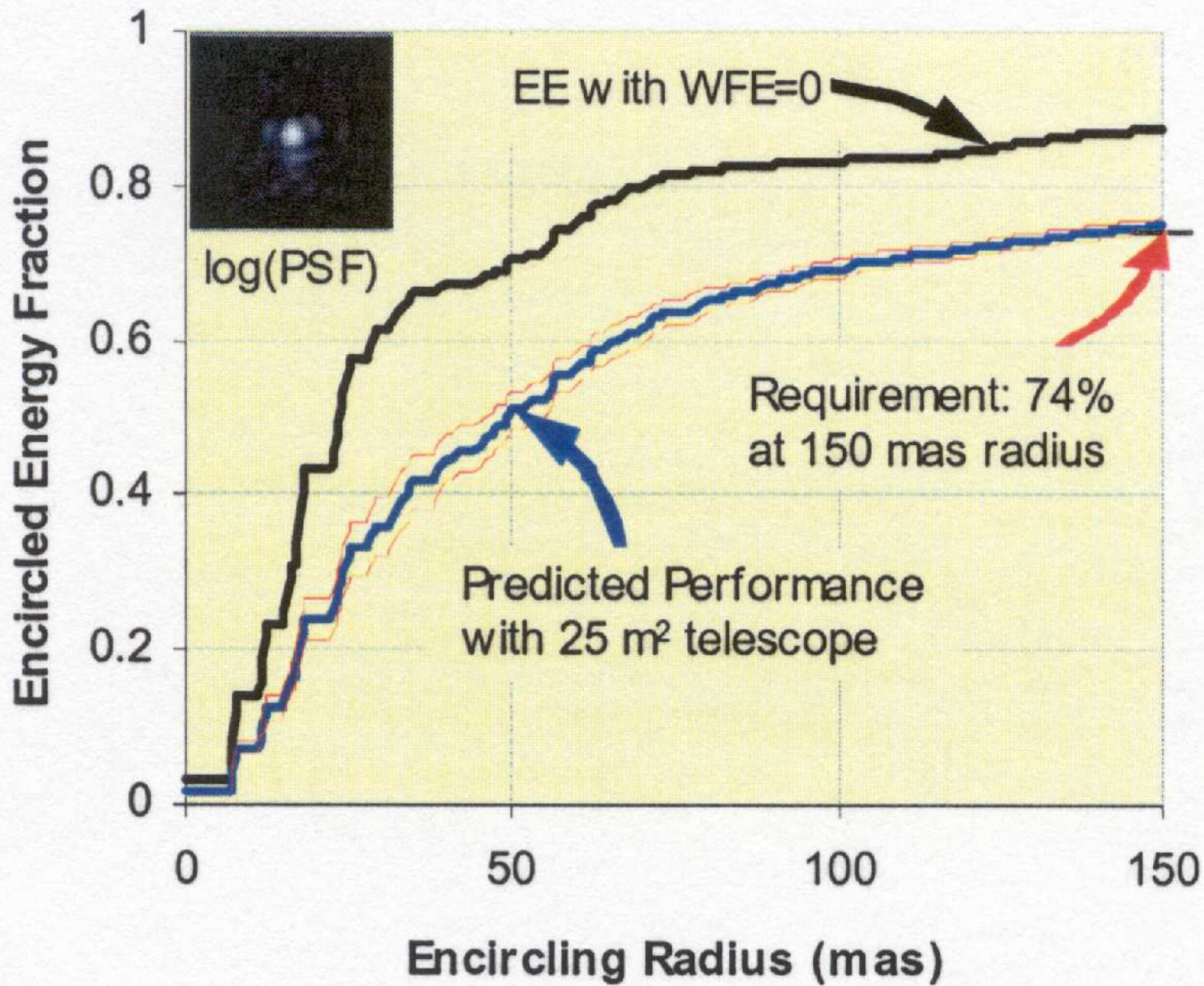


Edge-to-edge diameter is 6.60 m, but effective circular diameter is 5.85 m.
Cannot cleanly descope aperture without doing major harm to PSF.

<i>First light NIRC<i>am</i></i>		Initial Capture		Final Condition	
	1. Segment Image Capture		18 individual 1.6-m diameter aberrated sub-telescope images PM segments: < 1 mm, < 2 arcmin tilt SM: < 3 mm, < 5 arcmin tilt	PM segments: < 100 μm, < 2 arcsec tilt SM: < 3 mm, < 5 arcmin tilt	
2. Coarse Alignment Secondary mirror aligned Primary RoC adjusted		After Step 2 	Primary Mirror segments: < 1 mm, < 10 arcsec tilt Secondary Mirror : < 3 mm, < 5 arcmin tilt	WFE < 200 mm (rms)	
3. Coarse Phasing - Fine Guiding (PMSA piston)		After Step 3 	WFE: < 250 μm rms	WFE < 1 μm (rms)	
4. Fine Phasing		After Step 4 	WFE: < 5 μm (rms)	WFE < 110 nm (rms)	
5. Image-Based Wavefront Monitoring		After Step 5 	WFE: < 150 nm (rms)	WFE < 110 nm (rms)	

Figure 38. WFS&C commissioning and maintenance.

JWST's Wave Front Sensing and Control is similar to that at Keck and HET.
Successful demonstration of H/W and S/W on 6/1 scale model in 2006.



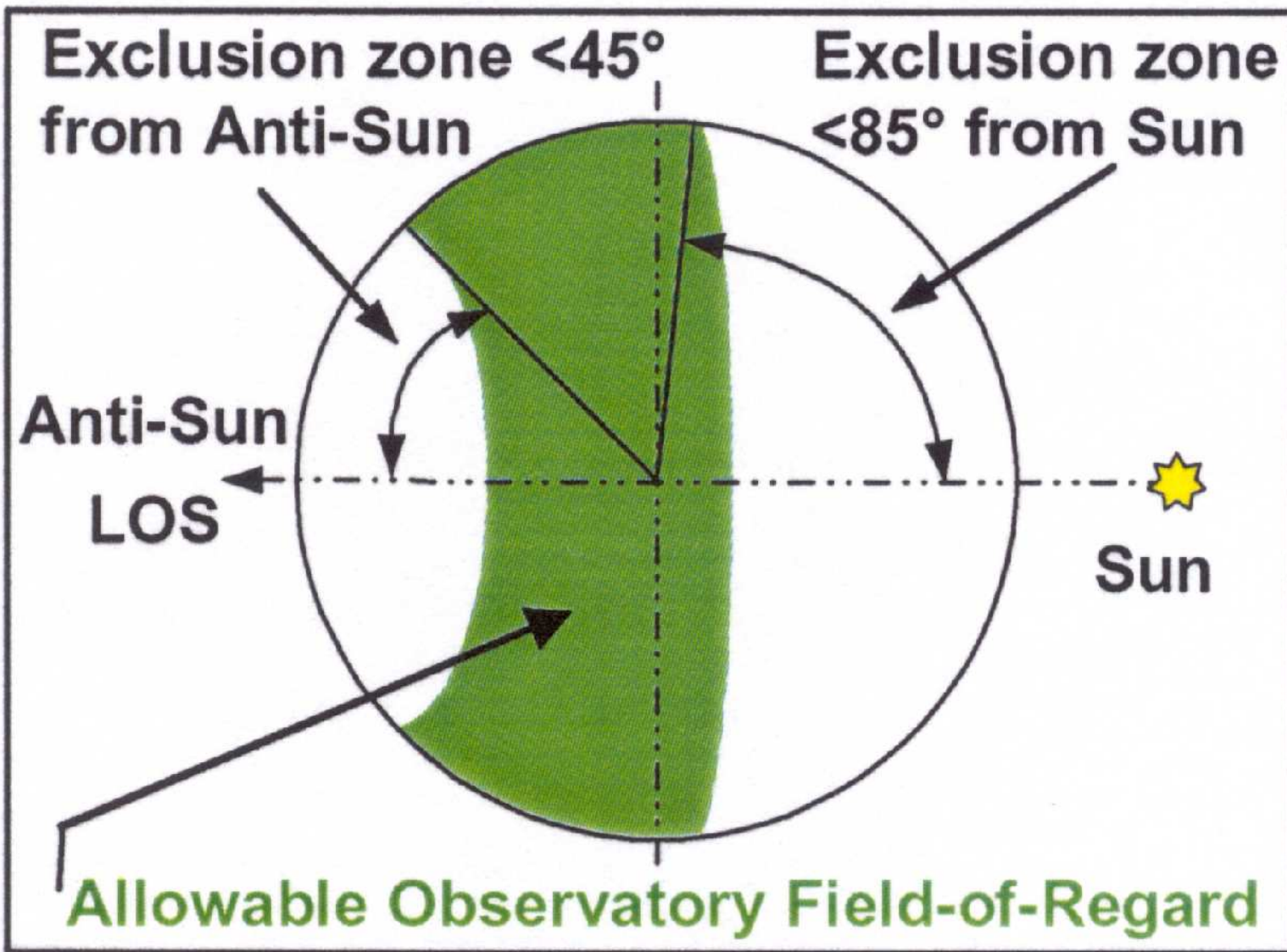


Figure 30. Observatory field of regard (FOR).

JWST can observe segments of sky that move around as it orbits the Sun.

• (2) What instruments will JWST have?

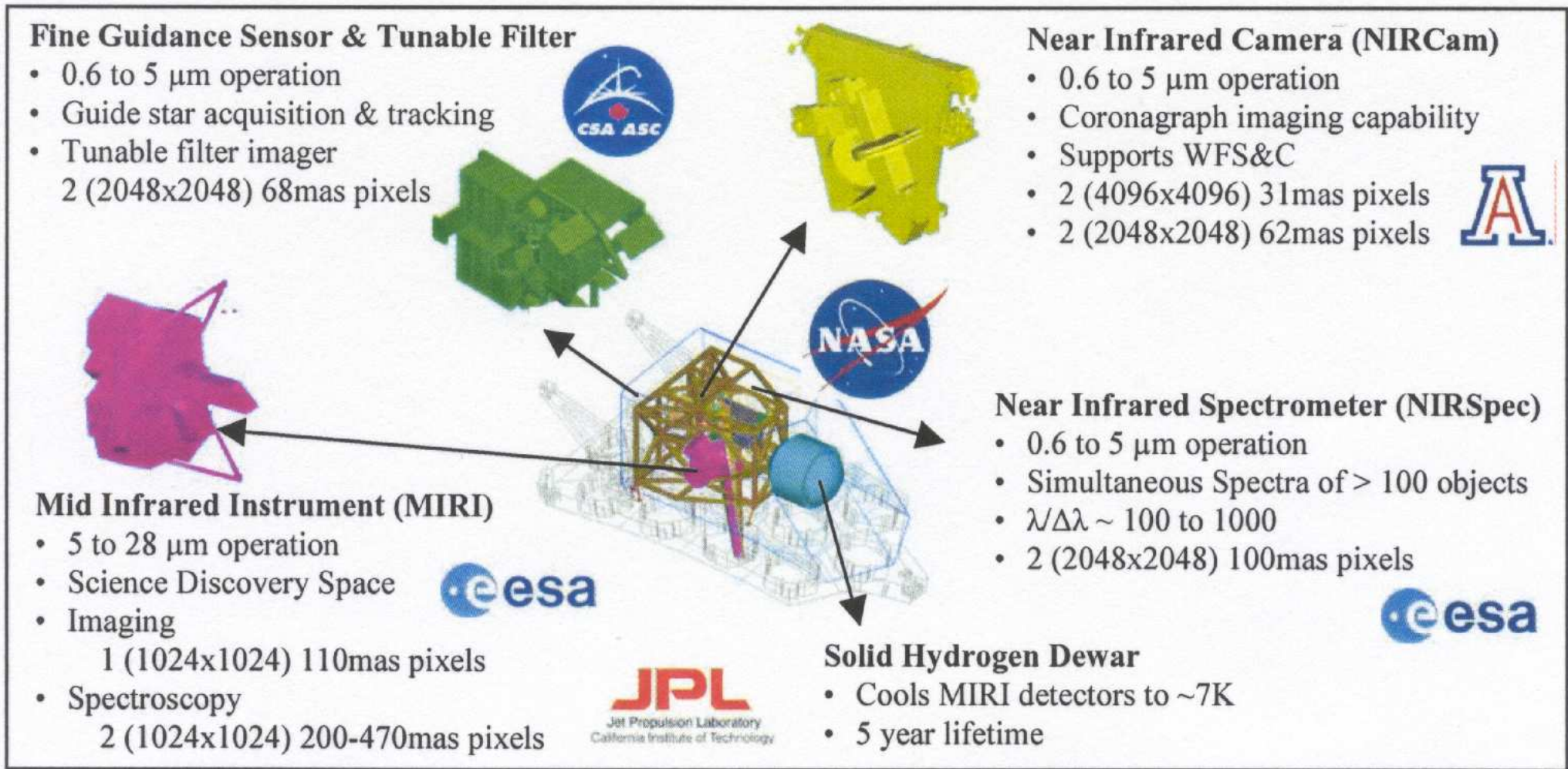


Figure 37. ISIM element and its science instrumentation.

The JWST instrument complement: US (UofA), ESA, and CSA.

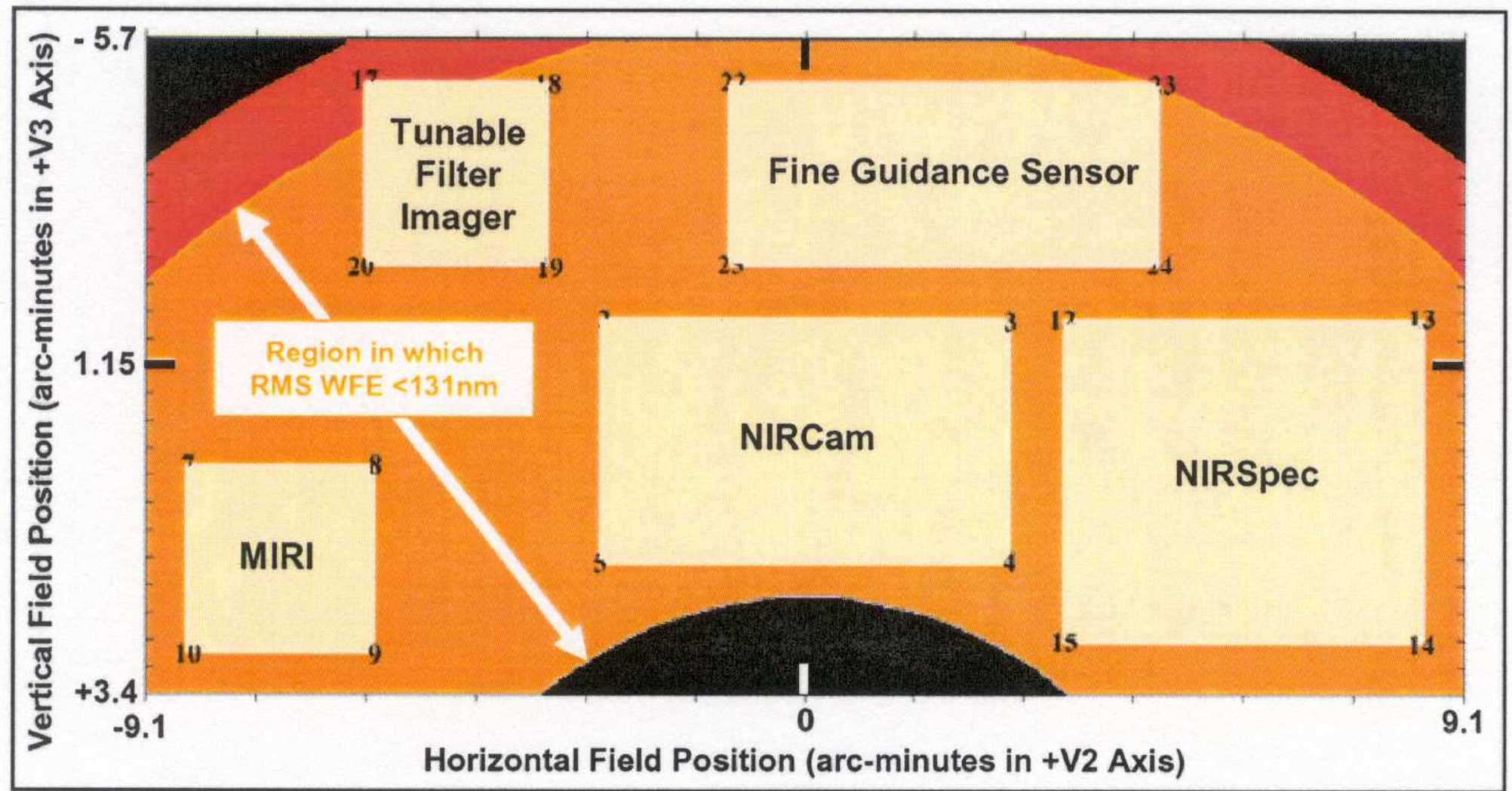
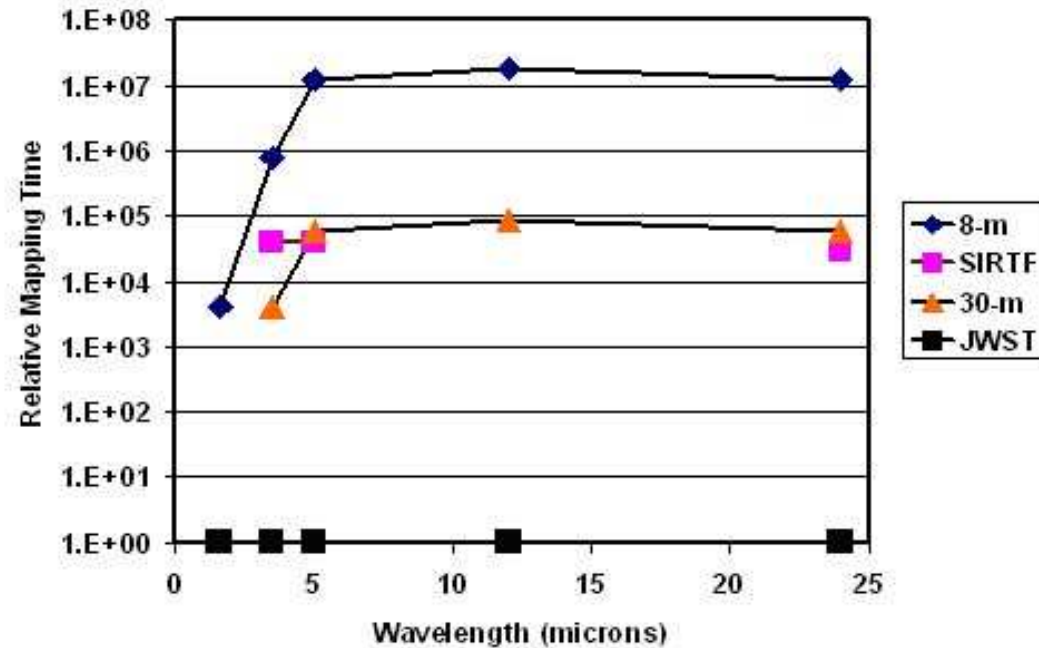
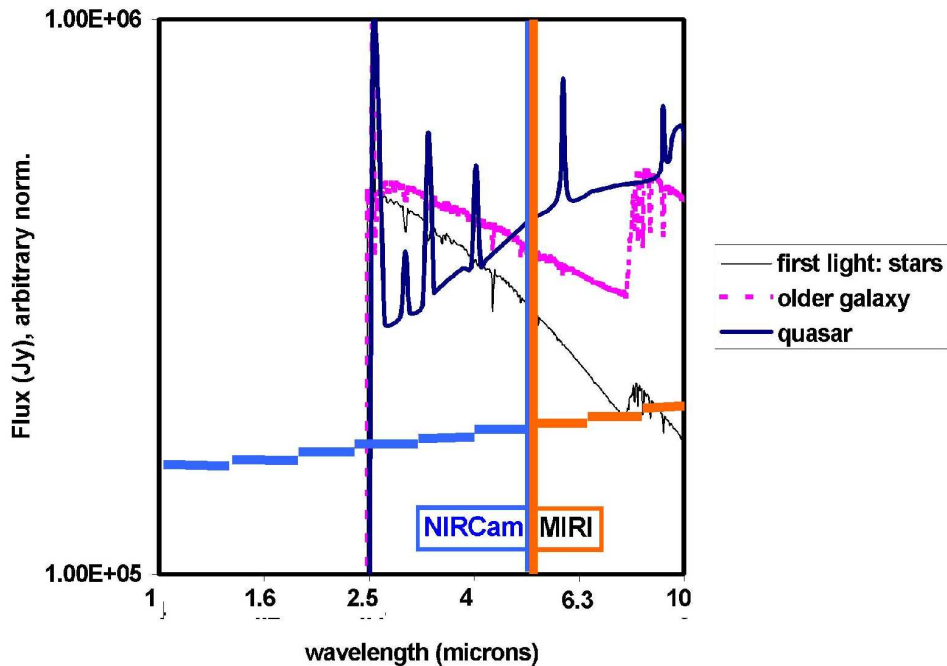


Figure 34. Placement of the ISIM instrument FPAs in the OTE field of view.

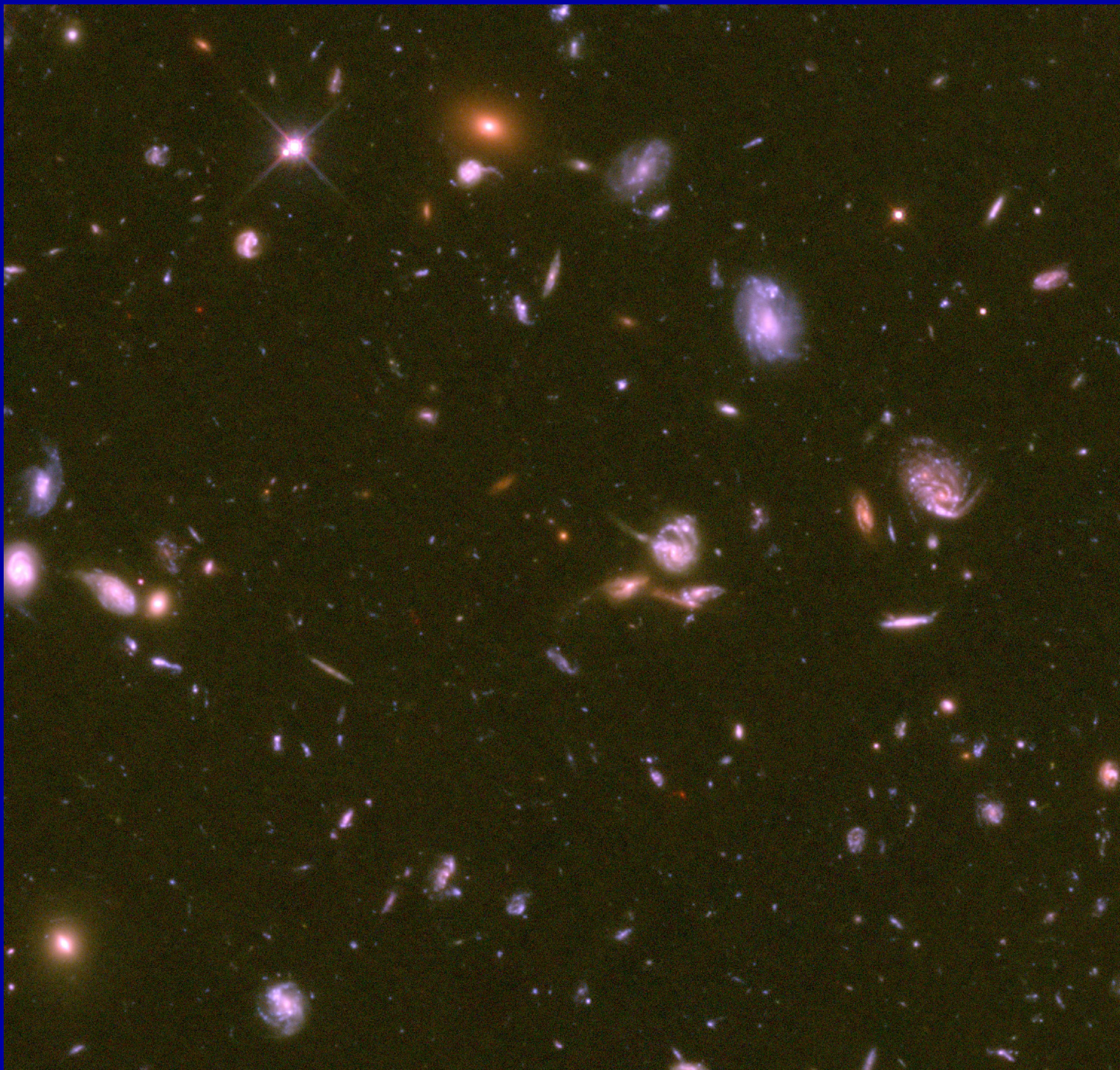
JWST instruments can in principle be used in parallel (not yet implemented).

- (2) What sensitivity will JWST have?



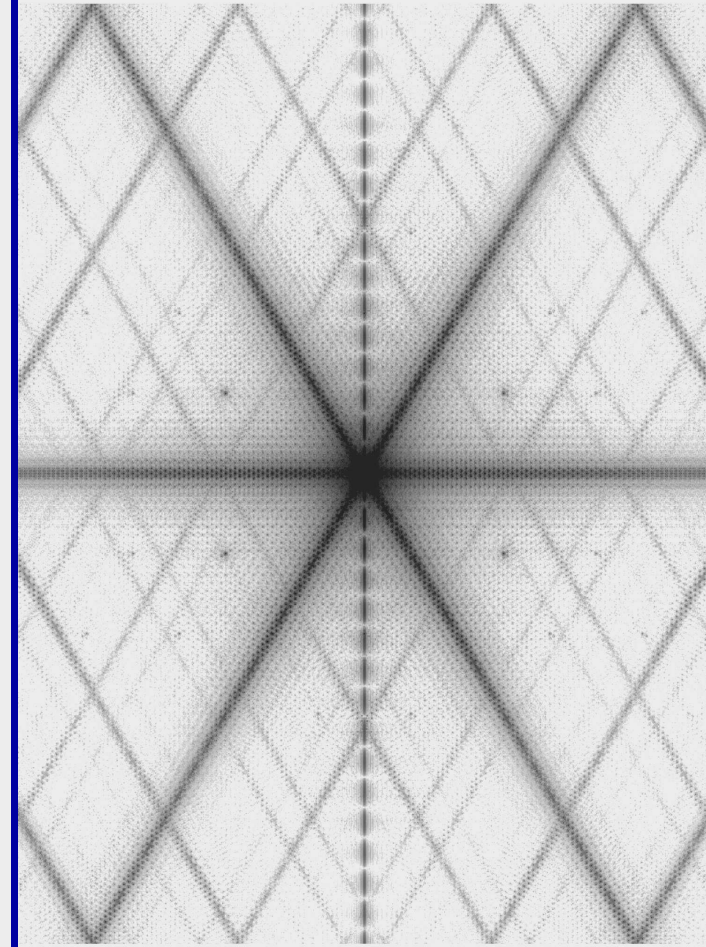
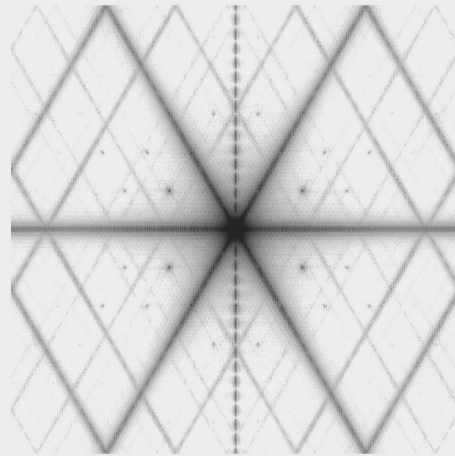
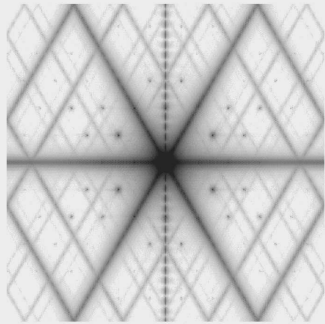
The NIRCam and MIRI sensitivity complement each other straddling $5 \mu\text{m}$ in wavelength, and together allow objects to be found to redshifts $z=15-20$ in $\sim 10^5$ sec (28 hrs) integration times.

The left panel shows the NIRCam and MIRI broadband sensitivity to a Quasar, a “First Light” galaxy dominated by massive stars, and a 50 Myr “old” galaxy, all at $z=20$. The right panel shows the relative survey time versus wavelength that Spitzer, a ground-based IR-optimized 8-m (Gemini) and a 30-m telescope would need to match JWST.



240 hrs HST/ACS in $V_i z'$ in the Hubble UltraDeep Field (HUDF)

6.5m JWST PSF's models (Ball Aerospace and GSFC):

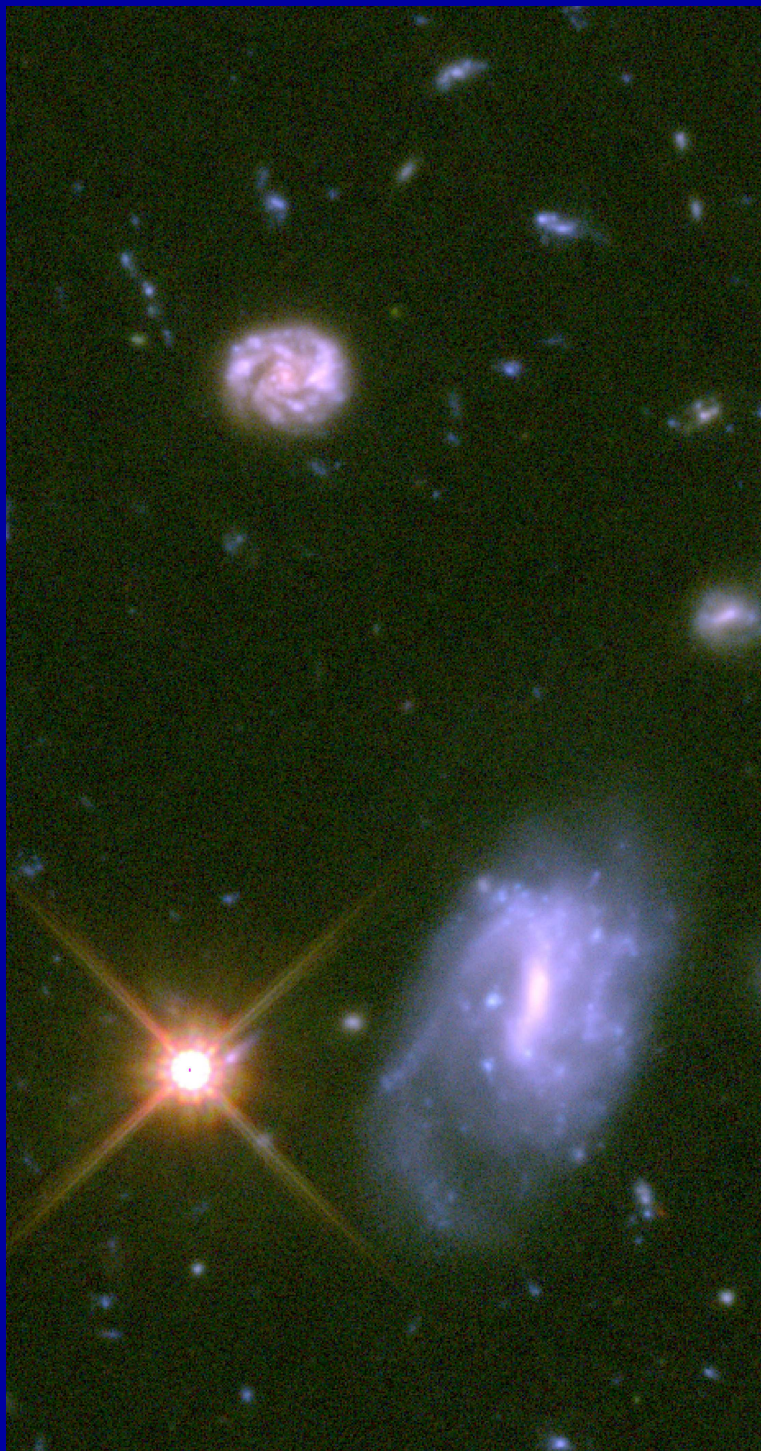


NIRCcam $0.7 \mu\text{m}$ $1.0 \mu\text{m}$ ($<150 \text{ nm WFE}$) $2.0 \mu\text{m}$ (diff. limit)

PSF's are shown at logarithmic stretch — they have $\gtrsim 74\%$ EE at $r \lesssim 0''.15$

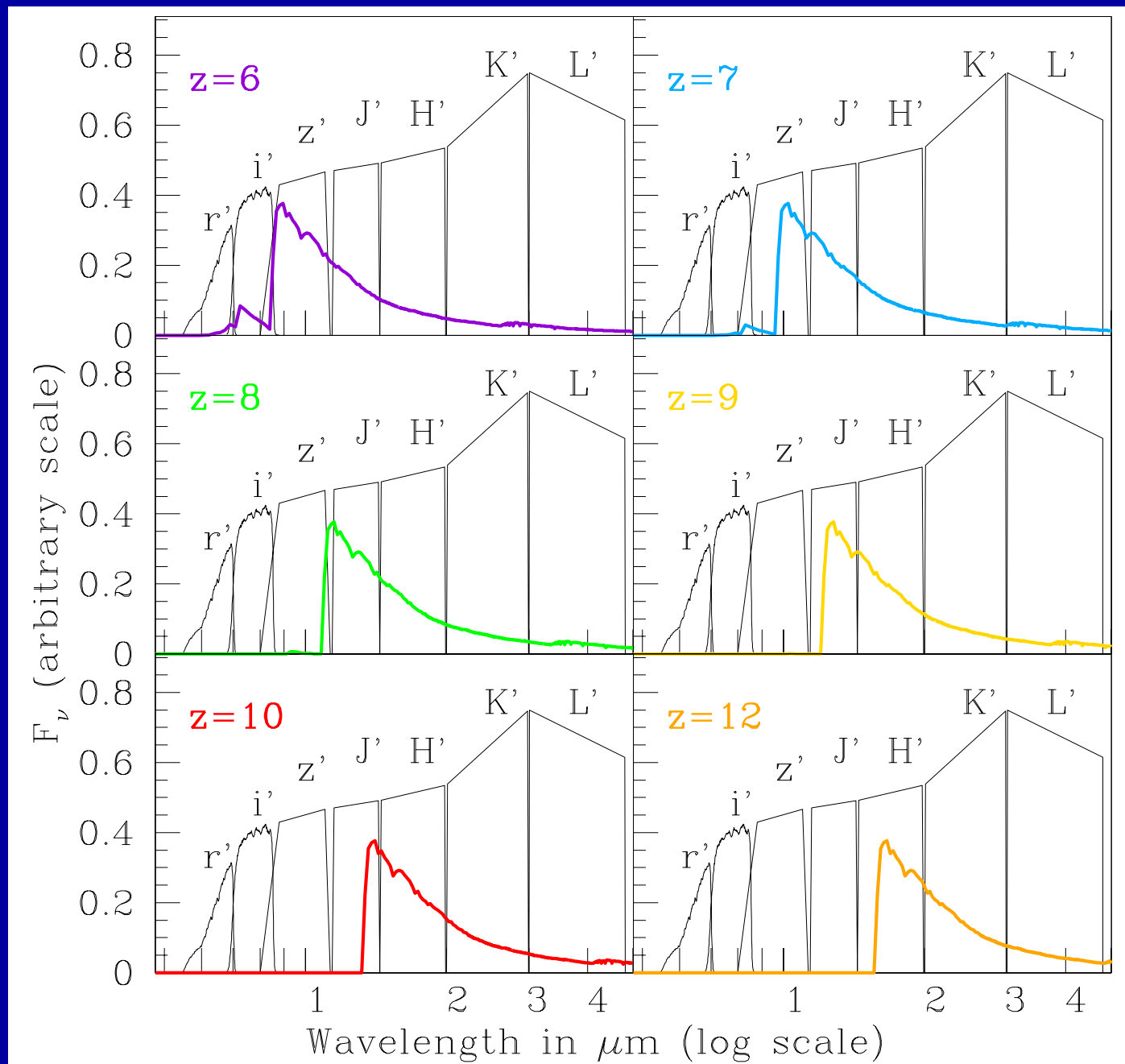


≈20 hrs JWST NIRCам at 0.7, 0.9, 2.0 μm in the HUDF



Truth \equiv 240 hrs HUDF Vi'z'

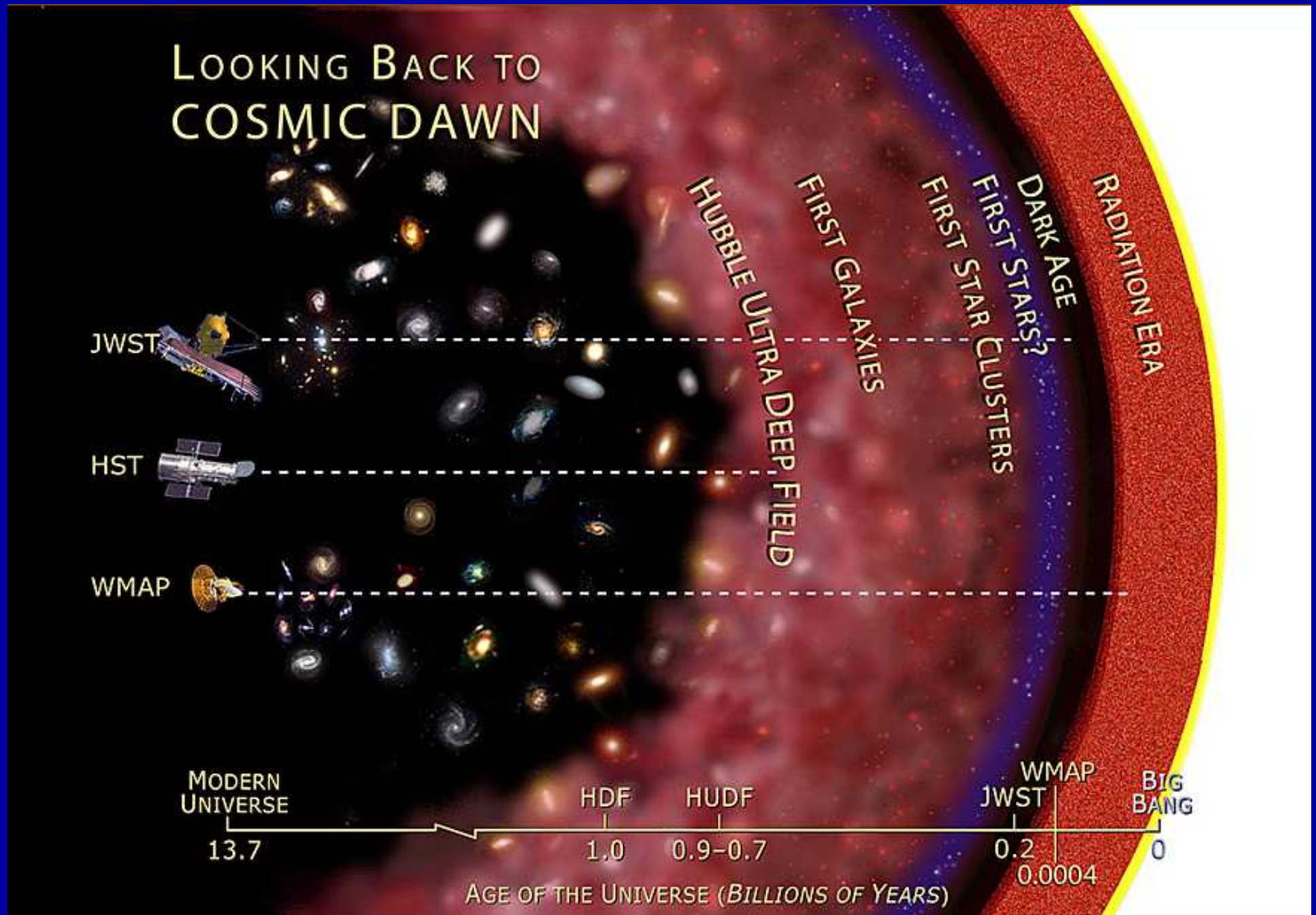
\lesssim 20 hrs JWST 0.7, 0.9, 2.0 μm



● Can't beat redshift: to see First Light, must observe near–mid IR.

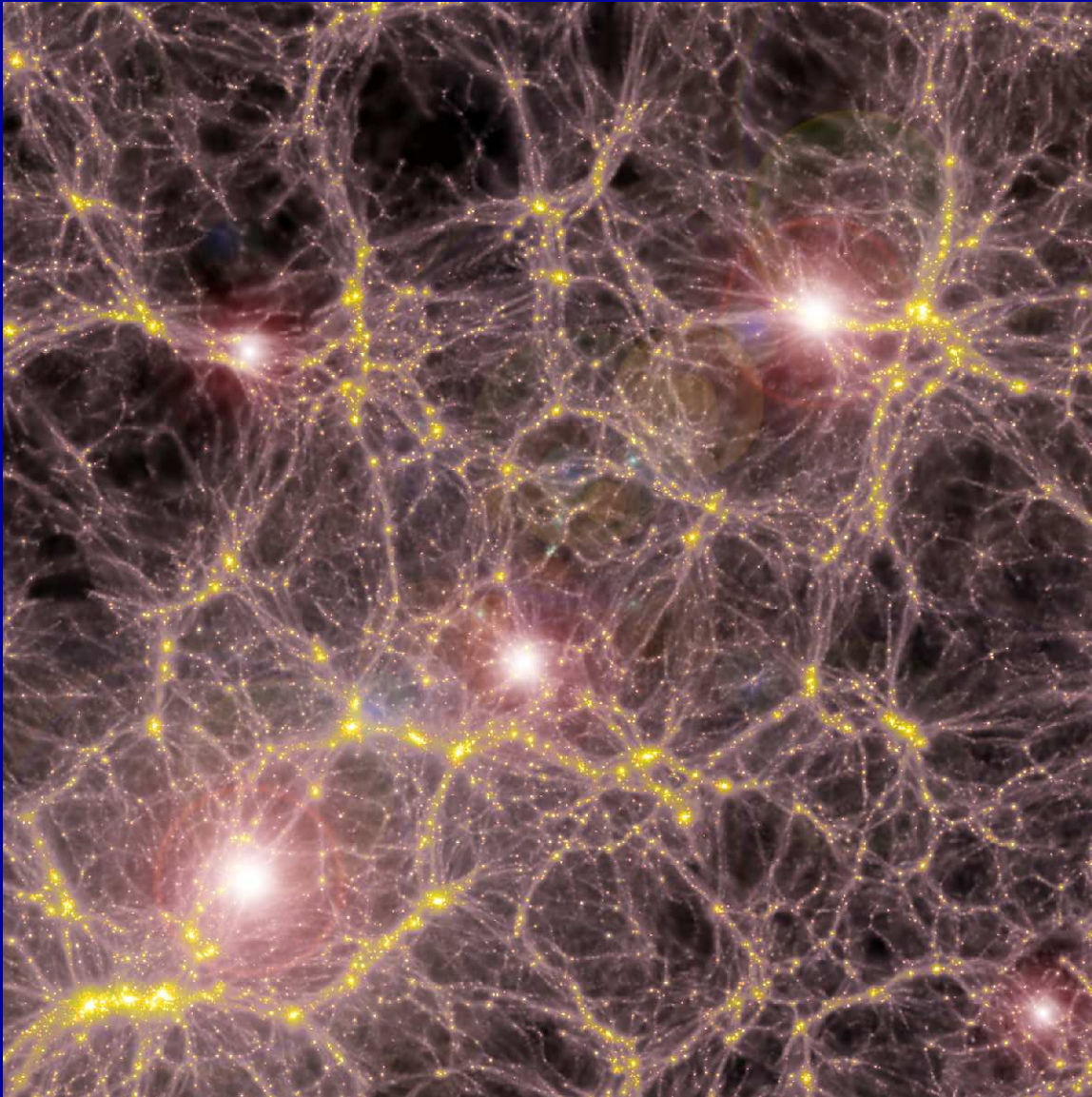
⇒ This is why JWST needs NIRC*am* at 0.8–5 μm and MIRI at 5–28 μm .

(3a) What is First Light, Reionization, and Galaxy Assembly?



NASA telescopes penetrating Cosmic Dawn, First Light, & Recombination

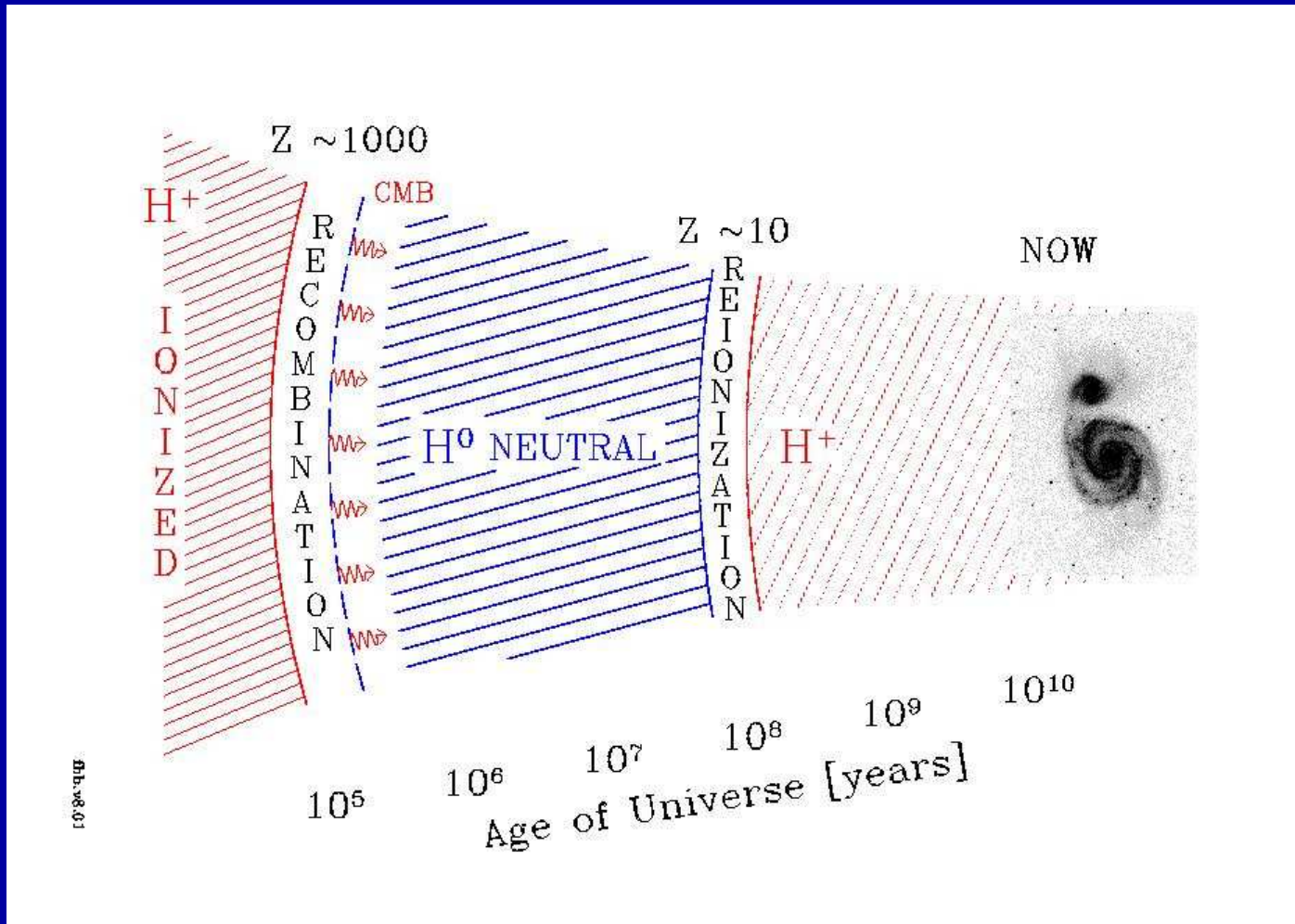
- (3a) What is First Light and Reionization?



- Detailed Hydrodynamical models (V. Bromm) show that formation of Pop III stars reionized universe for the first time at $z \lesssim 10-30$ (First Light).

- A this should be visible to JWST as the first Pop III star clusters, and perhaps their extremely luminous supernovae at $z \simeq 10 \rightarrow 30$.

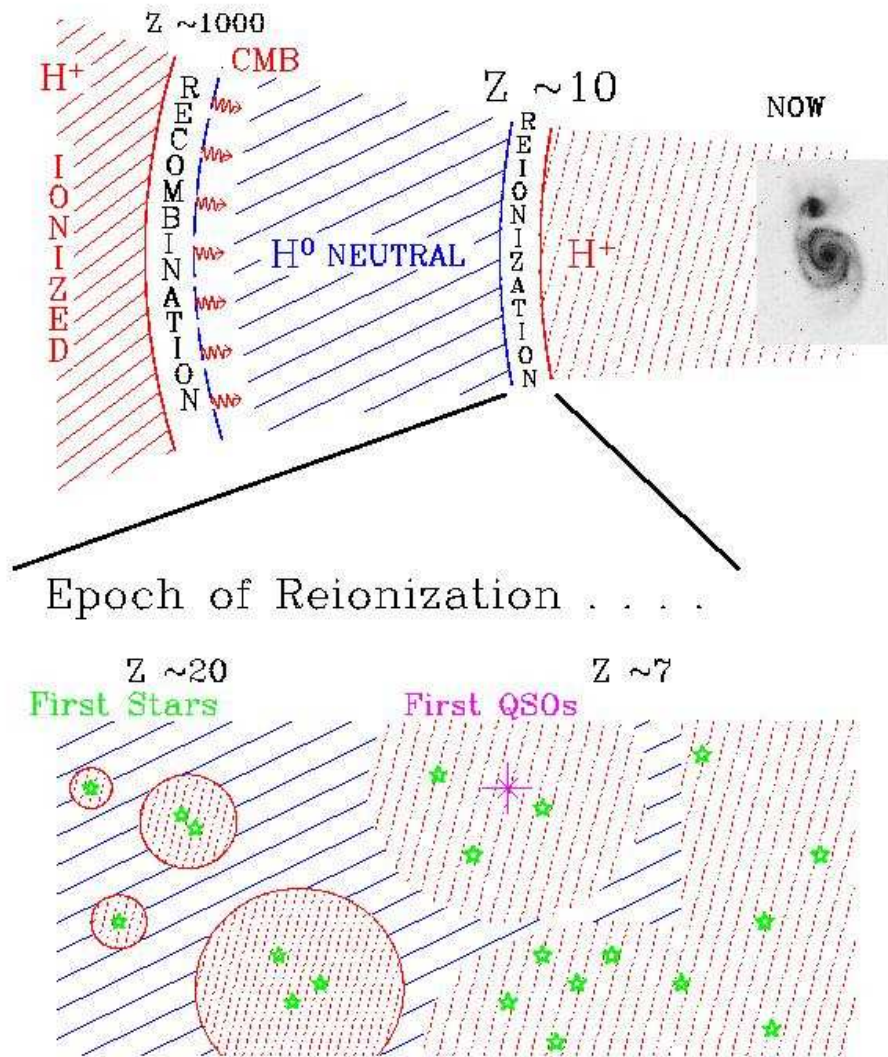
- (3a) What is First Light and Reionization?



WMAP: First light may have happened in 2 epochs (Cen 2003, Spergel 2006):

- (1) Population III stars with $\gtrsim 200 M_{\odot}$ at $z \simeq 11-20$ (First Light).
 - (2) First Population II stars (halo stars) form in dwarf galaxies of mass = 10^6 to $10^9 M_{\odot}$ at $z \simeq 6-9$, which complete reionization by $z \simeq 6$.
- \Rightarrow JWST needs NIRCам at $0.8-5 \mu\text{m}$ and MIRI at $5-28 \mu\text{m}$.

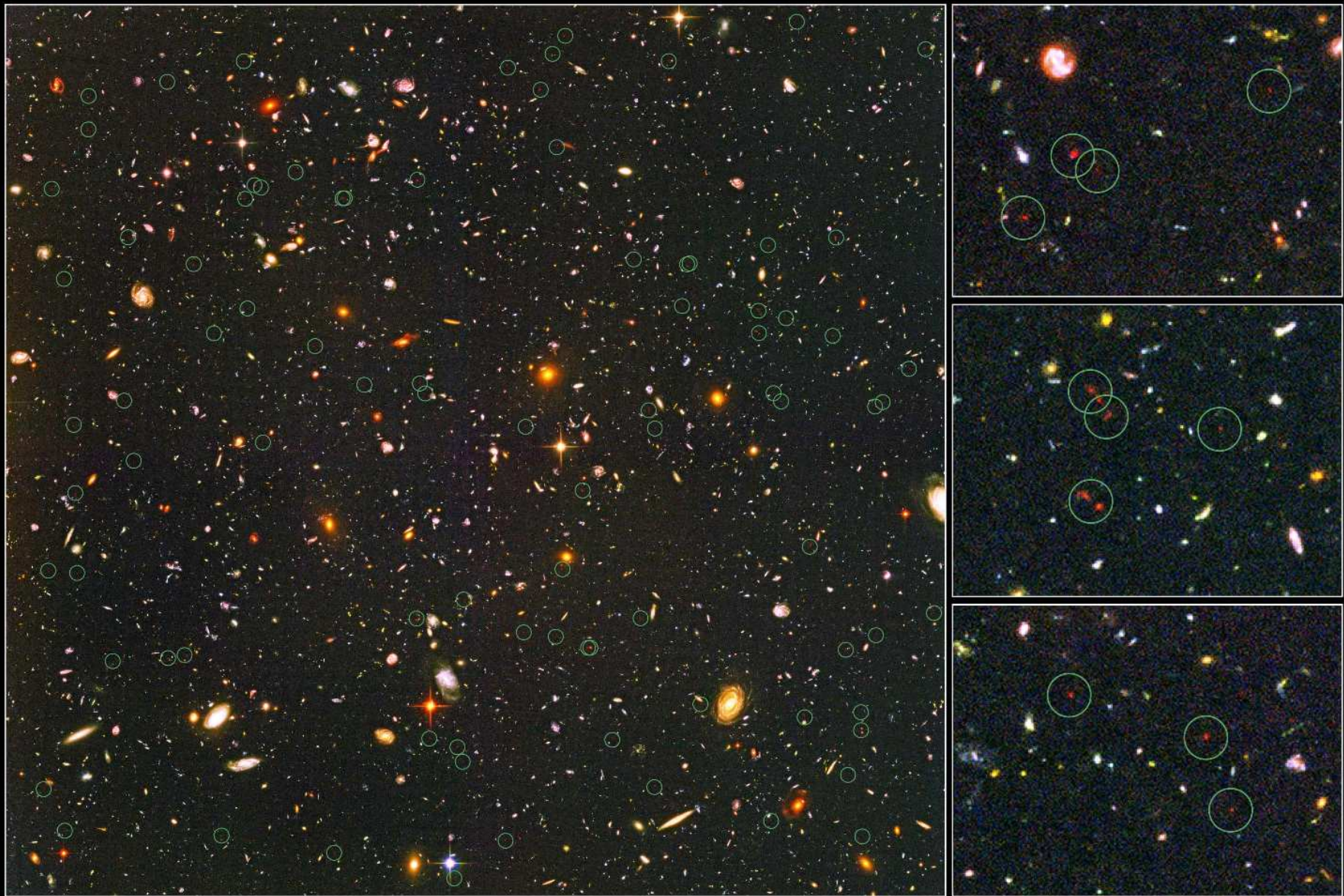
End of 'The Dark Age'



WMAP: First Light may have happened as following:

- (0) Dark Ages since recombination ($z=1089$) until first light objects started shining ($z=11-20$).
- (1) First Light when Population III stars start shining with mass $\gtrsim 200 M_{\odot}$ at $z \simeq 11-20$.
- (2) Pop III supernovae heated IGM, which could not cool and form normal Pop II halo stars until $z \simeq 9-10$.
- (3) This is followed by Pop II stars forming in dwarf galaxies (mass $\simeq 10^7 - 10^9 M_{\odot}$) at $z \simeq 6-9$, ending the epoch of reionization.

(Fig. courtesy of Dr. F. Briggs)



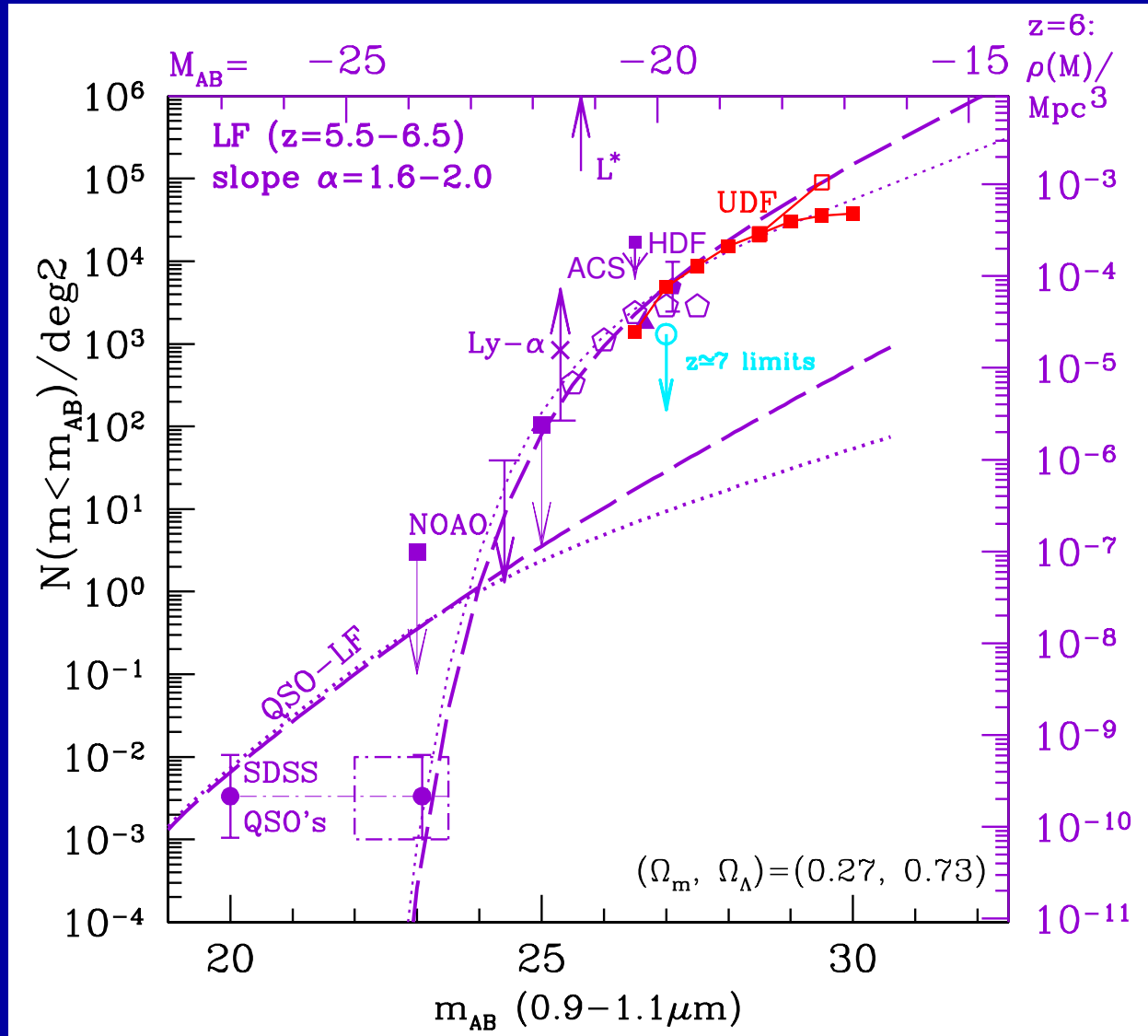
Distant Galaxies in the Hubble Ultra Deep Field
Hubble Space Telescope • Advanced Camera for Surveys

NASA, ESA, R. Windhorst (Arizona State University) and H. Yan (Spitzer Science Center, Caltech)

STScI-PRC04-28

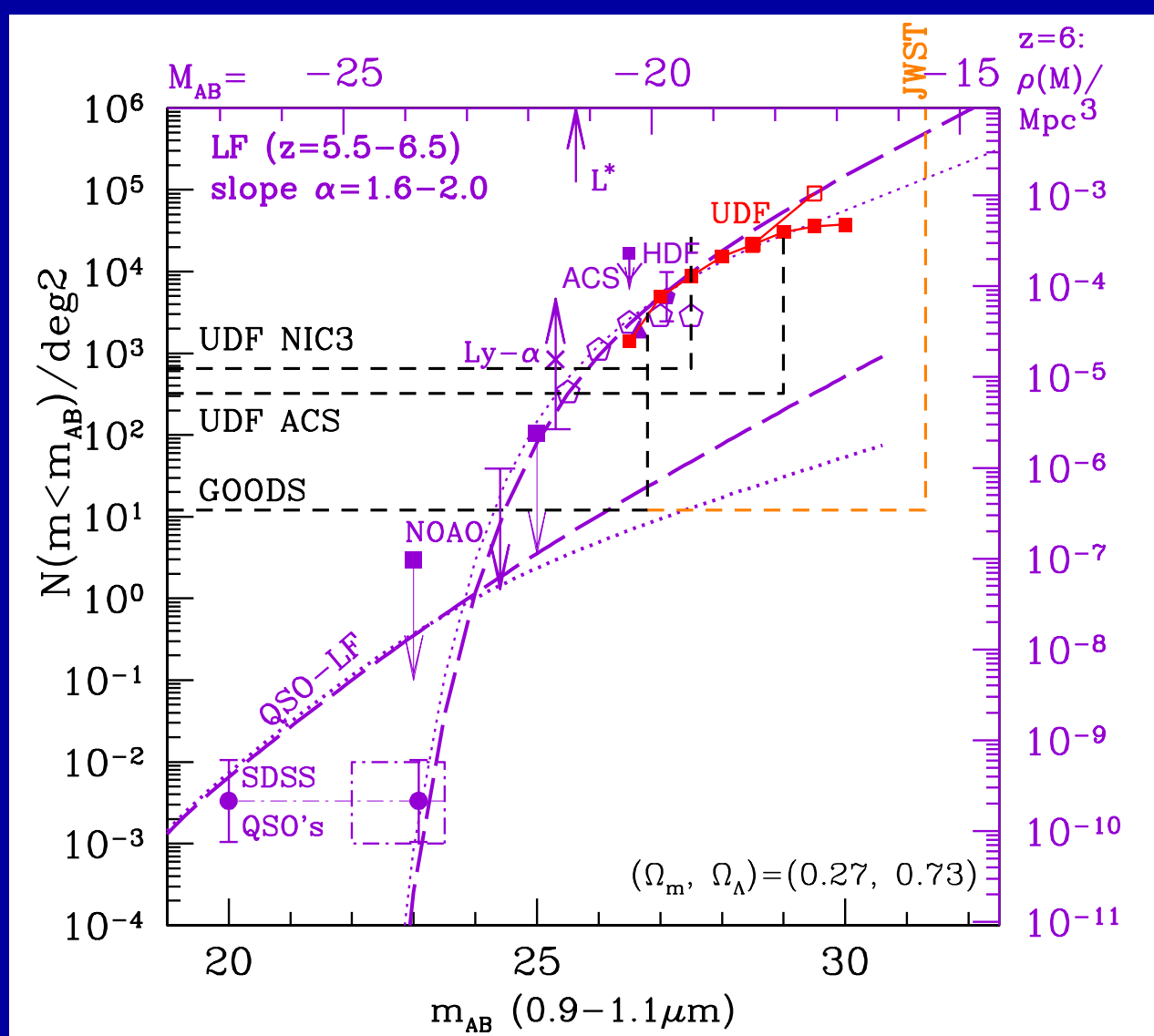
i-band drops in the HUDF: Most confirmed at $z \simeq 6$ (Malhotra et al. 2005)

- (3b) How JWST can measure First Light and Reionization

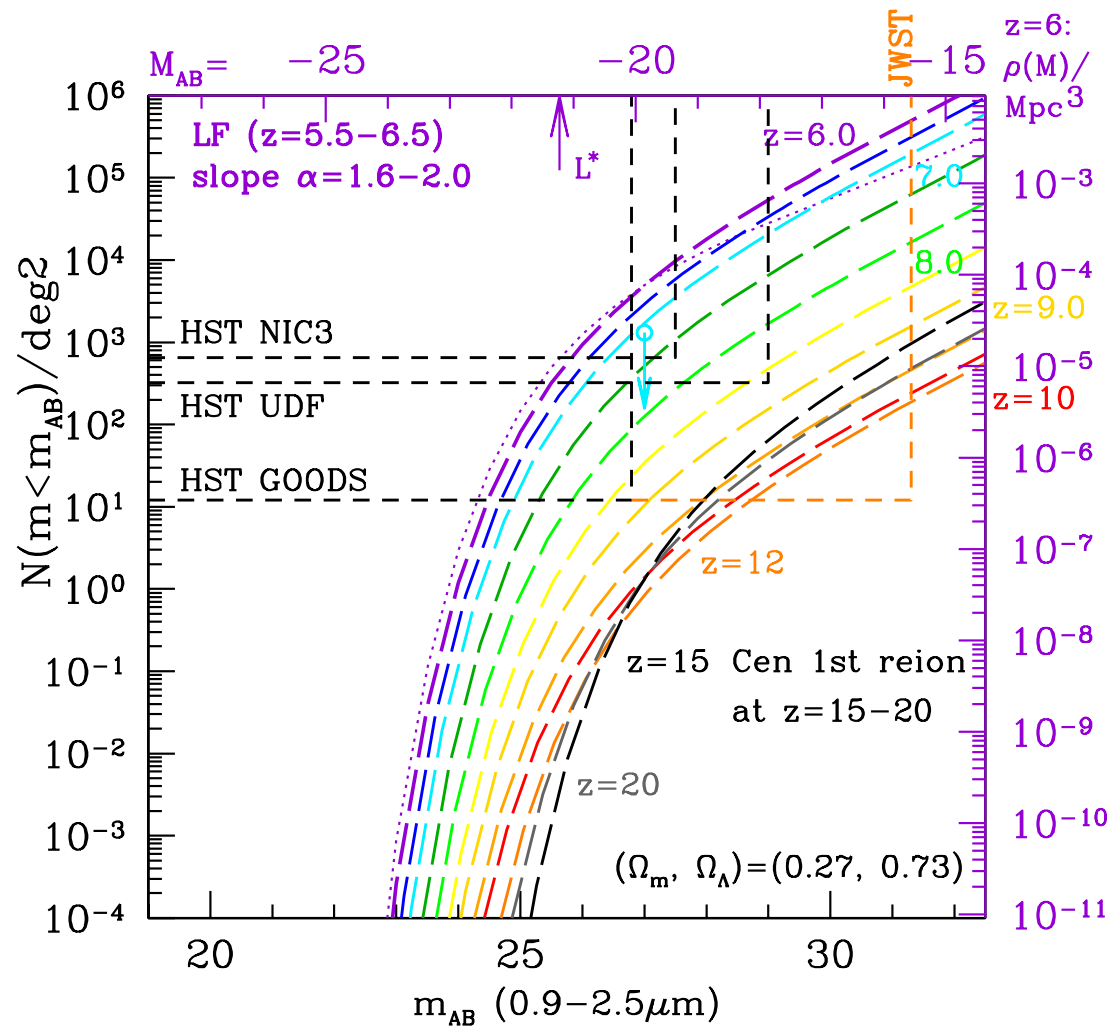


HUDF shows that luminosity function of $z \simeq 6$ objects (Yan & Windhorst 2004a, b) may be very steep: faint-end Schechter slope $|\alpha| \simeq 1.6-2.0$.

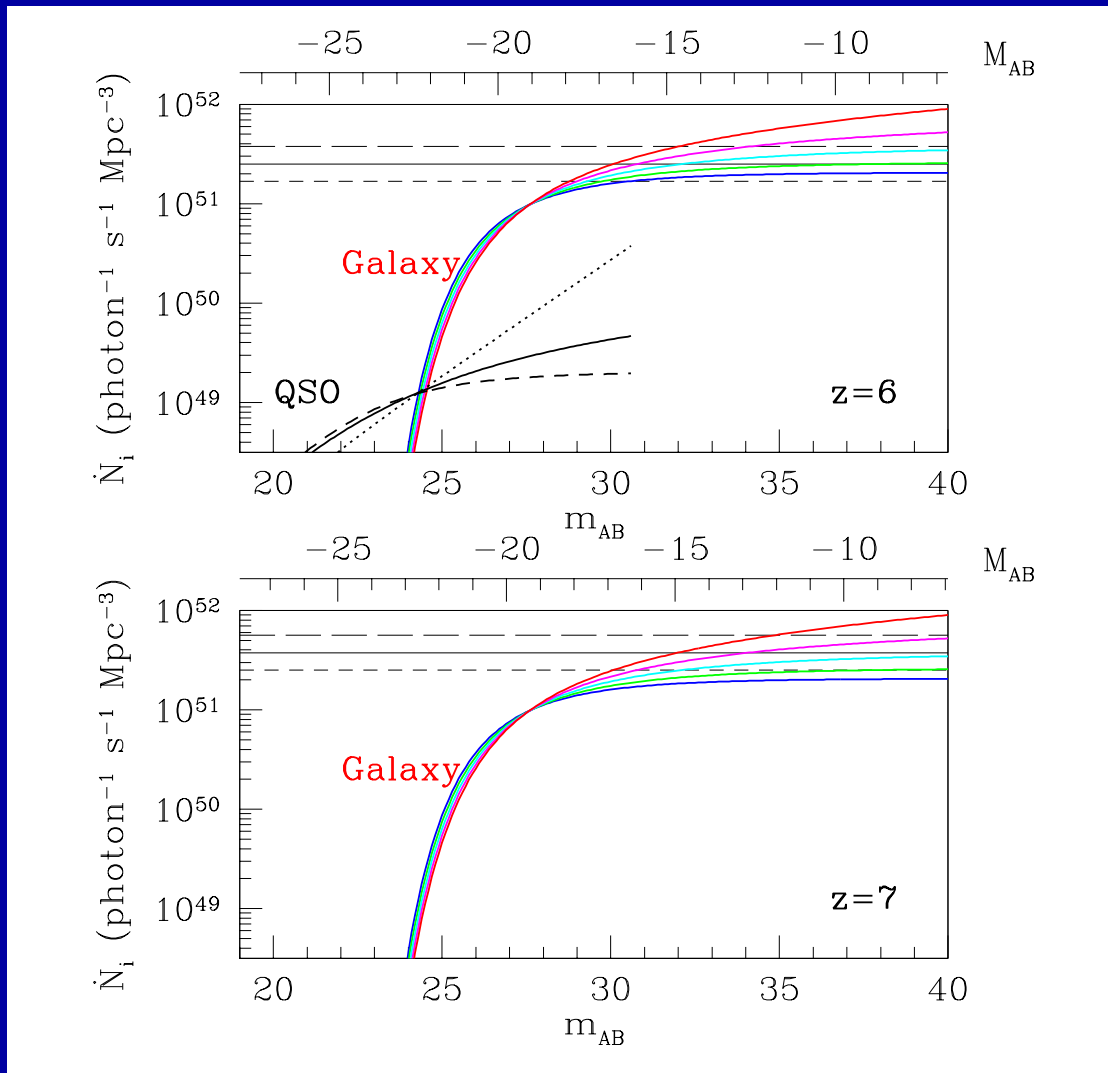
\Rightarrow Dwarf galaxies and not quasars likely completed the reionization epoch at $z \simeq 6$. This is what JWST will observe in detail to $z \gtrsim 20$.



- HST/ACS has made significant progress at $z \simeq 6$, surveying very large areas (GOODS, GEMS, COSMOS), or using very long integrations (HUDF). ACS can detect objects at $z \lesssim 6.5$, but its discovery space $A \cdot \Omega \cdot \Delta \log(\lambda)$ cannot map the entire reionization epoch. NICMOS similarly is limited to $z \lesssim 8-10$. JWST will be able to trace the entire reionization epoch.



- With proper survey strategy (area AND depth), JWST can trace the entire reionization epoch and detect the first star-forming objects.
- Objects at $z \gtrsim 9$ are rare, since volume element is small and JWST samples brighter part of LF. JWST needs the quoted sensitivity/aperture (A), field-of-view ($FOV = \Omega$), and wavelength range ($0.7-28 \mu\text{m}$).

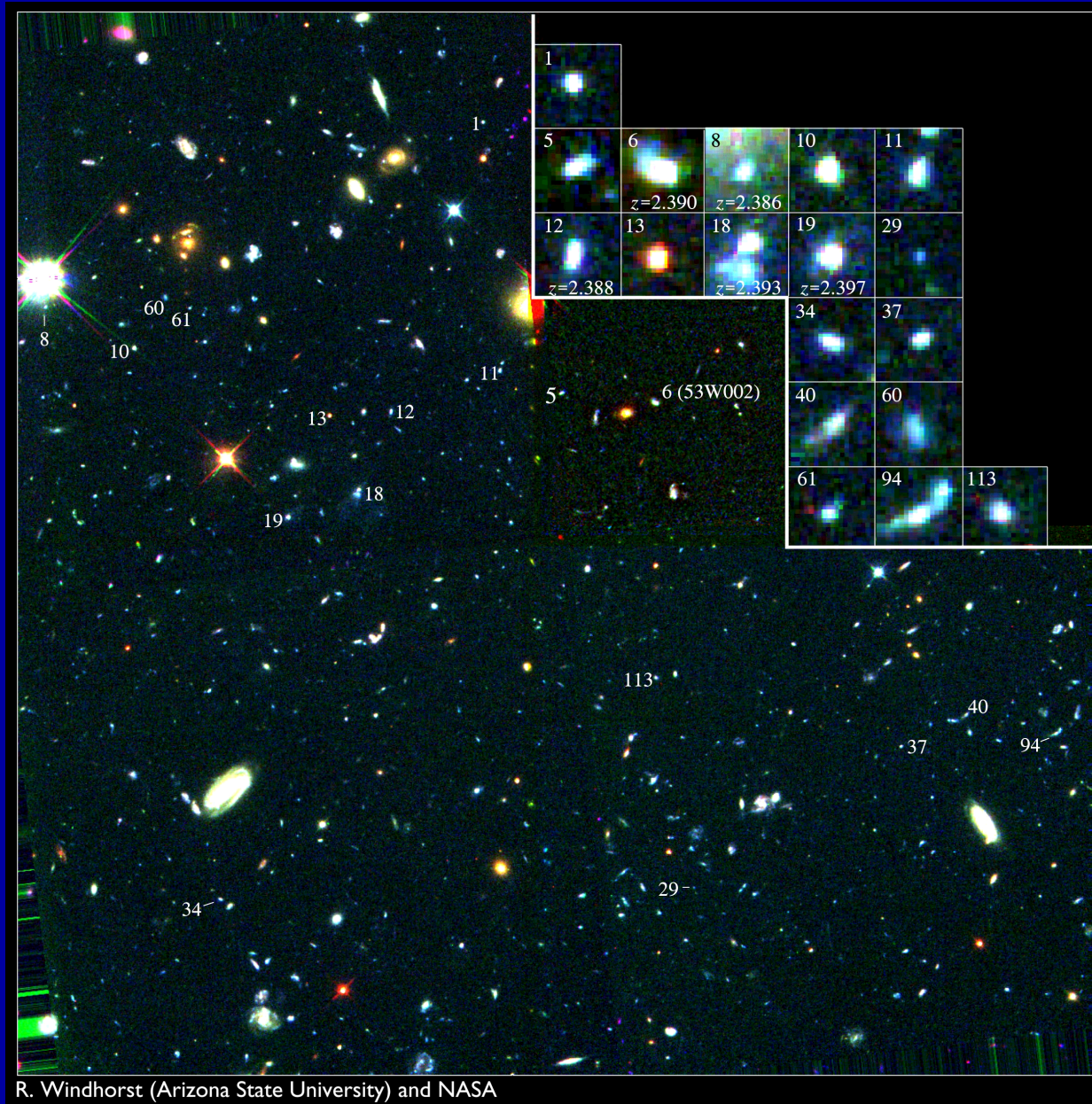


- A steep LF of $z \simeq 6$ objects (Yan & Windhorst 2004a, ApJL, 600, L1) could provide enough UV-photons to complete the reionization epoch at $z \simeq 6$.

- Pop II dwarf galaxies may not have started shining *per-vasively* much before $z \simeq 7-8$, or no H-I would be seen in the foreground of $z \gtrsim 6$ quasars.

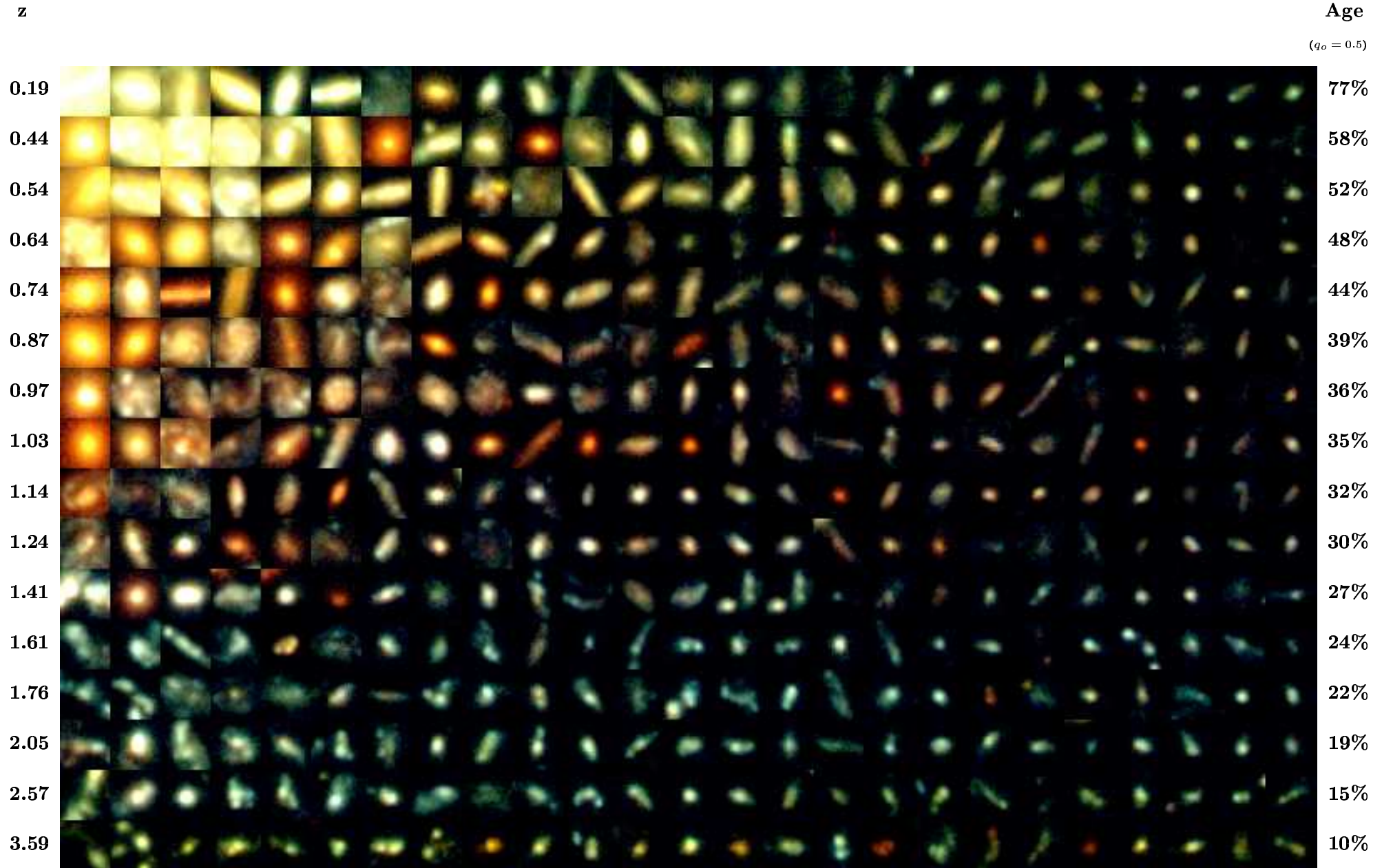
- JWST will measure this numerous population of dwarf galaxies from the end of the reionization epoch at $z \simeq 6$ into the epoch of First Light (Pop III stars) at $z \gtrsim 10$.

- (4) How JWST can measure Galaxy Assembly



One of the remarkable discoveries of HST was how numerous and small faint galaxies are — the building blocks of the giant galaxies seen today.

THE HUBBLE DEEP FIELD CORE SAMPLE ($I < 26.0$)



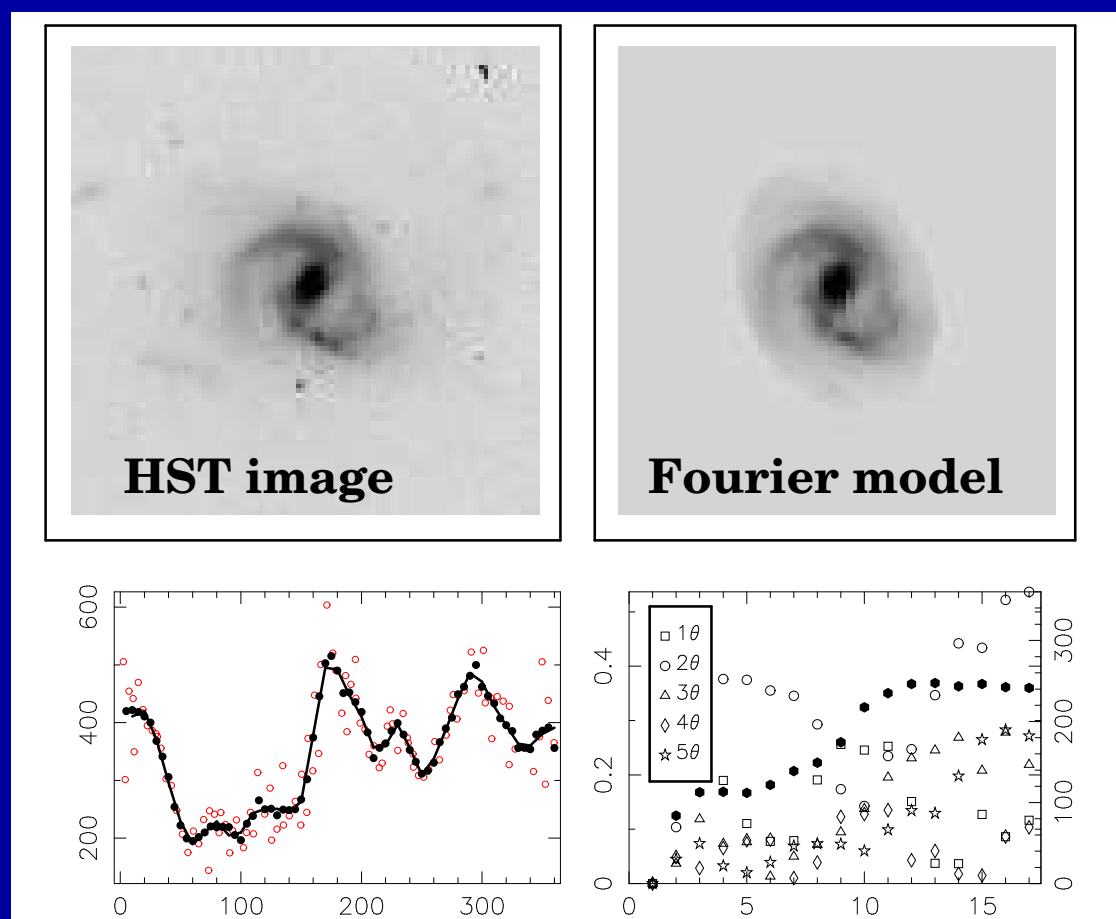
- (4) How JWST can measure Galaxy Assembly

- Galaxies of Hubble types formed over a wide range of cosmic time, but with a notable phase transition around $z \simeq 0.5-1.0$:

(1) Subgalactic units rapidly merge from $z \simeq 7 \rightarrow 1$ to grow bigger units.

(2) Merger products start to settle as galaxies with giant bulges or large disks around $z \simeq 1$. These evolved mostly passively since then, resulting in the giant galaxies that we see today.

- JWST can measure how galaxies of all types formed over a wide range of cosmic time, by accurately measuring their distribution over rest-frame structure and type as a function of redshift or cosmic epoch.

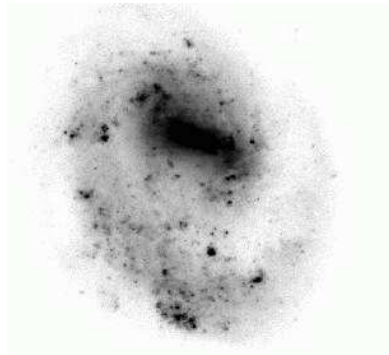


Fourier Decomposition is a robust way to measure galaxy morphology and structure in a quantitative way (Odehahn et al. 2002):

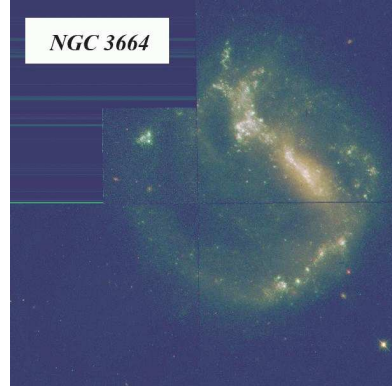
- (1) Fourier series are made in successive concentric annuli.
- (2) Even Fourier components indicate symmetric parts (arms, rings, bars).
- (3) Odd Fourier components indicate asymmetric parts (lopsidedness).
- (4) JWST can measure the evolution of each feature/class directly.

Massive Star Formation: Near and Far

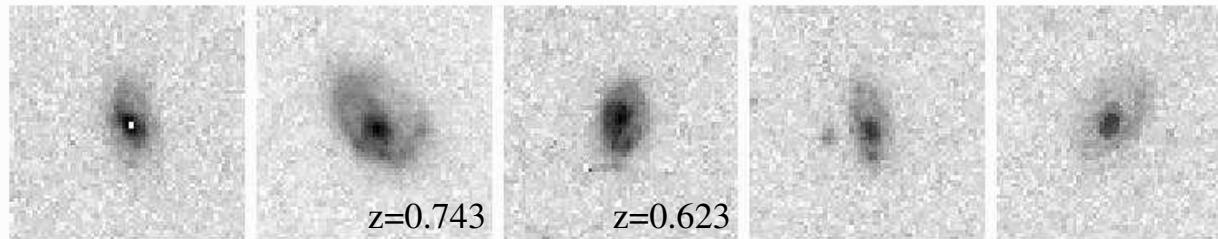
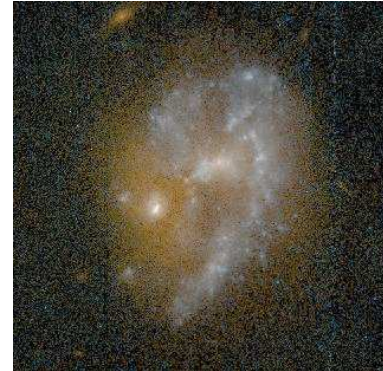
NGC 4618 (VATT, B)



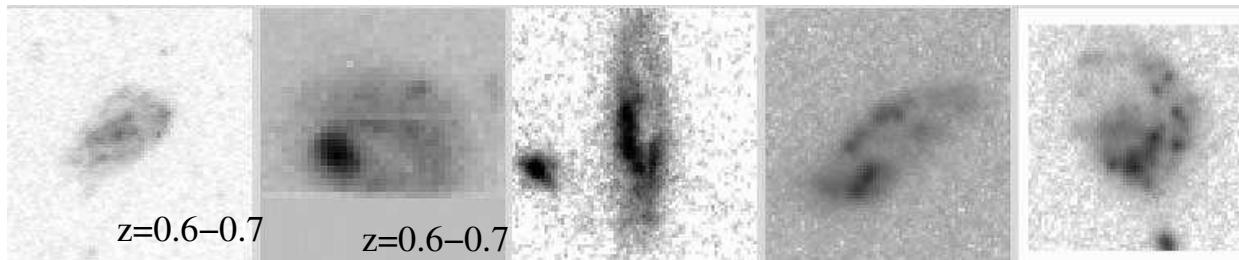
NGC 3664 (WFPC2)



UGC 5028 (HST,Cyc9)



BBP

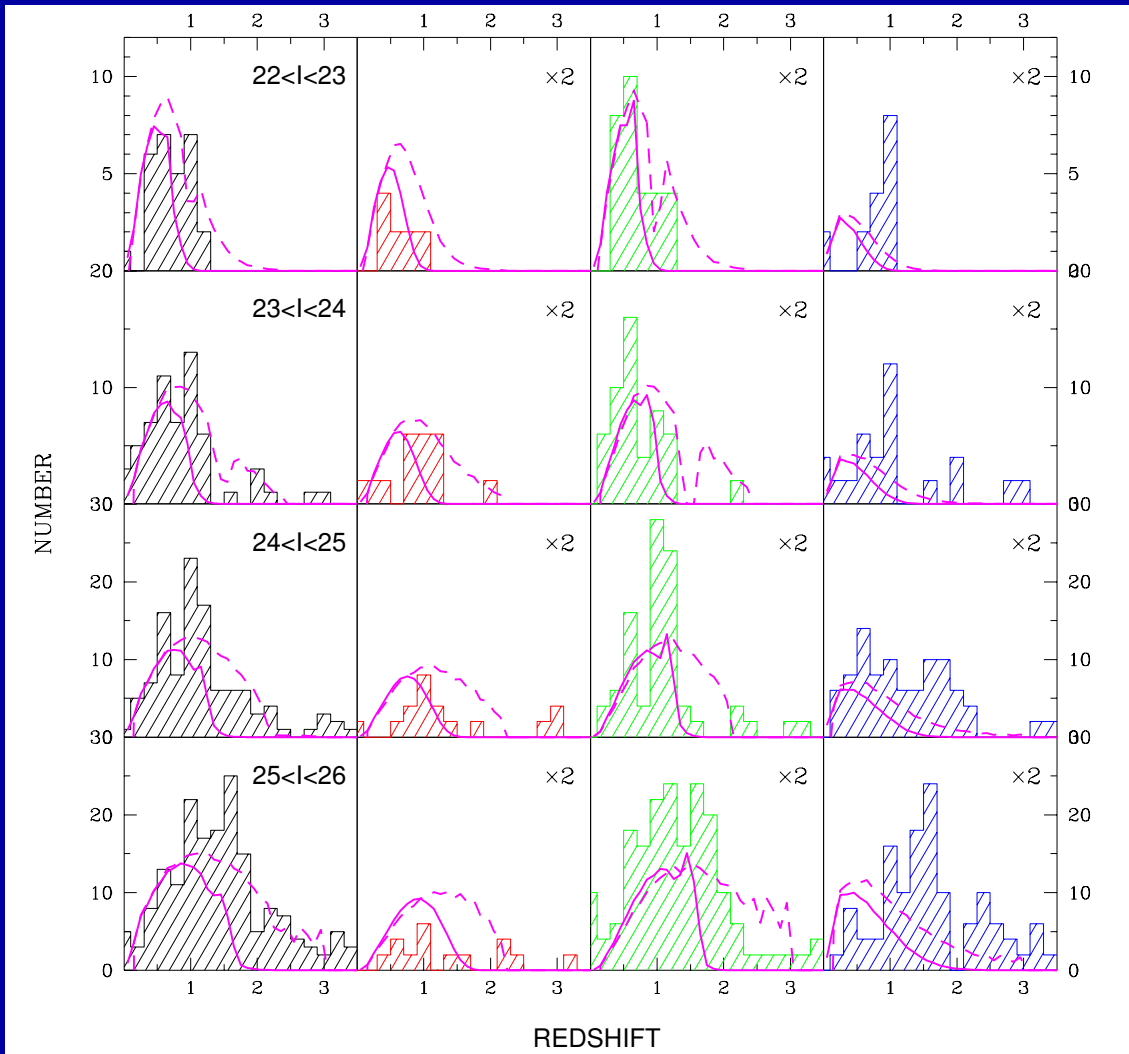


53W02

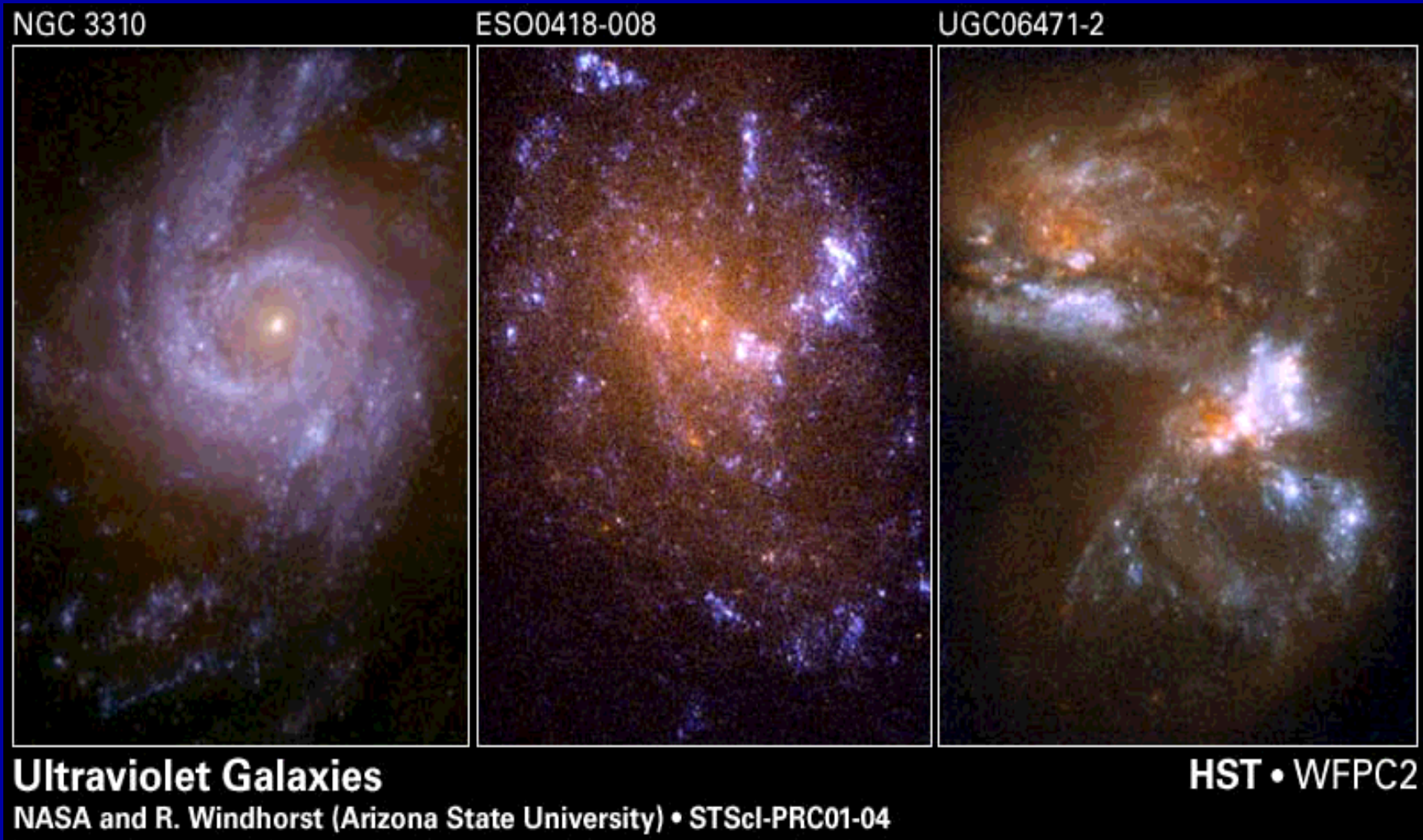
HDFS

Fourier Decomposition of nearby and distant galaxies in JWST images will directly trace the evolution of bars, rings, spiral arms, and other structural features. This measures the detailed history of galaxy assembly in the epoch $z \simeq 1-3$ when most of today's giant galaxies were made.

Total EII/S0 Sabc Irr/Mergers



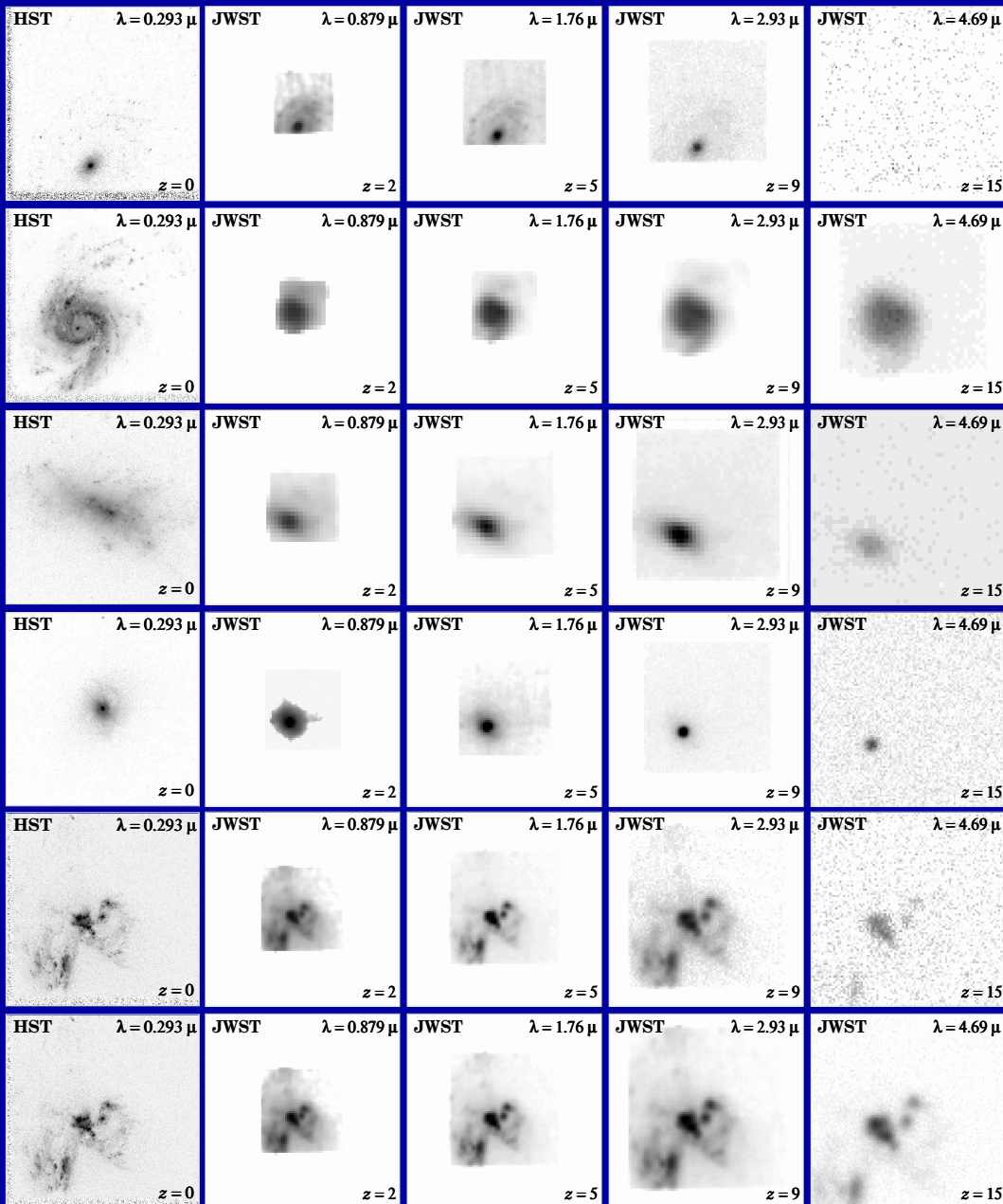
- JWST can measure how galaxies of all Hubble types formed over a wide range of cosmic time, by measuring their redshift distribution as a function of rest-frame type.
- For this, the types must be well imaged for large samples from deep, uniform and high quality multi-wavelength images, which JWST can do.



- The uncertain rest-frame UV-morphology of galaxies is dominated by young and hot stars, with often copious amounts of dust superimposed.
- This makes comparison with very high redshift galaxies seen by JWST complicated, although with good images a quantitative analysis of the restframe-wavelength dependent morphology and structure can be made.

(5) Predicted Galaxy Appearance for JWST at $z \simeq 1-15$

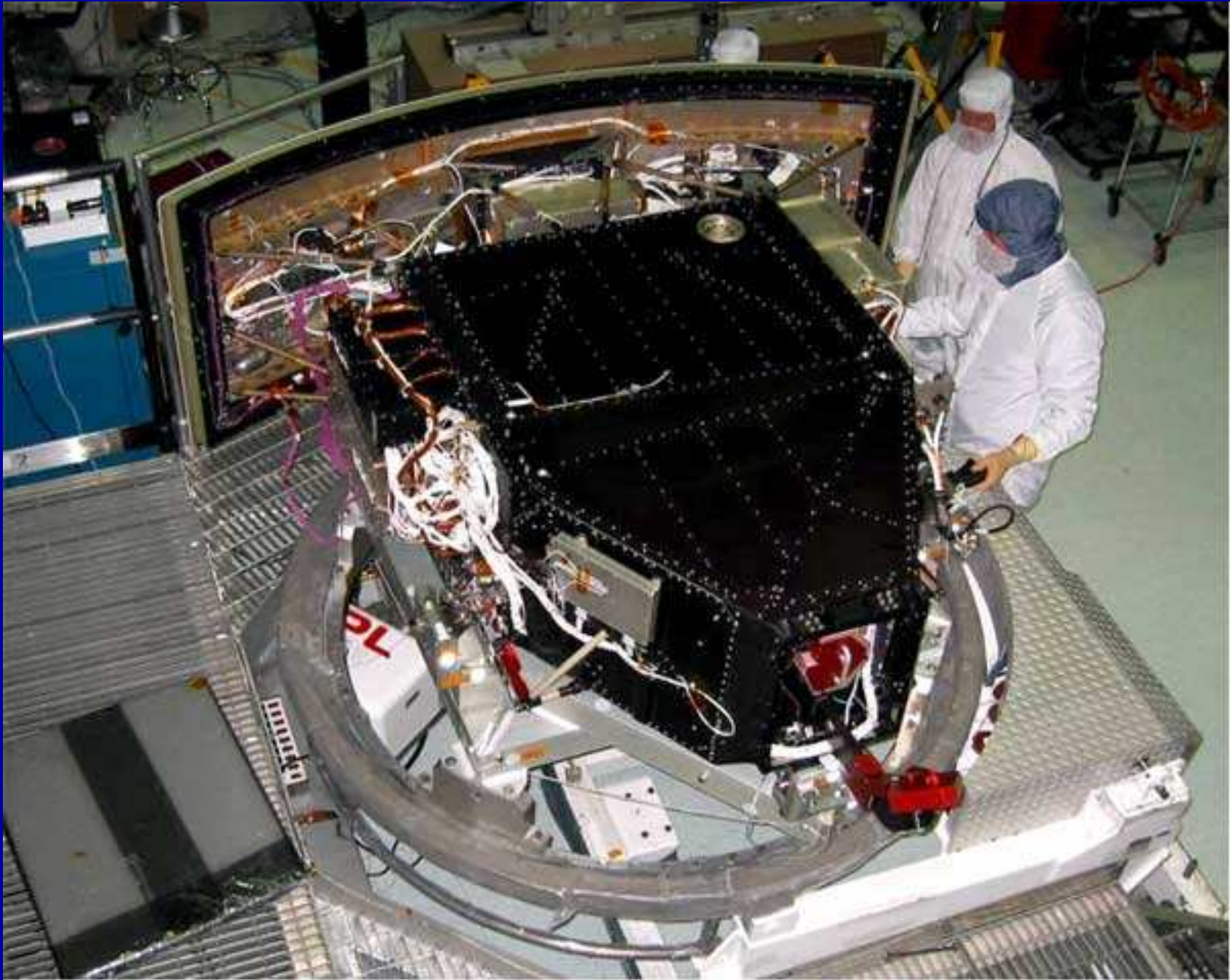
HST $z=0$ JWST $z=2$ $z=5$ $z=9$ $z=15$

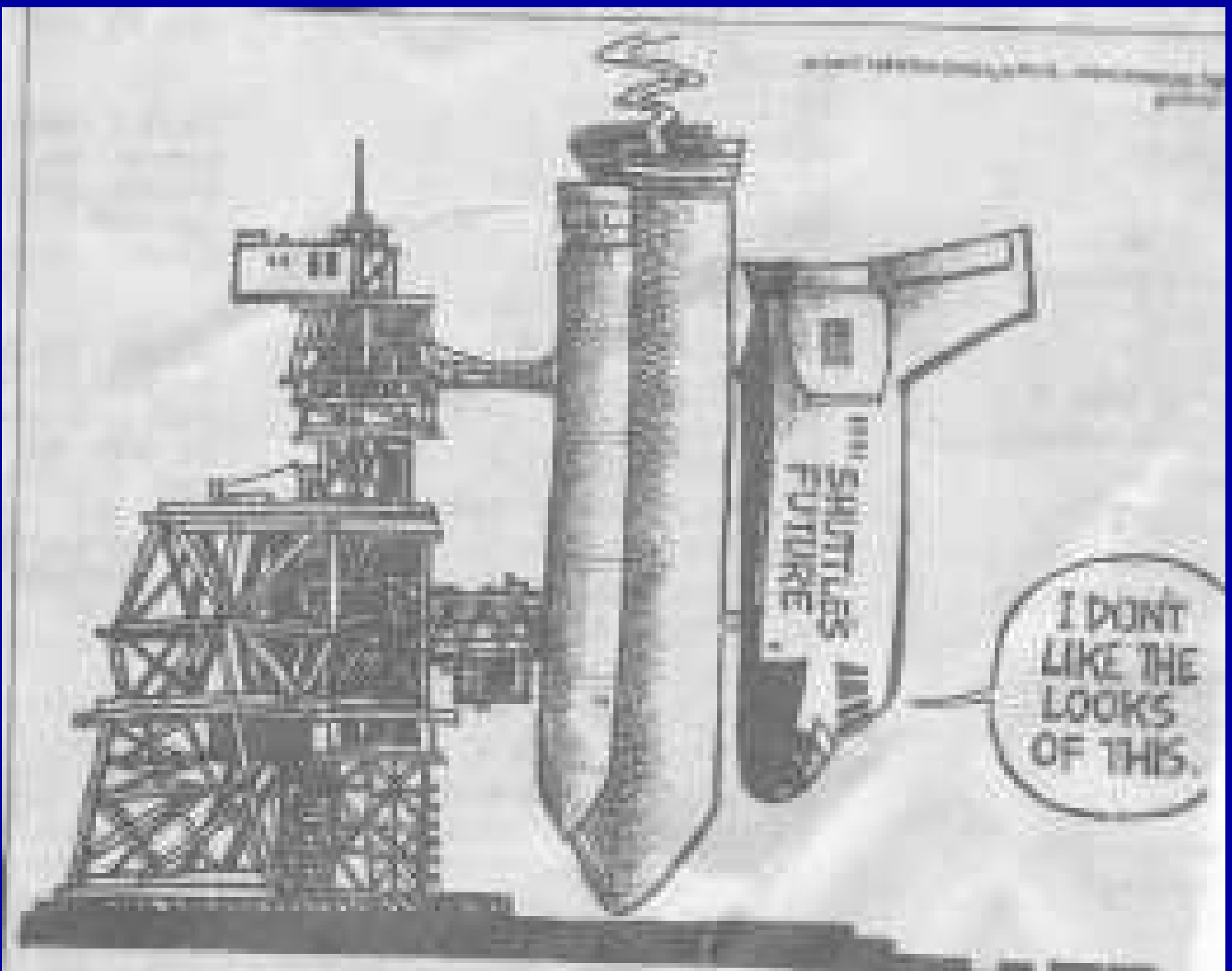


With proper restframe-UV training, JWST can quantitatively measure the evolution of galaxy morphology and structure over a wide range of cosmic time:

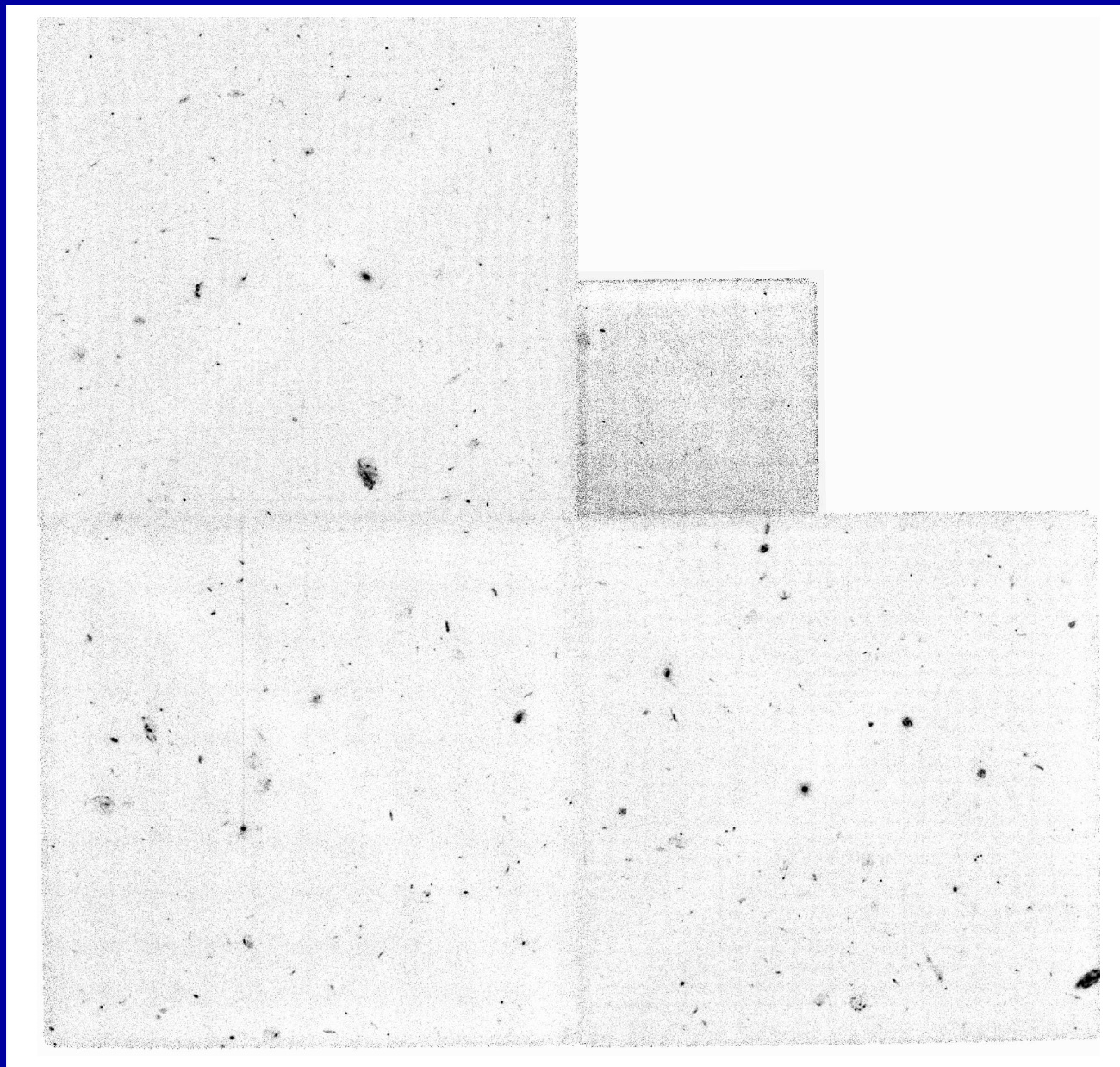
- (1) Most disks will SB-dim away at high z , but most formed at $z \lesssim 1-2$.
- (2) High SB structures are visible to very high z .
- (3) Point sources (AGN) are visible to very high z .
- (4) High SB-parts of mergers/train-wrecks are visible to very high z .

(6) What can WFC3 do, in particular in parallel to COS?





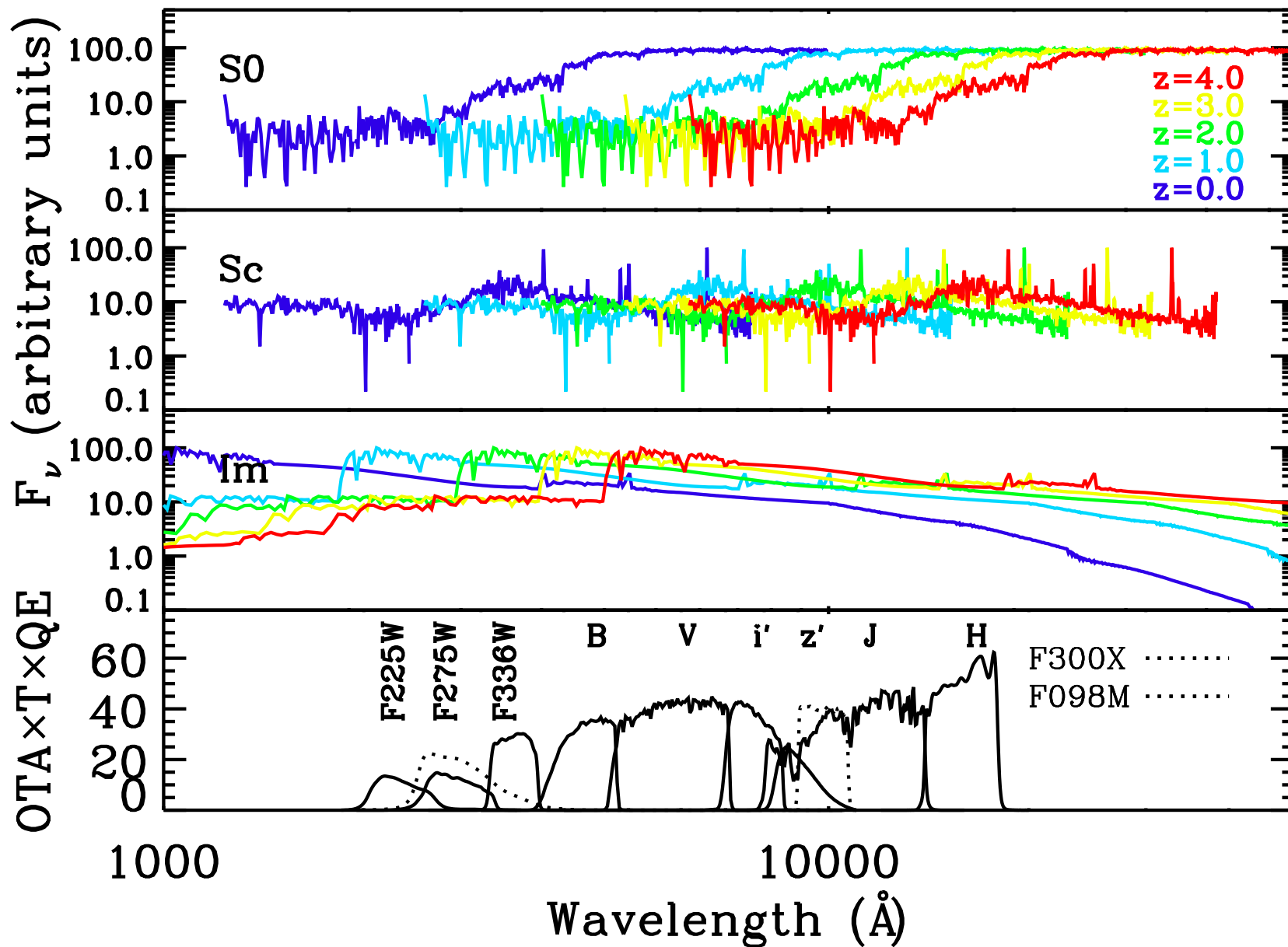
If no further big Shuttle issues, COS & WFC3 will get launched, so ...



77 orbits F300W WFPC2/HDF [$\simeq 1.4$ orbits WFC3]: $AB \lesssim 27.0$ mag ($10\text{-}\sigma$).

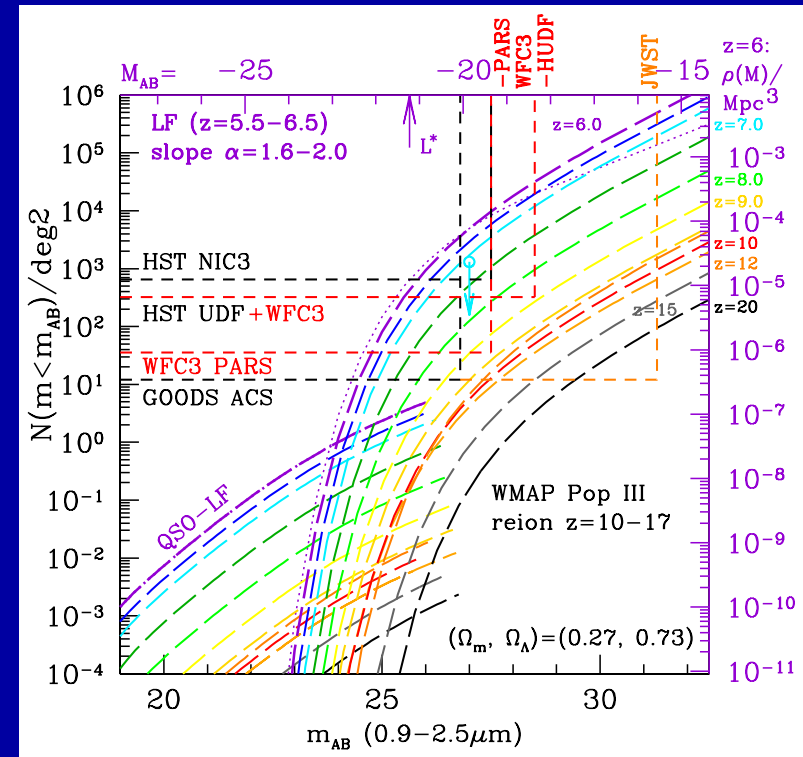
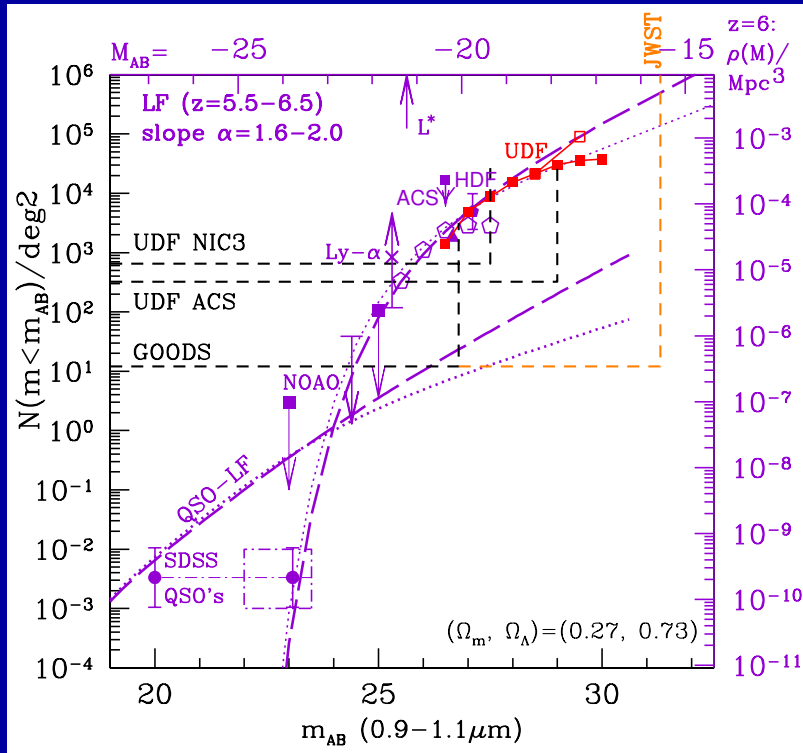
In 40 orbits F300X, a WFC3 HUDF will reach $AB \simeq 29.0$ ($10\text{-}\sigma$).

- The lack of deep UV images seriously limited the HUDF!



Cardinal WFC3 filters compared to BC03 galaxy SED templates at $z=0-4$.

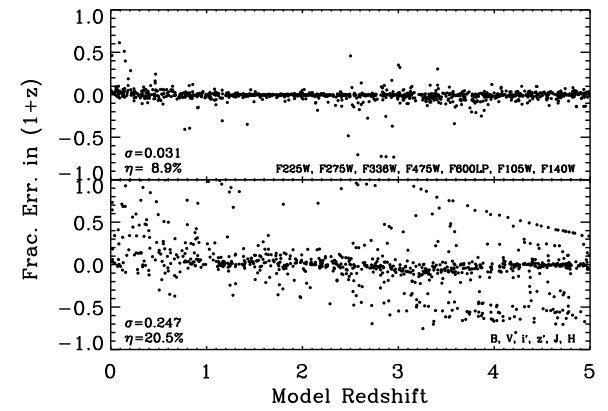
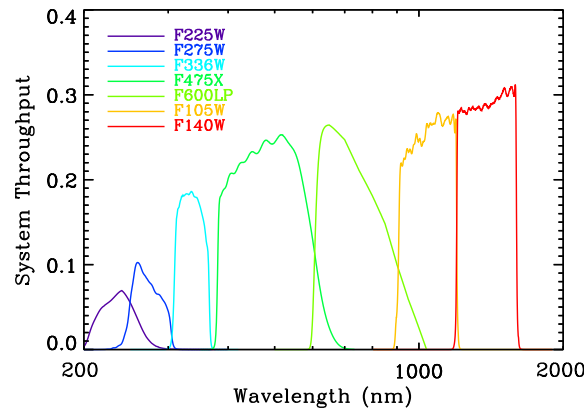
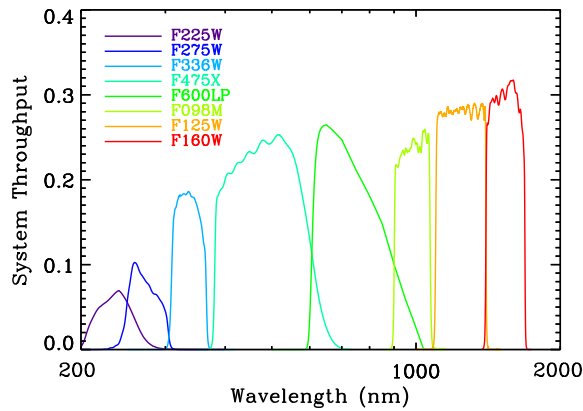
WFC3 Parallels can Map End of Reionization at $6 \lesssim z \lesssim 8-9$



Goals for WFC3 parallels:

- (1) Map the end of reionization for $6 \lesssim z \lesssim 8-9$. WFC3 can map dwarf galaxy formation from $z \simeq 9$ to $z \simeq 6$, which ended the reionization epoch at $z \simeq 6$.
- (2) Study size-distribution, light-profiles, and clustering of dwarf galaxies at $z \simeq 6-8$, constraining hierarchical formation models.
- (3) In conjunction SED models, constrain the UV escape fraction and dust content of the dwarf galaxy population at $z \simeq 6-8$.

WFC3 Parallels can Map Galaxy Assembly at $z \lesssim 5$.



● With WFC3, photo- z errors will go from $\sigma_z \simeq 0.25$ with the ACS/NIC3 filters to $\sigma_z \lesssim 0.02-0.03$ with 7-8 WFC3 filters to $AB \simeq 27.5-28$ mag, and vastly reduce the catastrophic photo- z failure fraction η . Goals are:

- (1) Map galaxy assembly from $z \simeq 0-5$.
- (2) High precision pixel-to-pixel studies of stellar populations, dust.
- (3) The UV luminosity density as a function of epoch.
- (4) Large scale structure can be mapped in redshift-space for $z \lesssim 5$ with an rms scatter in redshift that corresponds to $\lesssim 150$ Mpc.

● Hence, WFC3 parallels can trace the LSS about $6'$ ($\simeq 3$ Mpc) away from $z=0$ to $z=5$, which COS will map in absorption at much higher resolution.

Scheduling features required to get the most out of WFC3:

Enable all long (30–60 orbit) WFC3 parallels to COS:

- COS GTO's will do, and COS GO's are expected to do many 30–60 orbit primary observations.

- With the new compelling discovery space offered by WFC3, we must take advantage of these long COS primary observations by making sure that:

- (1) All WFC3 parallels to long COS primaries are enabled (for a few Cycles — HST transmitters permitting).

- (2) STScI finds ways to encourage (reward?) COS GO and GTO's to take WFC3 parallels to all their long COS exposures **with the SAME ORIENT.**

- (3) Or, if possible, rotate COS primaries between orbits by $\pm n \delta(\text{ORIENT}) \simeq \pm n 0.003^\circ$ (n such that FGS can do it), which at the WFC3 distance from COS corresponds to WFC3 dither steps of $\sim \pm n 0.02 \simeq \pm n 0.5$ WFC3 pixels. This process may not jeopardize the COS primaries.

(7) Conclusions

(1) JWST Project is technologically front-loaded and well on track:

- Most items at Technical Readiness Level 6 (TRL-6) by Jan. 2007 (*i.e.*, demonstration in a relevant environment — ground or space).

(2) JWST will map the epochs of First Light, Reionization, and Galaxy Assembly in detail. It will determine:

- The formation and evolution of the first (reionizing) Pop III star-clusters.
- The origin of the Hubble sequence in hierarchical formation scenarios.

(3) WFC3 will be a critical pathfinder for JWST:

- Estimate the density of the first Pop II star dominated dwarf galaxies at $z \simeq 6-9$ — determines optimum survey strategies for JWST.
- Measure photo- z 's with $\lesssim 0.02-0.03$ accuracy for $AB \lesssim 27-28$ mag and $z \simeq 0-5$ — galaxy assembly and $N(z)$ for precision LSS studies.
- WFC3 Parallels to COS are very powerful: we should plan for them!

SPARE CHARTS

- References and other sources of material shown:

<http://www.jwst.nasa.gov/>

<http://www.stsci.edu/jwst/>

<http://www.jwst.nasa.gov/ISIM/index.html>

<http://ircamera.as.arizona.edu/nircam/>

<http://ircamera.as.arizona.edu/MIRI/>

<http://www.stsci.edu/jwst/instruments/nirspec/>

<http://www.stsci.edu/jwst/instruments/nirspec/mems.html>

<http://www.stsci.edu/jwst/instruments/guider/>

Gardner, J. P., Mather, J. C., Clampin, M., Doyon, R., Greenhouse, M. A., Hammel, H. B., Hutchings, J. B., Jakobsen, P., Lilly, S. J., Long, K. S., Lunine, J. I., McCaughrean, M. J., Mountain, M., Nella, J., Rieke, G. H., Rieke, M. J., Rix, H.-W., Smith, E. P., Sonneborn, G., Stiavelli, M., Stockman, H. S., Windhorst, R. A., & Wright, G. S. 2006, *Space Science Reviews*, 123, 485–606 (astro-ph/0606175)

Mather, J., Stockman, H. 2000, *Proc. SPIE Vol. 4013*, p. 2-16, in “UV, Optical, and IR Space Telescopes and Instruments”, Eds. J. B. Breckinridge & P. Jakobsen (Berlin: Springer)

WFC3-SOC proposal to COS GTO team (Nov. 2002)

- (1) Carry out your primary GTO COS program as planned without disruption by WFC3 parallels.
- (2) Take WFC3 UVIS and IR (and ACS) parallels where-ever you can. Get WFC3 SOC input how to best take these WFC3 (and ACS) parallels.
- (3) Share (subset of) your WFC3 (and ACS) Parallels with WFC3 SOC members.
- (4) Expert WFC3 SOC members ($\sim 5-7$) will help you analyze these parallels (in mutual consultation and collaboration).

SUGGESTED PARALLEL SCIENCE GOALS:

(4.A) Systematic search for $z=6-8$ objects. Measure the LF around the epoch of reionization.

(4.B) MUV+Opt+near-IR imaging at $z \simeq 0-1$. Study stellar pops and dust with galaxy type and epoch.

WFC3-SOC proposal to COS GTO team (cont.)

- (5) All publications on parallels to COS GTO primary data in strict mutual agreement: COS GTO members can be co-author of any WFC3-SOC lead paper on these parallels.
- (6) JWST Interdisciplinary Scientist Rogier Windhorst will in a similar agreement share his 110 hours of James Webb Space Telescope time with the COS-GTO team in 2013–2017, which will do very high-z extensions of (4.A) and (4.B).
- (7) WFC3-SOC members will spend considerable ground-based telescope time in 2005-2010 to support goals (4.A) and (4.B): 6.5m Magellan & MMT, 11m LBT (McCarthy, Windhorst, others TBD), and share this similarly with the COS GTO team.
- (8) All items (1)–(7) to be formalized in a mutual agreeable MOU, in agreement with NASA policies. In particular, a strict agreement will be made to keep data in (1)–(7) between the two teams only.

WFC3-SOC Recommendations to STScI (Nov. 2006)

- **Specific requirements for HST Cycle $\gtrsim 17$ parallels:** With the unique, new and compelling discovery space offered by WFC3, the WFC3 SOC recommends that the community takes advantage of these long primary HST observations in Cycles $\gtrsim 17$, and recommends that STScI:
 - (1) Enables consistent short and long (30–60 orbit) WFC3 parallels to COS, ACS, NICMOS or FGS for several Cycles (transmitters permitting).
 - (2) Implements homogeneous WFC3 Parallels as following:
 - (a) Let GTO's and GO's "own" the WFC3 parallel time to their primary data (GO's – provided that they commit to take these in a homogeneous way);
 - (b) Hold a WFC3/COS community workshop, which helps define how GTO's and GO's best take homogeneous WFC3 parallels to all long COS exposures, with each given target held at approximately the **SAME ORIENT**.
 - (c) Reward these parallel APT efforts through (co-)authorship of papers on WFC3 parallel data, and perhaps extra funds to reduce/analyze the WFC3 parallels.

- (3) Aspects of HST Parallel scheduling: Parallels may not constrain primaries, but GTO's/GO's commit to take homogeneous WFC3 parallels in 7–8 filters and exposures times approximately as above, and to dither their primaries as following:

- (a) They will dither their ACS or NIC primary observations as usual; or

- (b) They will rotate their COS primaries between successive orbits by $\pm n \delta(\text{ORIENT}) \simeq \pm n 0.003^\circ$ (n such that FGS can do it), which at the WFC3 distance from COS corresponds to WFC3 dither steps of $\sim \pm n 0''.02 \simeq \pm n 0.5$ WFC3 pixels. This would improve WFC3 drizzle-ability, although it may not be essential;

We are open to other suggestions to optimize the yield of homogeneous WFC3 parallels, without posing undue constraints on the HST scheduling process.

Table 10. Predicted Performance of the JWST Observatory

Parameter	Capability
Wavelength	0.6 to 29 μm . Reflective gold coatings
Sensitivity	SNR=10, integration time = τ_i , $R=\lambda/\Delta \lambda$ and Zodiacal of 1.2 times that at north ecliptic pole
NIRCam	12 nJy (1.1 μm , $\tau_i=10,000\text{s}$, and $\lambda/\Delta \lambda = 4$)
NIRCam	10.4 nJy (2.0 μm , $\tau_i=10,000\text{s}$, and $\lambda/\Delta \lambda = 4$)
TFI	368 nJy (3.5 μm , $\tau_i=10,000\text{s}$, and $\lambda/\Delta \lambda = 100$)
NIRSpec	120 nJy (3.0 μm , $\tau_i=10,000\text{s}$, and $\lambda/\Delta \lambda = 100$)
NIRSpec	560 nJy (10 μm , $\tau_i=10,000\text{s}$, and $\lambda/\Delta \lambda = 5$)
MIRI	5000 nJy (21 μm , $\tau_i=10,000\text{s}$, and $\lambda/\Delta \lambda = 4.2$)
NIRSpec Med	$5.2 \times 10^{-22} \text{ Wm}^{-2}$ (2 μm , $\tau_i=100,000\text{s}$, $R= 1000$)
MIRI Spec	$3.4 \times 10^{-21} \text{ Wm}^{-2}$ (9.2 μm , $\tau_i=10,000\text{s}$, $R= 2400$)
MIRI Spec	$3.1 \times 10^{-20} \text{ Wm}^{-2}$ (22.5 μm , $\tau_i=10,000\text{s}$, $R= 1200$)
Spatial Resolution & Stability	Encircled Energy of 75% at 1 μm for 150mas radius Strehl ratio of ~ 0.86 at 2 μm . PSF stability better than 1%

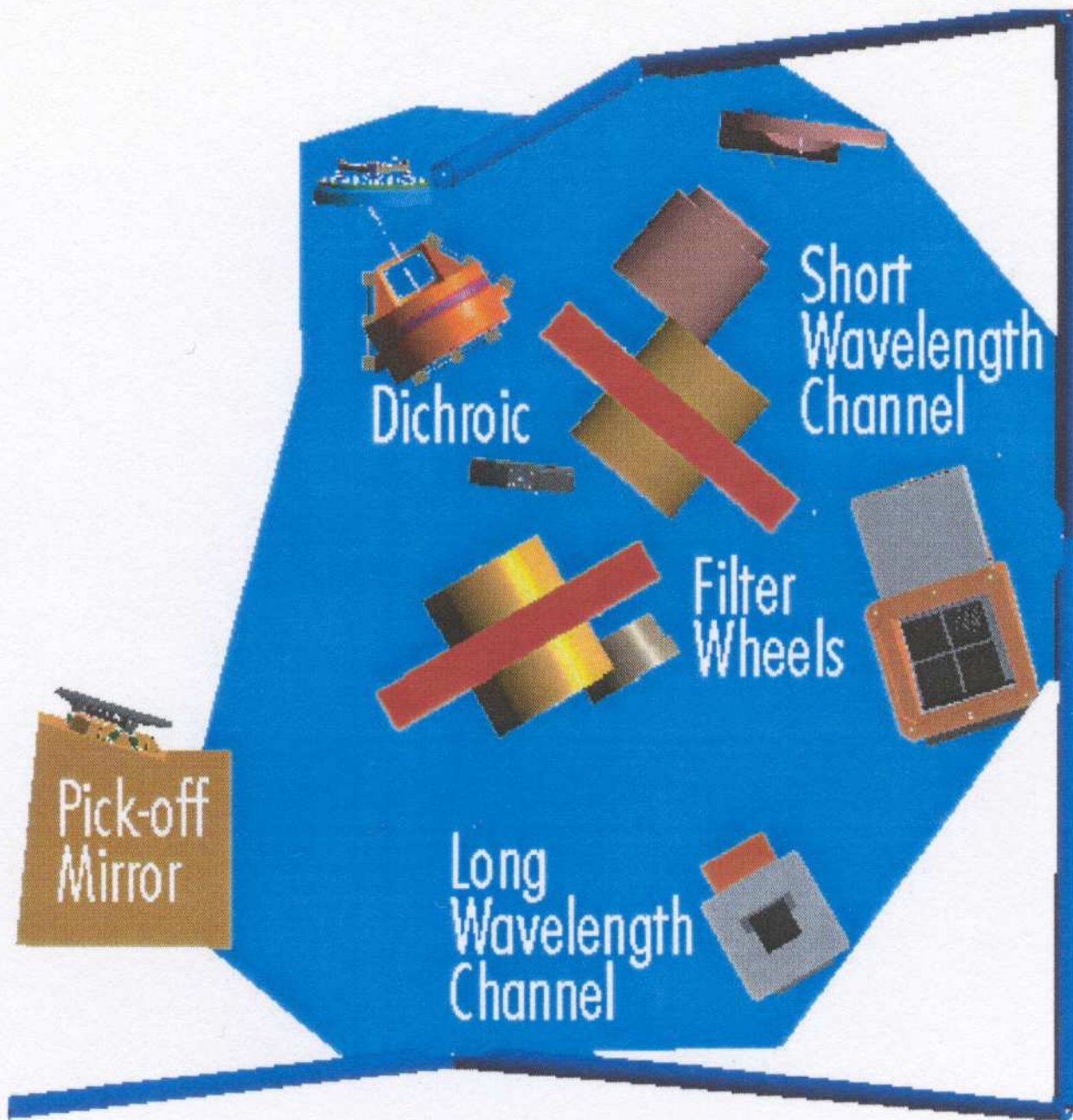


Figure 43. Optical layout of one of two NIRCcam imaging modules.

- (2) What instruments will JWST have?

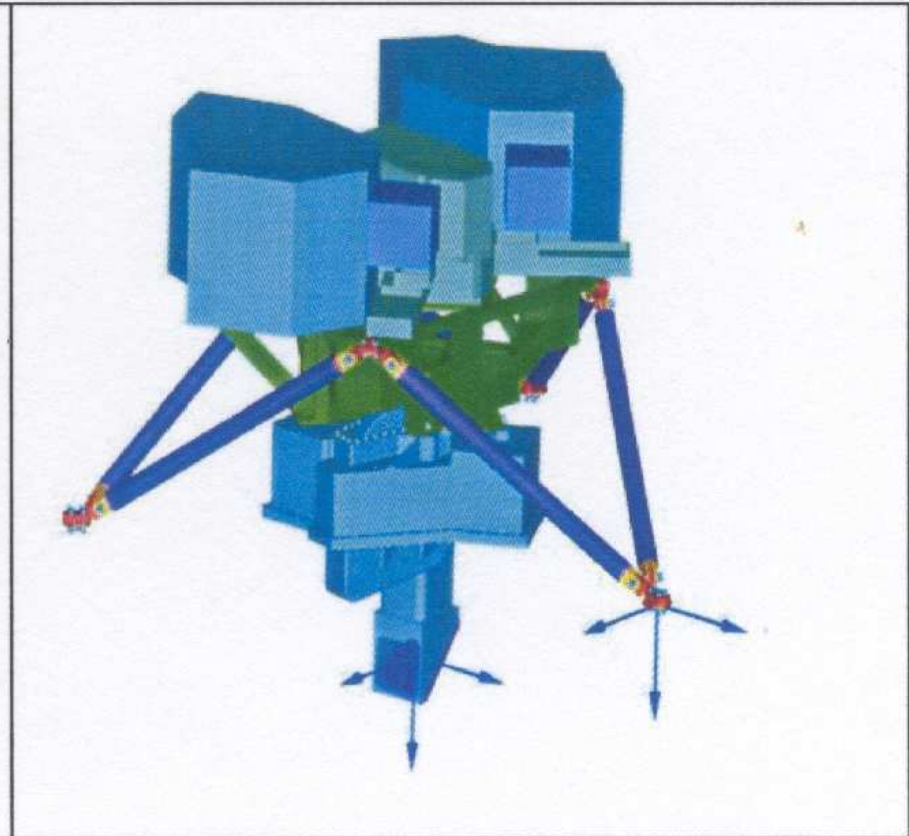
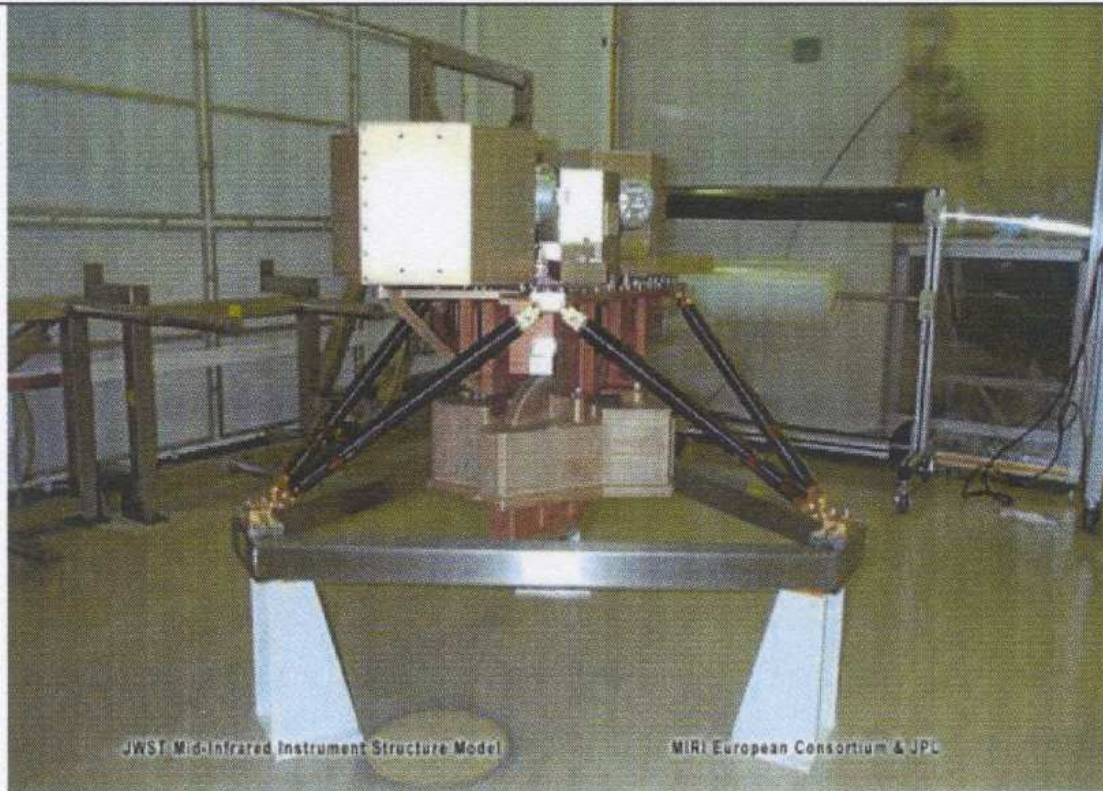


Figure 47. The MIRI structural and thermal model (left) compared to a computer design of the instrument (right).

The Mid-Infra-Red Instrument MIRI made by an UofA + JPL + ESA consortium will do imaging and spectroscopy from 5–28 μm . MIRI is actively cooled by a cryocooler, so that its lifetime is not limited by consumables.

MIRI IFUs fields of view

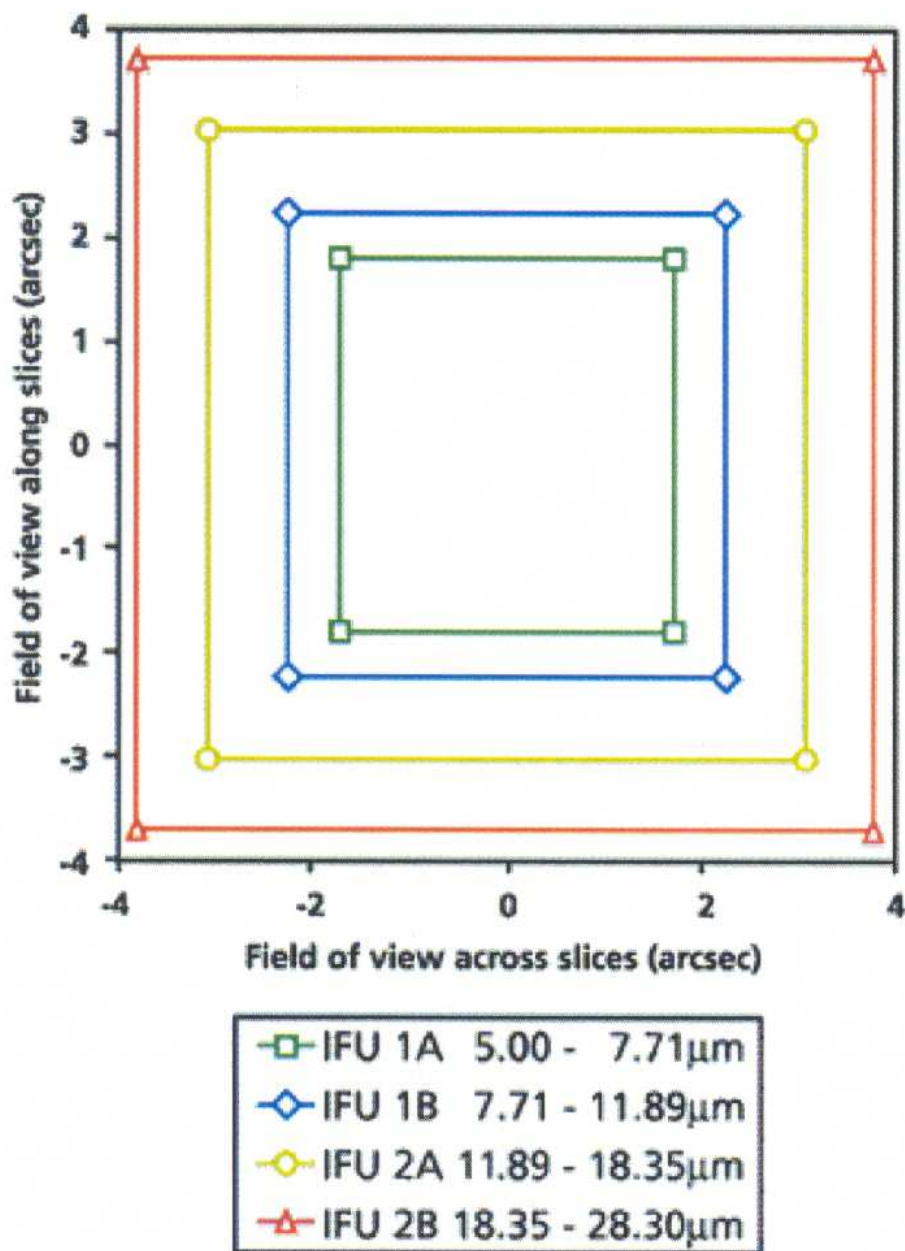


Figure 49. Fields of view of the MIRI IFU spectrograph.

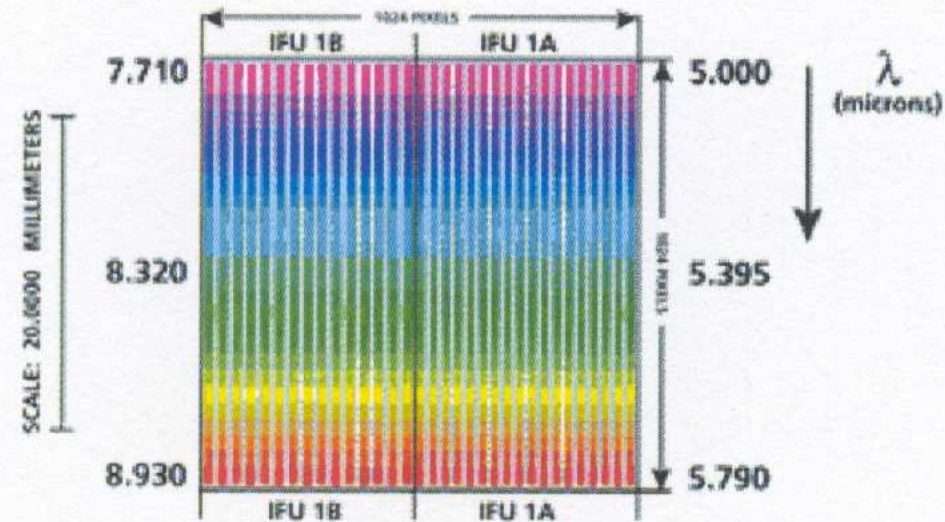
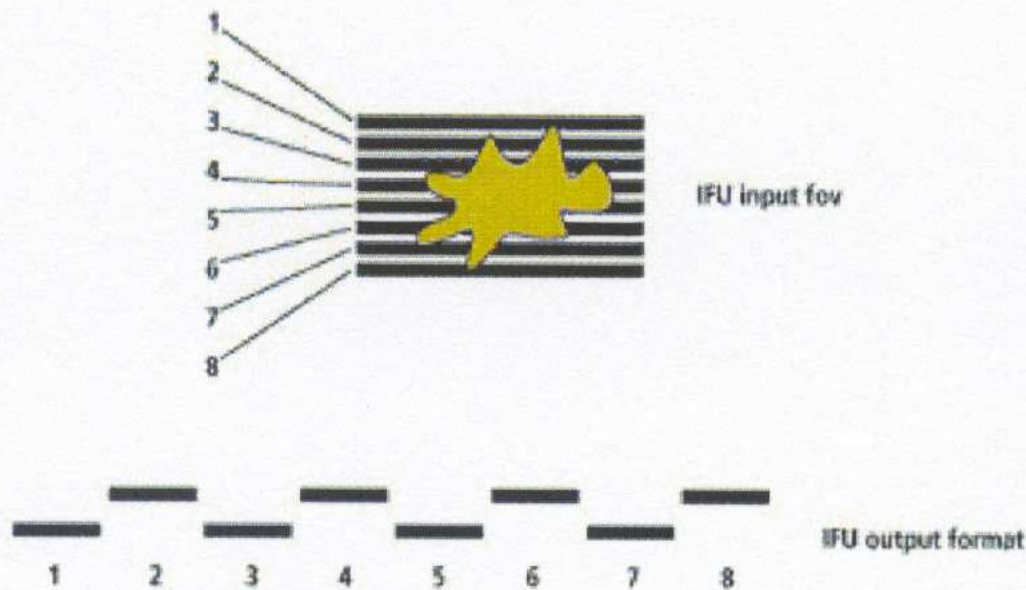


Figure 50. Schematic illustration of the MIRI IFU image slicer format (left) and dispersed spectra on detector (right)

The MIRI Integral Field Unit (IFU) has an image slicer that makes spatially resolved spectra at $5 \mu\text{m} \lesssim \lambda \lesssim 9 \mu\text{m}$.

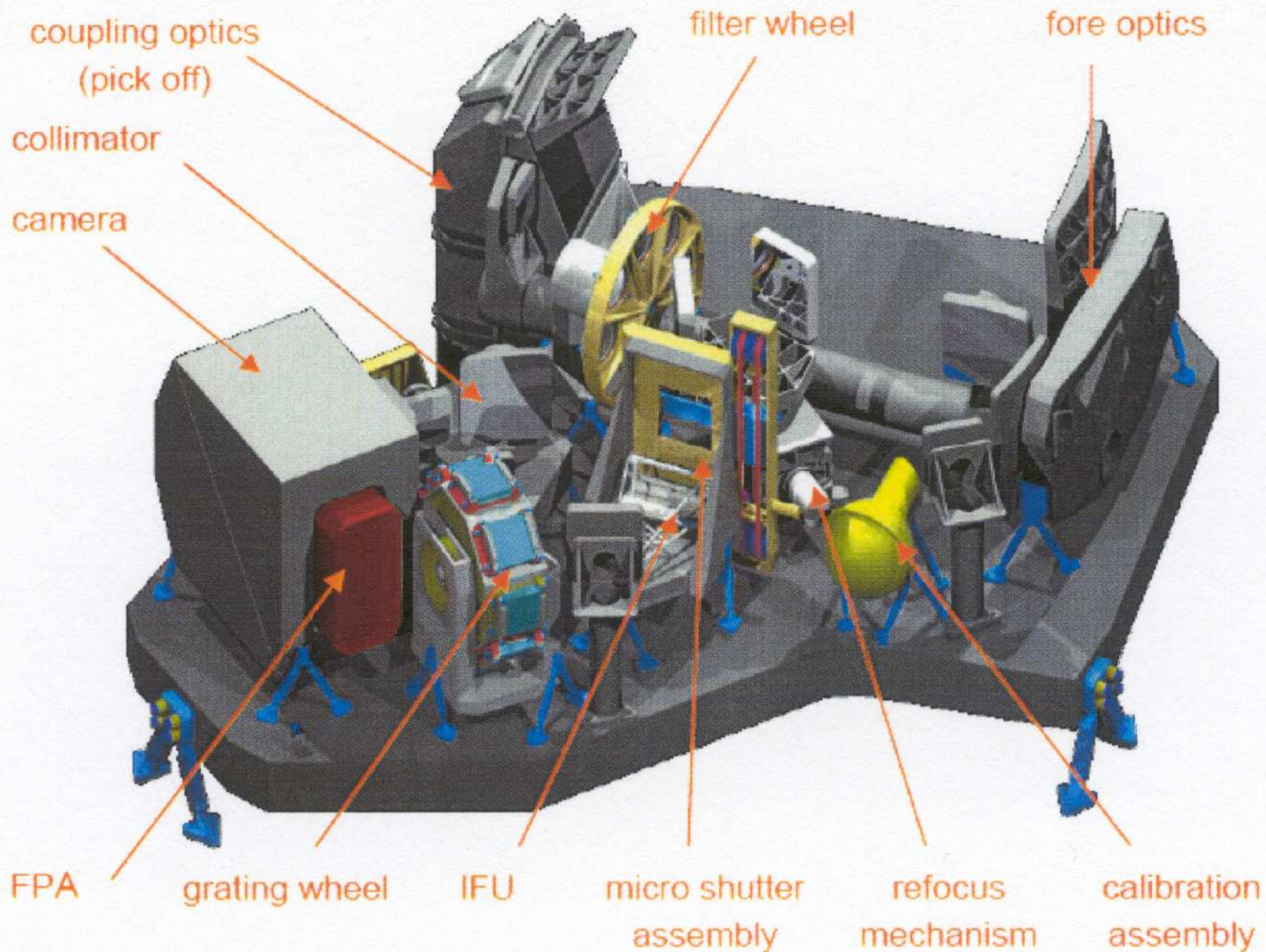


Figure 45. The NIRSpec instrument.

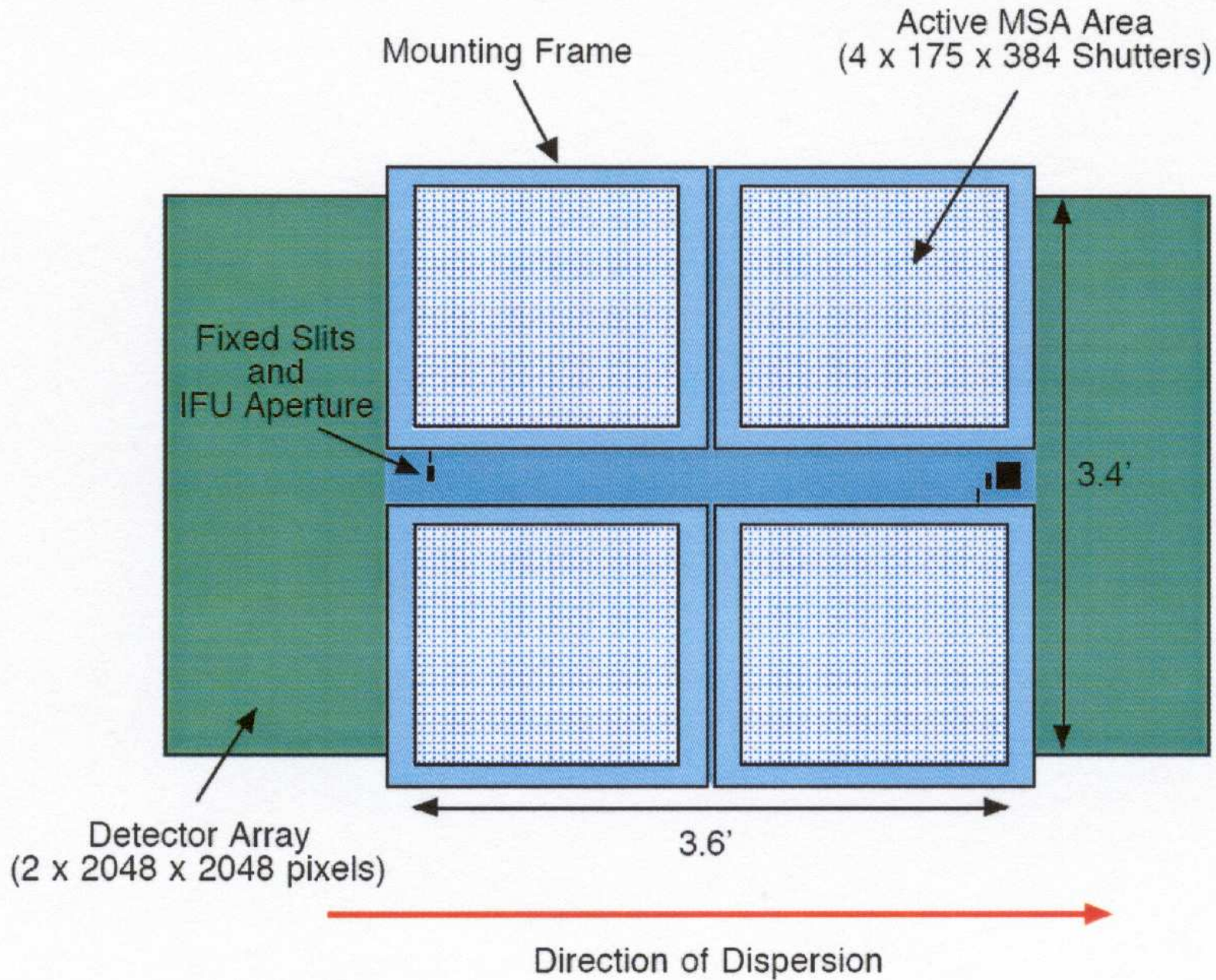
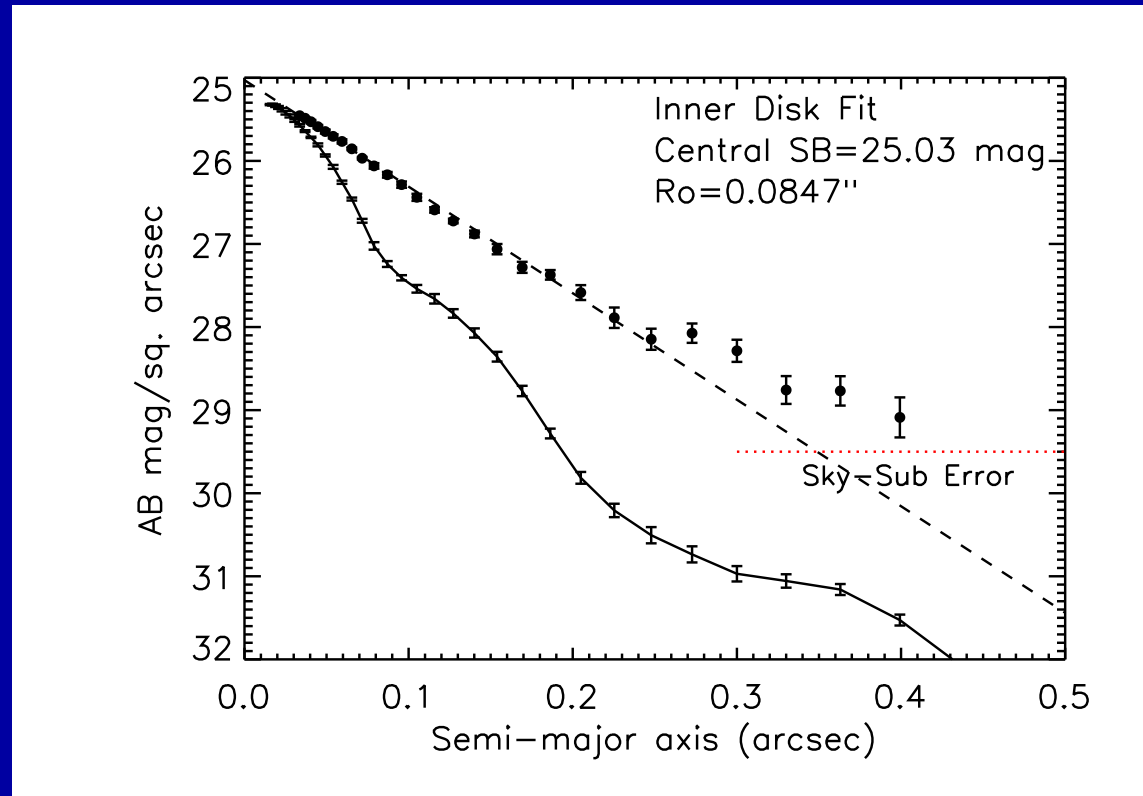
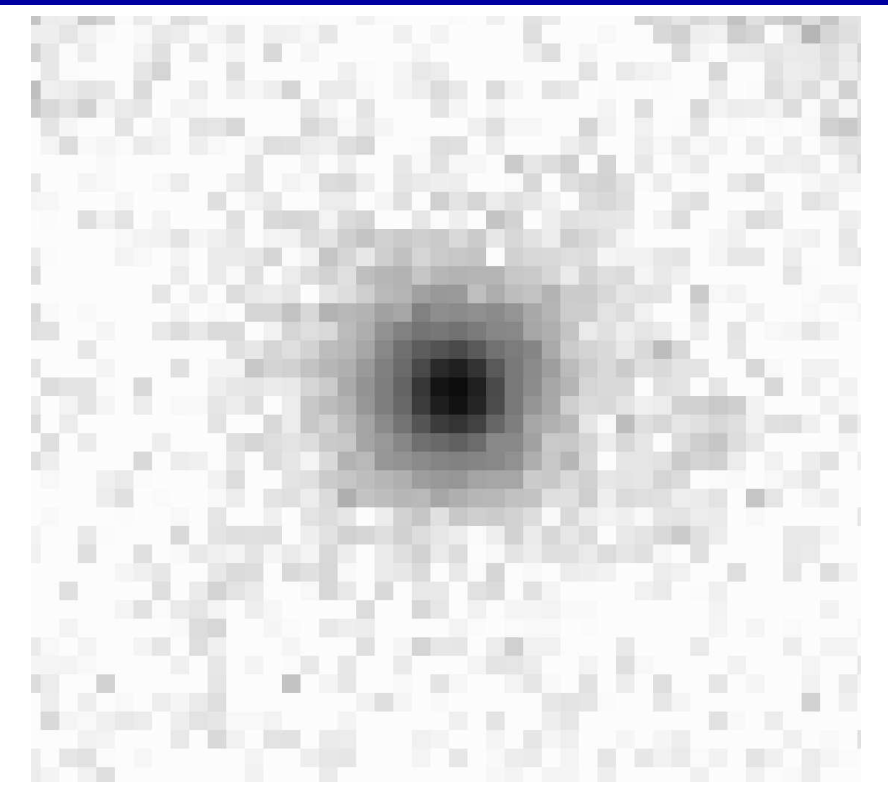


Figure 46. Schematic layout of the NIRSpec slit mask overlaid the detector array projected to the same angular scale.



Sum of 49 isolated i-drops:
 =5000 hrs HUDF z-band.
 [\simeq 330 hrs JWST $1 \mu\text{m}$]

ACS light-profile, PSF and sky-error:
 Deviates from exp. disk at $r_e \gtrsim 0.25$
 \Rightarrow Dyn. age ($z \simeq 6$) \simeq 100-200 Myr
 (cf. N. Hathi et al.2006)

HST/ACS cannot accurately measure individual light-profiles at $z \simeq 6$.

JWST can do this well for $z \gtrsim 6$ in very long integrations.

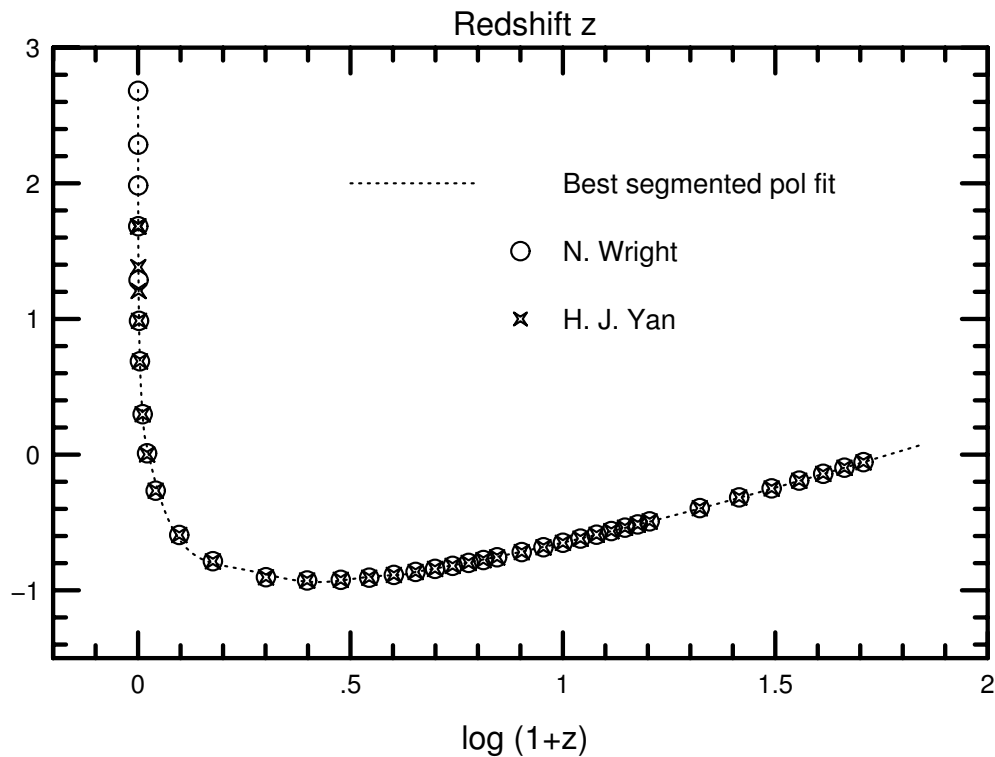
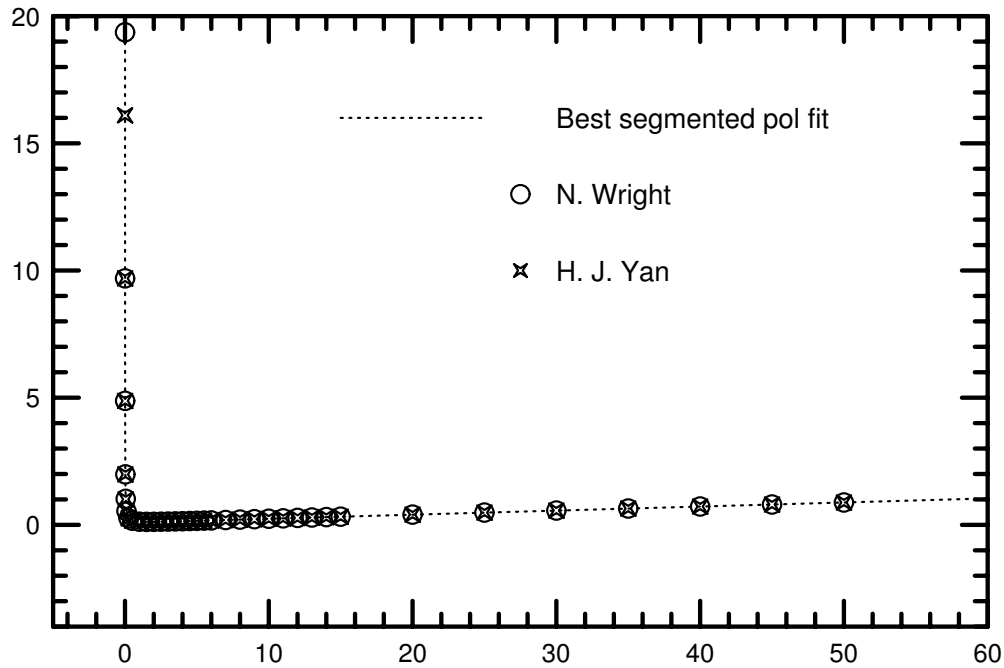
Dynamical timescale \simeq SED timescale \Rightarrow Bulk of SF at $z_{form} \simeq 7.0 \pm 0.5??$

(5) Details on JWST image simulations:

- All based on HST/WFPC2 F300W images from the HST mid-UV survey of nearby galaxies (Windhorst et al. 2002, ApJ Suppl. 143, 113).
- WMAP COSMOLOGY: $H_0=71$ km/s/Mpc, $\Omega_m=0.27$, $\Omega_\Lambda=0.73$.
- INSTRUMENT: 6.0 m effective aperture, diffraction limited at $\lambda \gtrsim 2.0 \mu\text{m}$, JWST/NIRCam, $0''.034/\text{pix}$, read-noise= $5.0 e^-$, dark-current= $0.02 e^-/\text{s}$, NEP-Sky($1.6 \mu\text{m}$)= $21.7 \text{ mag}/('')^2$ in L2, Zodi spectrum, $t_{exp}=4 \times 900\text{s}$.

Row	Telesc.	Redshift	λ (μm)	FWHM ($''$)
1	HST	$z \sim 0$	$0.293 \mu\text{m}$	$0''.04$
	JWST	$z=1.0$	$0.586 \mu\text{m}$	$0''.084$
	JWST	$z=2.0$	$0.879 \mu\text{m}$	$0''.084$
2	JWST	$z=3.0$	$1.17 \mu\text{m}$	$0''.084$
	JWST	$z=5.0$	$1.76 \mu\text{m}$	$0''.084$
	JWST	$z=7.0$	$2.34 \mu\text{m}$	$0''.098$
3	JWST	$z=09.0$	$2.93 \mu\text{m}$	$0''.122$
	JWST	$z=12.0$	$3.81 \mu\text{m}$	$0''.160$
	JWST	$z=15.0$	$4.69 \mu\text{m}$	$0''.197$

Theta-z relation for $H_0=71$, $\Omega_m=0.27$, $\Omega_\Lambda=0.73$



Angular size vs. redshift relation in a Lambda dominated cosmology of $H_0 = 71 \text{ km s}^{-1} \text{ Mpc}^{-1}$, $\Omega_m = 0.27$, $\Omega_\Lambda = 0.73$.

In the top panel the relation is nearly linear in $1/z$ for $z \lesssim 0.05$ (the small angle approximation) and linear in z for $z \gtrsim 3$ (the Lambda dominated universe).

All curvature occurs in the range $0.05 \lesssim z \lesssim 3$, which is coded up in the IRAF script that does the JWST simulations.

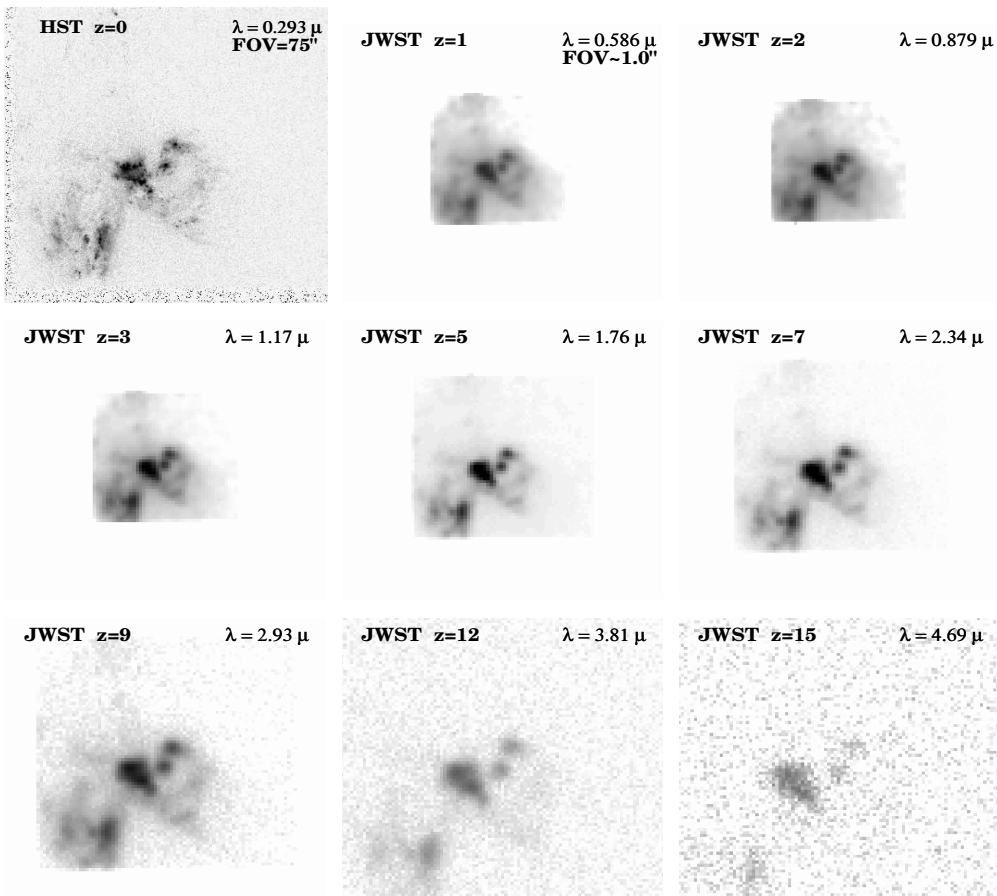


Fig. 4.06.a. JWST simulations based on HST/WFPC2 F300W images of the merger UGC06471-2 ($z=0.0104$). Note that the two unresolved star-bursting knots in the center remain visible until $z \sim 12$, beyond which the SB-dimming also kills their flux. This is the NOMINAL JWST [= (GOALS+REQUIREMENTS)/2].

ASSUMPTIONS: COSMOLOGY: $H_0=71$ km/s/Mpc, $\Omega_m=0.27$, and $\Omega_\Lambda=0.73$.

INSTRUMENT: 6.0 m effective aperture, JWST/NIRCam, $0.034''/\text{pix}$, $RN=5.0 e^-$, $\text{Dark}=0.020 e^-/\text{sec}$, NEP H-band $\text{Sky}=21.7 \text{ mag}/\text{arcsec}^2$ in L2, Zodiacal spectrum, $t_{exp}=1.0$ hrs, read-out every 900 sec ("NOMINAL").

Row 1: $z=0.0$ (HST $\lambda=0.293 \mu\text{m}$, $\text{FWHM}=0.04''$), $z=1.0$ (JWST $\lambda=0.586 \mu\text{m}$, $\text{FWHM}=0.084''$), and $z=2.0$ (JWST $\lambda=0.879 \mu\text{m}$, $\text{FWHM}=0.084''$). **Row 2:** $z=3.0$ (JWST $\lambda=1.17 \mu\text{m}$, $\text{FWHM}=0.084''$), $z=5.0$ (JWST $\lambda=1.76 \mu\text{m}$, $\text{FWHM}=0.084''$), and $z=7.0$ (JWST $\lambda=2.34 \mu\text{m}$, $\text{FWHM}=0.098''$). **Row 3:** $z=9.0$ (JWST $\lambda=2.93 \mu\text{m}$, $\text{FWHM}=0.122''$), $z=12.0$ (JWST $\lambda=3.81 \mu\text{m}$, $\text{FWHM}=0.160''$), and $z=15.0$ (JWST $\lambda=4.69 \mu\text{m}$, $\text{FWHM}=0.197''$)

The galaxy merger UGC06471-2 ($z=0.0104$) is a major and very dusty collision of two massive disk galaxies.

It shows two bright unresolved star-bursting knots to the upper-right of the center, which remain visible until $z \simeq 12$, beyond which the cosmic SB-dimming kills their flux. These are more typical for the small star-forming objects expected at $z \simeq 10-15$.

This is the NOMINAL JWST = (GOALS+REQUIREMENTS)/2.

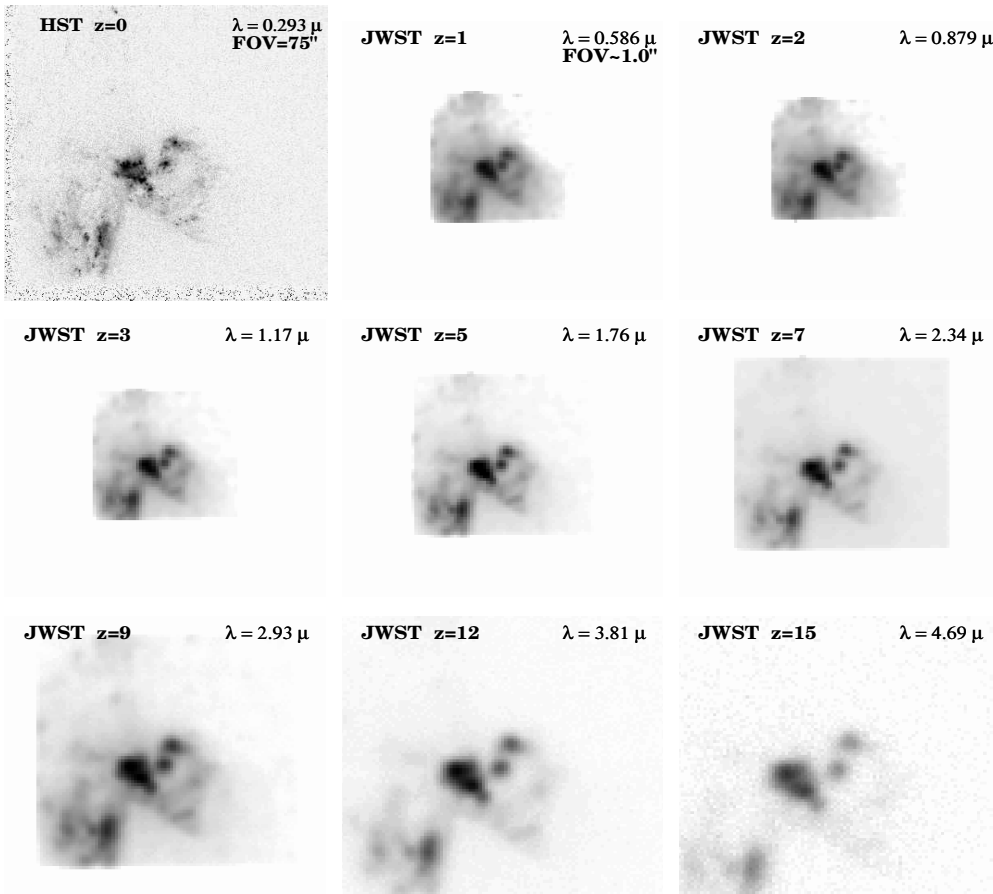


Fig. 4.06.c. JWST simulations based on HST/WFPC2 F300W images of the merger UGC06471-2 ($z=0.0104$). This is the BEST CASE JWST [meeting all GOALS, and $t_{exp}=100$ hrs]. The object is recognizable to $z \simeq 15$.

ASSUMPTIONS: COSMOLOGY: $H_0=71$ km/s/Mpc, $\Omega_m=0.27$, and $\Omega_\Lambda=0.73$.

INSTRUMENT: 6.0 m effective aperture, JWST/NIR camera, $0.034''$ /pix, $RN=3.0 e^-$, $Dark=0.010 e^-/sec$, NEP H-band $Sky=21.7 mag/arcsec^2$ in L2, Zodi spectrum, $t_{exp}=100.0$ hrs, read-out every 900 sec ("GOALS").

Row 1: $z=0.0$ (HST $\lambda=0.293\mu m$, $FWHM=0.04''$), $z=1.0$ (JWST $\lambda=0.586\mu m$, $FWHM=0.084''$), and $z=2.0$ (JWST $\lambda=0.879\mu m$, $FWHM=0.084''$). **Row 2:** $z=3.0$ (JWST $\lambda=1.17\mu m$, $FWHM=0.084''$), $z=5.0$ (JWST $\lambda=1.76\mu m$, $FWHM=0.084''$), and $z=7.0$ (JWST $\lambda=2.34\mu m$, $FWHM=0.098''$). **Row 3:** $z=9.0$ (JWST $\lambda=2.93\mu m$, $FWHM=0.122''$), $z=12.0$ (JWST $\lambda=3.81\mu m$, $FWHM=0.160''$), and $z=15.0$ (JWST $\lambda=4.69\mu m$, $FWHM=0.197''$)

The galaxy merger UGC06471-2 ($z=0.0104$).

This is the BEST CASE JWST. It assumes that all GOALS are met, and that $t_{exp}=100$ hrs. The whole object (including the two star-forming knots) is recognizable to $z \simeq 15$.

This does not imply that observing galaxies at $z=15$ with JWST will be easy. On the contrary, since galaxies formed through hierarchical merging, many objects at $z \simeq 10-15$ will be $10^1-10^4 \times$ less luminous, requiring to push JWST to its limits.

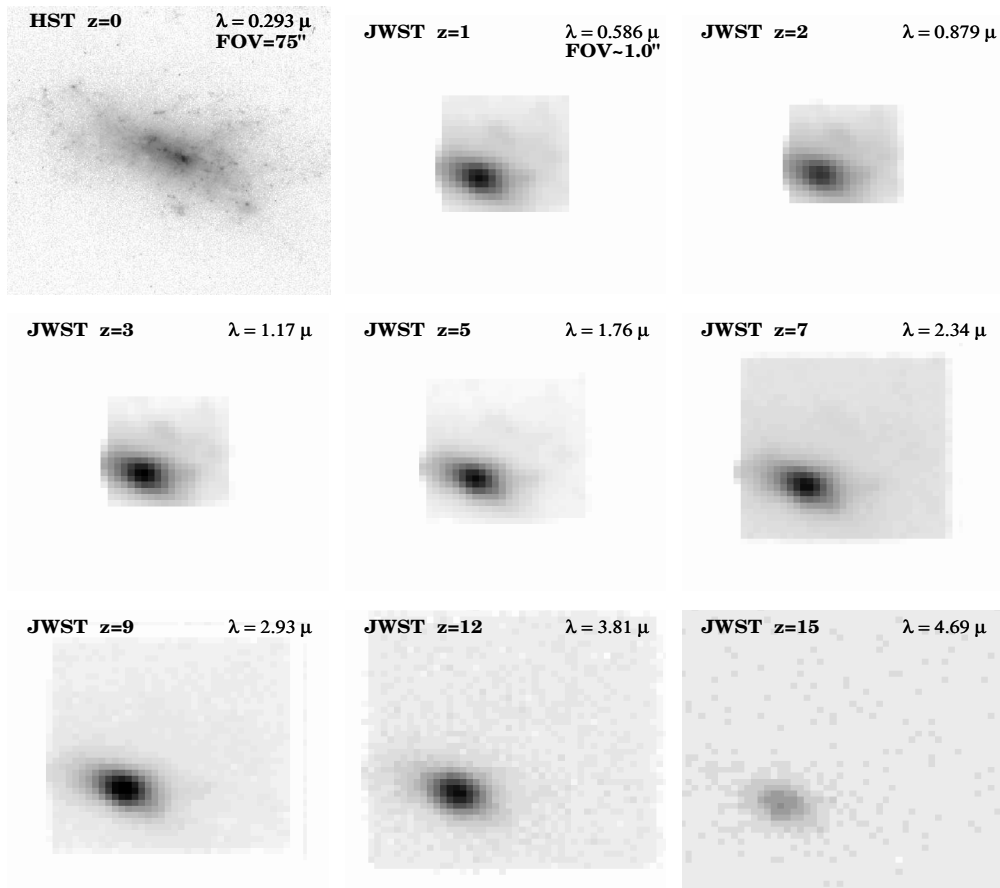


Fig. 4.01. JWST simulations based on HST/WFPC2 F300W images of the dwarf irregular NGC1140 ($z=0.0050$). This compact high SB object would be visible to $z \simeq 15$, but hard to classify at all $z \geq 1$.

ASSUMPTIONS: COSMOLOGY: $H_0=71$ km/s/Mpc, $\Omega_m=0.27$, and $\Omega_\Lambda=0.73$.

INSTRUMENT: 6.0 m effective aperture, JWST/NIRCam, $0.034''$ /pix, $RN=5.0 e^-$, $Dark=0.020 e^-/sec$, NEP H-band $Sky=21.7$ mag/arcsec² in L2, Zodiacal spectrum, $t_{exp}=1.0$ hrs, read-out every 900 sec.

Row 1: $z=0.0$ (HST $\lambda=0.293\mu m$, $FWHM=0.04''$), $z=1.0$ (JWST $\lambda=0.586\mu m$, $FWHM=0.084''$), and $z=2.0$ (JWST $\lambda=0.879\mu m$, $FWHM=0.084''$).

Row 2: $z=3.0$ (JWST $\lambda=1.17\mu m$, $FWHM=0.084''$), $z=5.0$ (JWST $\lambda=1.76\mu m$, $FWHM=0.084''$), and $z=7.0$ (JWST $\lambda=2.34\mu m$, $FWHM=0.098''$).

Row 3: $z=9.0$ (JWST $\lambda=2.93\mu m$, $FWHM=0.122''$), $z=12.0$ (JWST $\lambda=3.81\mu m$, $FWHM=0.160''$), and $z=15.0$ (JWST $\lambda=4.69\mu m$, $FWHM=0.197''$).

The compact high-SB dwarf irregular galaxy NGC1140 ($z=0.0050$).

With JWST, this object would be visible to $z \simeq 15$, but it will be hard to classify at all redshifts $z \geq 1$.

Note that the object indeed reaches a minimum angular size at $z \simeq 1.7$.

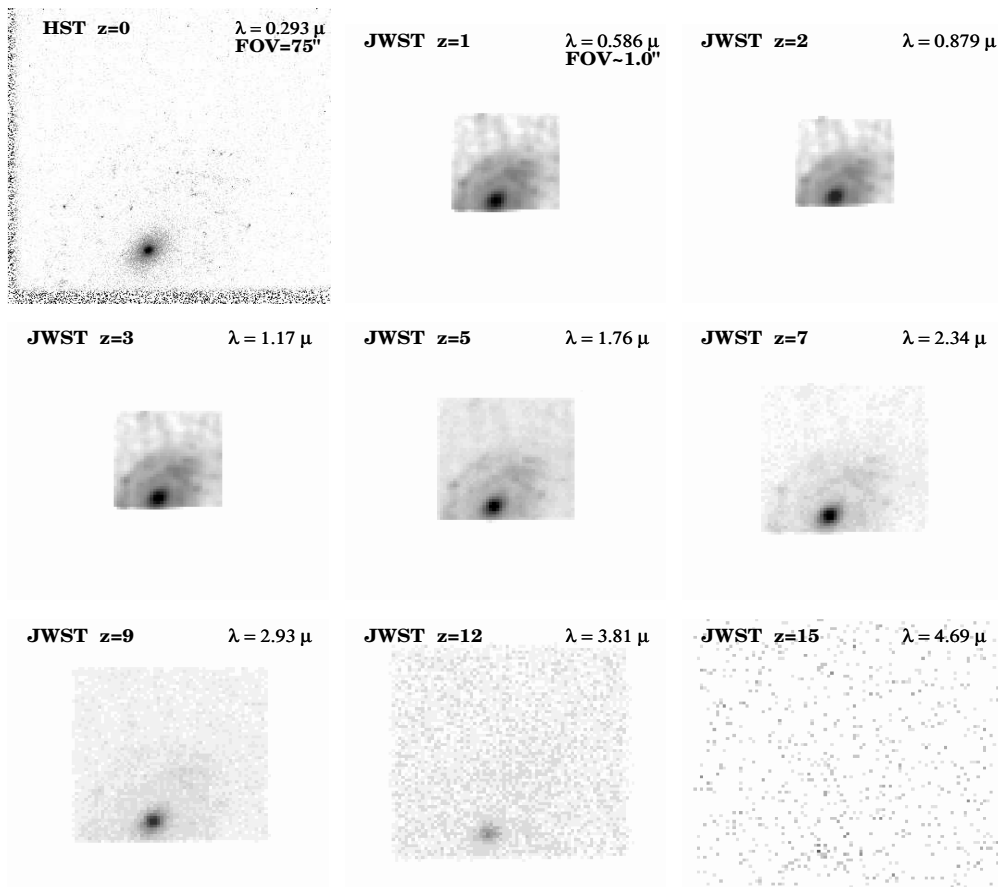


Fig. 4.02. JWST simulations based on HST/WFPC2 F300W images of the mid-type spiral NGC2551 (0.0078). Such an object would be visible to $z \simeq 10$, but only recognizable to $z \simeq 7$.

ASSUMPTIONS: COSMOLOGY: $H_0=71$ km/s/Mpc, $\Omega_m=0.27$, and $\Omega_\Lambda=0.73$.

INSTRUMENT: 6.0 m effective aperture, JWST/NIRCam, $0.034''$ /pix, $RN=5.0 e^-$, $Dark=0.020 e^-/sec$, NEP H-band $Sky=21.7$ mag/arcsec² in L2, Zodiacal spectrum, $t_{exp}=1.0$ hrs, read-out every 900 sec.

Row 1: $z=0.0$ (HST $\lambda=0.293\mu m$, $FWHM=0.04''$), $z=1.0$ (JWST $\lambda=0.586\mu m$, $FWHM=0.084''$), and $z=2.0$ (JWST $\lambda=0.879\mu m$, $FWHM=0.084''$).

Row 2: $z=3.0$ (JWST $\lambda=1.17\mu m$, $FWHM=0.084''$), $z=5.0$ (JWST $\lambda=1.76\mu m$, $FWHM=0.084''$), and $z=7.0$ (JWST $\lambda=2.34\mu m$, $FWHM=0.098''$).

Row 3: $z=9.0$ (JWST $\lambda=2.93\mu m$, $FWHM=0.122''$), $z=12.0$ (JWST $\lambda=3.81\mu m$, $FWHM=0.160''$), and $z=15.0$ (JWST $\lambda=4.69\mu m$, $FWHM=0.197''$).

The mid-type spiral NGC2551 ($z=0.0078$) would be visible out to $z \simeq 10$, but only recognizable out to $z \simeq 7$.

Its disk is in principle visible to $z \gtrsim 5-7$. Hence, if such objects are not seen by JWST at $z \lesssim 3$, then disks likely form at $z \lesssim 3$.

With HST we have seen glimpses of this, but with JWST these will become robust conclusions.

$\lambda = 0.293 \mu\text{m}$
FOV=75"

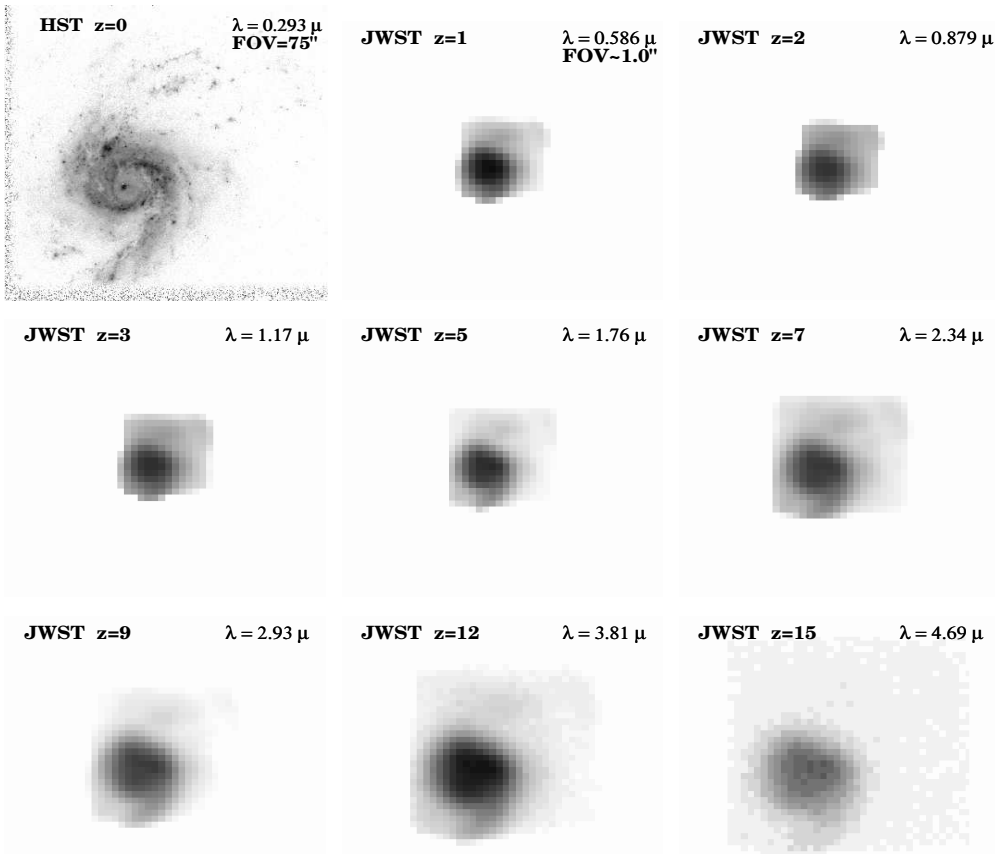


Fig. 4.03. JWST simulations based on HST/WFPC2 F300W images of the high-SB starbursting dwarf spiral galaxy NGC3310 (0.0033). The minimum in the Θ - z relation at $z \simeq 1.7$ and the JWST diffraction limit at $\lambda \geq 2.2 \mu\text{m}$ — combined with the object's very high rest-frame UV SB — conspire to improve the effective JWST resolution on the mid-UV morphology of this object from $z \simeq 2$ to $z \simeq 7$.

ASSUMPTIONS: COSMOLOGY: $H_0 = 71 \text{ km/s/Mpc}$, $\Omega_m = 0.27$, and $\Omega_\Lambda = 0.73$. INSTRUMENT: 6.0 m effective aperture, JWST/NIRCam, $0.034''/\text{pix}$, $\text{RN} = 5.0 \text{ e}^-$, $\text{Dark} = 0.020 \text{ e}^-/\text{sec}$, NEP H-band Sky = $21.7 \text{ mag/arcsec}^2$ in L2, Zodiacal spectrum, $t_{\text{exp}} = 1.0 \text{ hrs}$, read-out every 900 sec.

Row 1: $z=0.0$ (HST $\lambda=0.293 \mu\text{m}$, $\text{FWHM}=0.04''$), $z=1.0$ (JWST $\lambda=0.586 \mu\text{m}$, $\text{FWHM}=0.084''$), and $z=2.0$ (JWST $\lambda=0.879 \mu\text{m}$, $\text{FWHM}=0.084''$). **Row 2:** $z=3.0$ (JWST $\lambda=1.17 \mu\text{m}$, $\text{FWHM}=0.084''$), $z=5.0$ (JWST $\lambda=1.76 \mu\text{m}$, $\text{FWHM}=0.084''$), and $z=7.0$ (JWST $\lambda=2.34 \mu\text{m}$, $\text{FWHM}=0.098''$). **Row 3:** $z=9.0$ (JWST $\lambda=2.93 \mu\text{m}$, $\text{FWHM}=0.122''$), $z=12.0$ (JWST $\lambda=3.81 \mu\text{m}$, $\text{FWHM}=0.160''$), and $z=15.0$ (JWST $\lambda=4.69 \mu\text{m}$, $\text{FWHM}=0.197''$)

The very high-SB, compact starbursting dwarf spiral galaxy NGC3310 ($z=0.0033$).

The minimum in the Θ - z relation at $z \simeq 1.7$ and the JWST diffraction limit at $\lambda \geq 2.2 \mu\text{m}$ — combined with the object's very high rest-frame UV-SB — conspire to improve the effective JWST resolution on the mid-UV morphology of this object from $z \simeq 2$ to $z \simeq 7$.

A rather exceptional case of where nasty cosmology doesn't appear to cost you prohibitive sensitivity, but gains you resolution!

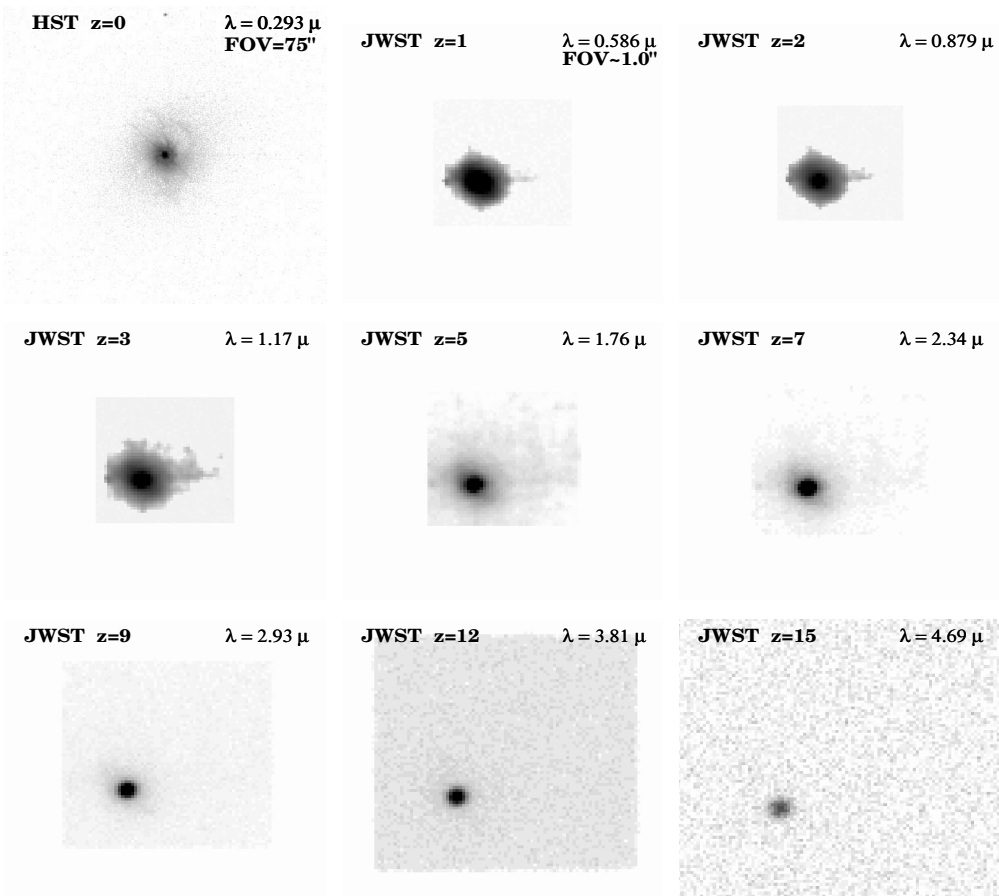


Fig. 4.04. JWST simulations based on HST/WFPC2 F300W images of the Seyfert galaxy NGC3516 (0.0088). Note that the faint nebula surrounding the AGN in the mid-UV at $z=0$ essentially disappears at $z \geq 7$, so that at high redshifts such objects would look like a pure AGN.

ASSUMPTIONS: COSMOLOGY: $H_0=71$ km/s/Mpc, $\Omega_m=0.27$, and $\Omega_\Lambda=0.73$.

INSTRUMENT: 6.0 m effective aperture, JWST/NIRCam, $0.034''$ /pix, RN=5.0 e^- , Dark=0.020 e^- /sec, NEP H-band Sky=21.7 mag/arcsec² in L2, Zodiacal spectrum, $t_{exp}=1.0$ hrs, read-out every 900 sec.

Row 1: $z=0.0$ (HST $\lambda=0.293\mu\text{m}$, FWHM=0.04''), $z=1.0$ (JWST $\lambda=0.586\mu\text{m}$, FWHM=0.084''), and $z=2.0$ (JWST $\lambda=0.879\mu\text{m}$, FWHM=0.084''). **Row 2:** $z=3.0$ (JWST $\lambda=1.17\mu\text{m}$, FWHM=0.084''), $z=5.0$ (JWST $\lambda=1.76\mu\text{m}$, FWHM=0.084''), and $z=7.0$ (JWST $\lambda=2.34\mu\text{m}$, FWHM=0.098''). **Row 3:** $z=9.0$ (JWST $\lambda=2.93\mu\text{m}$, FWHM=0.122''), $z=12.0$ (JWST $\lambda=3.81\mu\text{m}$, FWHM=0.160''), and $z=15.0$ (JWST $\lambda=4.69\mu\text{m}$, FWHM=0.197'')

The Seyfert galaxy NGC3516 ($z=0.0088$) has a faint nebula surrounding its AGN in the mid-UV, while at longer wavelengths the surrounding elliptical galaxy is present (not shown here).

The nebula surrounding the AGN is essentially SB-dimmed away at $z \geq 7$, so that at high redshifts these objects would look like purely stellar objects ("quasars").

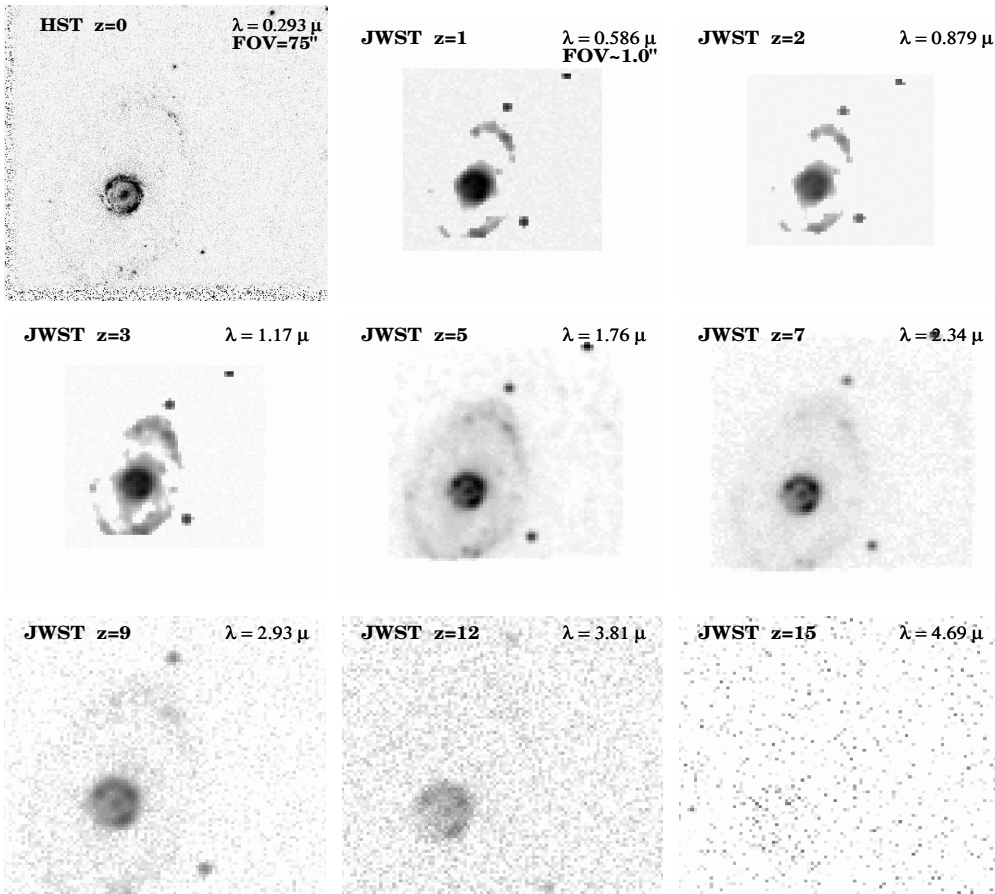


Fig. 4.05. JWST simulations based on HST/WFPC2 F300W images of the barred ring galaxy NGC6782 (0.0125). Note again that for $z \simeq 2$ – 7 , the effective resolution on the bright star-forming ring improves with increasing redshift, until the $(1+z)^4$ -dimming completely kills it for $z \geq 10$.

ASSUMPTIONS: COSMOLOGY: $H_0=71$ km/s/Mpc, $\Omega_m=0.27$, and $\Omega_\Lambda=0.73$.

INSTRUMENT: 6.0 m effective aperture, JWST/NIRCam, $0.034''$ /pix, $RN=5.0 e^-$, $Dark=0.020 e^-/sec$, NEP H-band Sky= 21.7 mag/arcsec² in L2, Zodiacal spectrum, $t_{exp}=1.0$ hrs, read-out every 900 sec.

Row 1: $z=0.0$ (HST $\lambda=0.293\mu m$, FWHM= $0.04''$), $z=1.0$ (JWST $\lambda=0.586\mu m$, FWHM= $0.084''$), and $z=2.0$ (JWST $\lambda=0.879\mu m$, FWHM= $0.084''$). **Row 2:** $z=3.0$ (JWST $\lambda=1.17\mu m$, FWHM= $0.084''$), $z=5.0$ (JWST $\lambda=1.76\mu m$, FWHM= $0.084''$), and $z=7.0$ (JWST $\lambda=2.34\mu m$, FWHM= $0.098''$). **Row 3:** $z=9.0$ (JWST $\lambda=2.93\mu m$, FWHM= $0.122''$), $z=12.0$ (JWST $\lambda=3.81\mu m$, FWHM= $0.160''$), and $z=15.0$ (JWST $\lambda=4.69\mu m$, FWHM= $0.197''$)

The barred ring galaxy NGC6782 (0.0125) shows that at $z \simeq 2$ to $z \simeq 7$, the effective resolution on its high-SB bright star-forming ring improves with increasing redshift, until the $(1+z)^4$ -dimming completely kills it for $z \gtrsim 10$ – 12 .

Another good case showing why cosmology is not “WYSIWYG”.